R. & M. No. 3752

R. & M. No. 3752

PROCUREMENT EXECUTIVE, MINISTRY OF DEFENCE

AERONAUTICAL RESEARCH COUNCIL

REPORTS AND MEMORANDA

Notes on the Approximate Solution of Lifting-Surface Theory Used in the R.A.E. Standard Method

By J. WEBER

Aerodynamics Dept., R.A.E., Farnborough

LONDON: HER MAJESTY'S STATIONERY OFFICE

1974

PRICE £2·80 NET

Notes on the Approximate Solution of Lifting-Surface Theory Used in the R.A.E. Standard Method

By J. WEBER

Aerodynamics Dept., R.A.E., Farnborough

Reports and Memoranda No. 3752*
February, 1973

Summary

The downwash induced by planar vorticity distributions has been computed by exact linear theory and by the R.A.E. Standard Method to examine the accuracy of the approximate method. The results on wings of infinite span with load distributions which are uniform across the span are used to derive a modification of the downwash equation of the approximate method. It is shown that this modification can explain some of the difference between the exact and the approximate results for the spanwise C_L distribution of a plane wing of infinite span at an angle of incidence. The downwash distributions on finite wings of constant chord, unswept and sweptback by 45 degrees, with given load distributions, computed by the exact and the approximate method are compared. The lift distribution for wings of given shape derived by the approximate method is also compared with more accurate results.

* Replaces R.A.E. Technical Report 73044-A.R.C. 34 766

LIST OF CONTENTS

1. Introduction

The 'R.A.E. Standard Method'[1,2] used for the design of swept wings with subsonic attached flow is based on linear theory; some non-linear effects are taken into account using specific theoretical twodimensional and threedimensional results.

In the original framework, developed at a time when fast electronic computers were not yet available, the velocity field predicted by linear theory was not determined by exact computation but some approximations were introduced. Recently, computer programs have been written, *see* e.g. Refs. 3 and 4, for evaluating the velocity field induced by given planar singularity distributions. We are, therefore, now able to examine the validity of the approximations made in the Standard Method. We use in these notes the label 'R.A.E. Standard Method' for the original approximate solution of lifting-surface theory, based on Küchemann's work.[2,5] The framework of the R.A.E. Standard Method can, of course, be retained when the velocity fields from planar singularity distributions are computed exactly. In this Report, we compare downwash distributions calculated by the approximate method with those calculated by exact linear theory; we also examine the accuracy of the approximate method when it is used to solve the direct lifting-surface problem (to find the load distribution for a given downwash distribution).

The Standard Method makes use of the downwash induced by distributions of infinite swept vortices which are of constant strength along the span. In the past, the induced downwash distribution away from the centre section has not been computed exactly but only an approximation has been used. For the first two Birnbaum distributions of the vorticity along the chord, we have therefore computed the downwash at various spanwise stations for angles of sweep of 30, 45 and 60 degrees. These results are discussed in Section 2.

To evaluate the downwash on finite wings of given load distribution, we have used the computer program developed by Sells.[3] The accuracy of the numerical results from the Sells program is such that, for the purpose of the present study, we may call them 'exact'. The results from Sells' program have least accuracy near the tip, but we shall see that there the difference between the approximate results and those from Sells' program are so large that small inaccuracies in the results from Sells' program do not affect the comparison.

We consider two planforms:

(i) an unswept rectangular wing of aspect ratio 6,

(ii) a swept wing, $\phi = 45$ degrees, of constant chord and aspect ratio 6.

The chosen load distributions are such that the type of chordwise distribution is the same along the span but C_L varies spanwise. We have chosen two types of chordwise load distribution, namely, the first and second Birnbaum distribution, and two spanwise C_L distributions, namely, the elliptic distribution and one where C_L is constant over the inner 80 per cent of the semi-span and where C_L decreases elliptically over the outer part of the wing, *see* Table 1. (With the second type of C_L distribution, *i.e.* for the load distributions (3) and (4), the second spanwise derivative $\partial^2 l(\xi, \eta)/\partial\eta^2$ is discontinuous at $\eta = 0{\cdot}8$. The Sells program is written for load distributions for which the derivative $\partial^2 l(\xi, \eta)/\partial\eta^2$ is a continuous function. The discontinuity is important only when computing the downwash at the position of the discontinuity. For the load distributions (3) and (4), we do not therefore consider the downwash at the spanwise station $\eta = 0{\cdot}8$.)

The downwash which these load distributions induce in the wing plane, $z = 0$, has been computed at the nine chordwise stations

$$\xi = \frac{x - |y| \tan \phi}{c} = \frac{1 - \cos \theta}{2},$$

with $\theta = n\pi/8$, $n = 0, 1, \ldots, 8$, at various spanwise stations. The centre section, $\eta = 0$, has not been considered since, for the chosen load distributions, the downwash for the swept wing in the plane $z = 0$ would be logarithmically infinite.

The formulae used in the Standard Method to derive approximate values of the downwash are given in Section 3.1. Numerical values from the approximate method are compared with the exact values, for the rectangular wings in Section 3.2 and for the swept wings in Section 3.3.

The results obtained in Section 2, for wings of infinite span and uniform spanwise load distributions, suggest a modification to the original basic downwash equation of the Standard Method. This modification entails also a modification to the sectional lift slope used in the Standard Method in the derivation of the spanwise C_L distribution. These modifications are discussed in Sections 4.1 and 4.2.

For the special case of an uncambered wing of infinite span, sweptback by 45 degrees, at an angle of incidence, Hui[6] has calculated the spanwise C_L distribution by solving the downwash equation of lifting-surface theory. Away from the centre section, Hui's values for C_L are appreciably smaller than those of the Standard Method. In Section 4.3, we examine the cause of this difference.

In Section 4.4, we consider how much the difference between the downwash from the exact and the approximate method affects the results for the inverse problem of finding the load distribution for a given wing, in particular the spanwise C_L distribution. For this purpose, we use the load distributions derived by Sells (Ref. 10 and unpublished work) by means of an iterative procedure, in which the accuracy of a load distribution is checked by computing the downwash using the program of Ref. 3. We have also studied wings which are warped such that the chordwise slope is equal to the difference between the approximate and the exact downwash induced by the load distributions (1) and (2) of Section 3.

We stress again that we examine in this Report the downwash only at spanwise stations away from the centre section and only in the plane of the singularity distributions. We restrict the discussion to wings of constant chord.

2. Downwash Induced on Swept Wings of Infinite Span by Load Distributions which are Uniform across the Span

We use a system of rectangular coordinates x, y, z; the plane $z = 0$ is the wing datum plane, the line $y = z = 0$ the centre section of a swept wing and the point $x = y = z = 0$ the apex of the wing. ϕ denotes the angle of sweep. We consider the velocity component v_z parallel to the z-axis; v_z is positive if the velocity vector is directed upwards. We denote the downwash $-v_z(x, y, z)$ by $w(x, y, z)$.

The value of the downwash which is induced by a single swept vortex through $x = y = 0$ in the plane $z = 0$ of strength Γ is given by the equation

$$w(x,y,z) = \frac{\Gamma}{4\pi\cos\phi}\left\{\frac{x + y\tan\phi}{(x + y\tan\phi)^2 + \dfrac{z^2}{\cot^2\phi}}\left[1 - \frac{y\cos\phi - x\sin\phi}{\sqrt{x^2 + y^2 + z^2}}\right] + \right.$$
$$\left. + \frac{x - y\tan\phi}{(x - y\tan\phi)^2 + \dfrac{z^2}{\cos^2\phi}}\left[1 + \frac{y\cos\phi + x\sin\phi}{\sqrt{x^2 + y^2 + z^2}}\right]\right\}. \tag{1}$$

For $y \geqslant 0$, we introduce the coordinate ξ, where

$$x = y\tan\phi + \xi, \tag{2}$$

and obtain

$$w(x,y,z) = \frac{\Gamma}{4\pi\cos\phi}\left\{\frac{\xi}{\xi^2 + \dfrac{z^2}{\cos^2\phi}}\left[1 + \frac{y + \xi\sin\phi\cos\phi}{\sqrt{y^2 + 2\xi y\sin\phi\cos\phi + \xi^2\cos^2\phi + z^2\cos^2\phi}}\right] + \right.$$
$$\left. + \frac{2y\tan\phi + \xi}{(2y\tan\phi + \xi)^2 + \dfrac{z^2}{\cos^2\phi}}\left[1 - \frac{y(\cos^2\phi - \sin^2\phi) - \xi\sin\phi\cos\phi}{\sqrt{y^2 + 2\xi y\sin\phi\cos\phi + \xi^2\cos^2\phi + z^2\cos^2\phi}}\right]\right\}. \tag{3}$$

For $y \to \infty$, we obtain from equation (3) the value for the downwash of the infinite sheared vortex; $w_{2D}(\xi, z)$:

$$w_{2D}(\xi, z) = \frac{\Gamma}{2\pi\cos\phi}\frac{\xi}{\xi^2 + \dfrac{z^2}{\cos^2\phi}}. \tag{4}$$

For the centre section $y = 0$, we obtain from equations (3) and (4):

$$w(\xi, 0, z) - w_{2D}(\xi, z) = \frac{\Gamma}{2\pi\cos\phi}\frac{\sin\phi\,\xi^2}{\left[\xi^2 + \dfrac{z^2}{\cos^2\phi}\right]\sqrt{\xi^2 + z^2}}. \tag{5}$$

For $y \neq 0$, $z = 0$, we obtain

$$w(\xi, y, 0) - w_{2D}(\xi, 0) = \frac{\Gamma}{2\pi\cos\phi}\frac{\tan\phi}{\xi[2y\tan\phi + \xi]} \times [\sqrt{y^2 + 2y\xi\sin\phi\cos\phi + \xi^2\cos^2\phi} - y]. \tag{6}$$

We consider wings of constant chord (which we choose as unity) and infinite span in a mainstream of velocity V_0. We choose $V_0 = 1$ so that in the following w denotes the ratio w/V_0 between the downwash and the velocity of the free stream. We assume that the strength of the load distribution is constant along the span, *i.e.* $l(x, y) = -\Delta C_p(x, y) = l(\xi)$. The vorticity is related to the pressure difference by the relation

$$l(\xi) = \cos\phi 2\gamma(\xi), \tag{7}$$

so that the strength of an elemental strip of vortices, which are parallel to the leading edge, is

$$\gamma(\xi)\, dn = \gamma(\xi)\cos\phi\, d\xi = \tfrac{1}{2}l(\xi)\, d\xi,$$

where dn is a length measured normal to the leading edge of the wing. Integration of equations (5) and (6) gives for the downwash the equations:

$$w(\xi, 0, z) - w_{2D}(\xi, z) = \frac{\sin\phi}{2\pi}\int_0^1 \gamma(\xi')\frac{(\xi - \xi')^2\, d\xi'}{\left[(\xi - \xi')^2 + \dfrac{z^2}{\cos^2\phi}\right]\sqrt{(\xi - \xi')^2 + z^2}} \tag{8}$$

and

$$w(\xi, y, 0) - w_{2D}(\xi, 0) =$$

$$= \frac{1}{2\pi}\int_0^1 \gamma(\xi')\frac{\tan\phi}{(\xi - \xi')[2y\tan\phi + \xi - \xi']} \times$$

$$\times \left[\sqrt{y^2 + 2y(\xi - \xi')\sin\phi\cos\phi + (\xi - \xi')^2\cos^2\phi} - y\right] d\xi'. \tag{9}$$

For large values of y and $\phi \neq 0$, we may expand the integrand of equation (9) in terms of powers of $(\xi - \xi')/y$ and we obtain

$$w(\xi, y, 0) - w_{2D}(\xi, 0) =$$

$$= \frac{\sin\phi\cos\phi}{4\pi y}\int_0^1 \gamma(\xi')\left\{1 - \sin\phi\cos\phi\frac{\xi - \xi'}{2y} - \cos^2\phi(1 - 2\sin^2\phi)\left(\frac{\xi - \xi'}{2y}\right)^2 + \ldots\right\} d\xi'$$

$$= \frac{\sin 2\phi}{8\pi y}\left\{\left[1 - \frac{\xi}{4y}\sin 2\phi - \left(\frac{\xi}{2y}\right)^2\cos^2\phi\cos 2\phi + \ldots\right]\int_0^1 \gamma(\xi')\, d\xi' + \right.$$

$$\left. + \frac{1}{4y}\left[\sin 2\phi + \frac{\xi}{y}2\cos^2\phi\cos 2\phi + \ldots\right]\int_0^1 \xi'\gamma(\xi')\, d\xi' + \ldots\right\}$$

$$= \frac{\sin 2\phi}{8\pi y}\left\{1 - \frac{\xi - \xi_{CP}}{4y}\sin 2\phi + \ldots\right\}\int_0^1 \gamma(\xi')\, d\xi', \tag{10}$$

where $\xi_{CP} = \int_0^1 \xi'\gamma(\xi')\, d\xi' / \int_0^1 \gamma(\xi')\, d\xi'$ is the position of the centre of pressure of the load distribution $l(\xi)$.

Equation (10) shows that for large values of y the difference between the downwash from a distribution of swept vortices and that of the corresponding infinite sheared distribution is to a large degree independent of the chordwise distribution of vorticity and depends mainly on the total circulation, $\int_0^1 \gamma(\xi')\, d\xi'$, as would be expected. Equation (10) shows further that, for a given distribution $\gamma(\xi)$ and large y, the term $w(\xi, y, 0) - w_{2D}(\xi, 0)$ is largest for $\phi = 45$ degrees.

For the first and second Birnbaum distributions, $\gamma(\xi) = 2\sqrt{(1 - \xi)/\xi}$ and $\gamma(\xi) = 8\sqrt{\xi(1 - \xi)}$, we have calculated values of $w(\xi, y, 0) - w_{2D}(\xi, 0)$ by equation (9). For $\phi = 45$ degrees, some values are plotted in Fig. 1. We note that, for $y > 0{\cdot}6$ say, the values of $w - w_{2D}$ do not depend a great deal on the distribution $\gamma(\xi)$; they are very similar to the approximate values given by equation (10) for large y, shown by the dotted lines. The chordwise distribution of $w - w_{2D}$ is the more dependent on the distribution of $\gamma(\xi)$ the closer the station is to the centre section. We have added in Fig. 1 values for $w - w_{2D}$ at the centre section $y = 0$ at the distance $z = 0{\cdot}04$. Since the values of $w(\xi, 0, z) - w_{2D}(\xi, z)$ tend logarithmically to infinity for $z \to 0$, the values of $w - w_{2D}$ vary rapidly with z. Therefore, the values at $z = 0{\cdot}04$ are only to indicate the type of downwash induced at the surface of a wing with finite thickness.

In Fig. 2, we have plotted values of $w - w_{2D}$ for various angles of sweep. We have mentioned before that it follows from equation (10) that, with given $\gamma(\xi)$ (*i.e.* given $w_{2D}(\xi)$ but not fixed $l(\xi)$, *see* equation (7)) and large values of y, the term $w - w_{2D}$ is largest for $\phi = 45$ degrees; Fig. 2 shows that this is true for $y \geqslant 0{\cdot}4$. For small values of y, the value of ϕ for which $w - w_{2D}$ reaches a maximum depends on the values of ξ and z and on the distribution $\gamma(\xi)$. To illustrate this, we quote from Ref. 7 the approximate relation for the additional downwash at the centre section, $w(\xi, 0, z) - w_{2D}(\xi, z)$, when $\gamma(\xi) = A + B\xi$ and z is small compared with ξ, $1 - \xi$ and 1:

$$w(\xi, 0, z) - w_{2D}(\xi, z) = -\frac{\sin\phi}{2\pi}\left\{(A + B\xi)\log\frac{4\xi(1-\xi)}{z^2} + B(1 - 2\xi)\right\} + \frac{1}{2\pi}(A + B\xi)\log\frac{1 + \sin\phi}{1 - \sin\phi}. \quad (11)$$

For $\xi = 0{\cdot}5$, the maximum value of $w - w_{2D}$ is reached when $\cos\phi = [-\log z]^{-\frac{1}{2}}$. With $z = 0{\cdot}04$ this gives $\phi \approx 56$ degrees. We note that the value of ϕ increases with decreasing z. Fig. 3 shows for $\gamma(\xi) = 2\sqrt{(1-\xi)/\xi}$ how $w - w_{2D}$ at the centre section at $z = 0{\cdot}04$ varies with ϕ.

It follows from equations (8) and (9) that the function $[\phi/|\phi|][w - w_{2D}]$ is independent of the sign of ϕ for $y = 0$ but not for $y \neq 0$. To demonstrate how much the function depends on the sign of ϕ, we have plotted in Fig. 4 some values of $w - w_{2D}$ for $\phi = 45$ degrees and for $\phi = -45$ degrees.

We consider now how the results given above compare with those obtained from the approximate downwash equation suggested by Küchemann. The latter reads

$$w_K(\xi, y, z) = \frac{1}{2\pi}\int_0^1 \gamma(\xi', y)\frac{d\xi'}{\xi - \xi'} + \tfrac{1}{2}\tan(\lambda(y)\phi)\gamma(\xi; y). \quad (12)$$

(Within linear theory, this equation has been suggested for values of z appropriate to the surface of the wing or (for $y \neq 0$) also for $z = 0$.) For the special case considered above, $w - w_{2D}$ is thus approximated at the centre section and at $y \neq 0$ by the function

$$w_K - w_{2D} = \tfrac{1}{2}\tan(\lambda(y)\phi)\gamma(\xi) \quad (13)$$

where

$$\lambda(y) = \sqrt{1 + \left(2\pi\frac{\tan\phi}{\phi}y\right)^2} - 2\pi\frac{\tan\phi}{\phi}y. \quad (14)$$

This implies that the function $w_K(\xi, y, 0) - w_{2D}(\xi, 0)$ has the same shape for all values of y. We note from Figs. 1 and 2 that this is a rather crude approximation for $y > 0{\cdot}1$. A comparison of values for $w - w_{2D}$ from equation (9) with those from equation (13) is made in Fig. 5. Some of the resulting changes to the twodimensional wing shape

$$\Delta z(\xi, y) = \int_\xi^1 [w(\xi', y, 0) - w_{2D}(\xi', 0)]\, d\xi' \quad (15)$$

are shown in Fig. 6. We note that (for both chordwise load distributions), for $\phi = 45$ degrees, the approximate equation (13) produces less twist than the exact equation (9). For the first Birnbaum distribution, the exact camber lines for $y = $ const. and $y \geqslant 0{\cdot}1$ are very nearly circular arcs whilst the approximate camber lines (which are of the type $m = 0{\cdot}5$ given in Fig. 4 of Ref. 8) have the maximum ordinate further forward, at $\xi = 0{\cdot}29$. To appreciate the difference in camber shape, we quote the type of twodimensional load distribution related to the camber lines: for the approximate camber line it is $\sqrt{(1-\xi)/\xi}\log[(1-\xi)/\xi]$, whilst it is $\sqrt{\xi(1-\xi)}$ for the circular arc.

The spanwise variation of the twist,

$$\Delta\alpha(y) = \int_0^1 [w(\xi, y, 0) - w_{2D}(\xi, 0)]\, d\xi, \quad (16)$$

is shown in Fig. 7, together with

$$\Delta\alpha_K(y) = \frac{\pi}{2}\tan(\lambda(y)\phi). \quad (17)$$

We note that $\Delta\alpha_K(y)$ predicts the type of distribution quite well, but does not give the actual values of $\Delta\alpha$ accurately. For the function $\lambda(y)$ not only the formula given by equation (14) has been used but also a function which is independent of ϕ, namely the limit for $\phi \to 0$ of the expression given by equation (14):

$$\lambda(y) = \sqrt{1 + (2\pi y)^2} - 2\pi y. \tag{18}$$

We have, therefore, plotted the values of $\Delta\alpha_K$ for both formulae for λ. Fig. 7 may suggest that it is preferable to use for $\lambda(y)$ the values given by equation (18). This would however not be advisable for $\phi > 60$ degrees say, because equations (17) and (18) produce values for $\Delta\alpha_K$ which increase monotonically with increasing ϕ whilst we have learnt that, for large y, the exact $\Delta\alpha$ has a maximum value at $\phi = 45$ degrees. For small y, Fig. 2 suggests that $\Delta\alpha$ has the maximum value for ϕ smaller than 90 degrees. We note further that the values of $w - w_{2D}$ for $y = 0$, $z = 0{\cdot}04$, plotted in Fig. 3, do not show the large increase with increasing ϕ as given by the term $\frac{1}{2}\tan\phi\gamma(\xi)$.

3. Comparison of Downwash Distributions on Finite Wings with Given Load Distribution Computed by the R.A.E. Standard Method with those from Exact Linear Theory

3.1. Prediction of the Downwash by the Standard Method

For an unswept wing of large aspect ratio, the Standard Method is identical with Prandtl's theory of a lifting wing. The vorticity vector is split into the spanwise and streamwise components. The downwash at a point x, y produced by the spanwise vortices is approximated by the downwash induced by a twodimensional distribution of vorticity which has the same strength as the threedimensional distribution at the spanwise station y. The contribution to the downwash which is induced by the chordwise component of the vorticity over the wing and by the trailing vortices behind the wing is assumed to be nearly constant over the chord of the wing and equal to half the downwash induced far behind the wing, *i.e.* in the Trefftz plane.

Thus for an unswept wing with a given load distribution $l(x, y) = 2\gamma(x, y)$, the downwash $w(x, y)$ is approximated by the sum $w_{2D}(x, y) + \alpha_{i0}(y)$ where

$$w_{2D}(x, y) = \frac{1}{4\pi}\int_{x_{LE}(y)}^{x_{TE}(y)} l(x', y)\frac{dx'}{x - x'} \tag{19}$$

and

$$\begin{aligned}\alpha_{i0}(y) &= \tfrac{1}{2}w(x = \infty, y)\\ &= \frac{1}{8\pi}\iint\limits_{\substack{\text{wing}\\ \text{area}}} \frac{\partial}{\partial y'} l(x', y')\, dx' \frac{dy'}{y - y'}.\end{aligned} \tag{20}$$

This approximation can be derived from the exact equation of linear theory:

$$\begin{aligned}w(x, y, z = 0) &= \frac{1}{8\pi}\iint_S \frac{l(x', y')}{(y - y')^2}\left[1 + \frac{x - x'}{\sqrt{(x - x')^2 + (y - y')^2}}\right] dx'\, dy'\\ &= \frac{1}{8\pi}\frac{\partial}{\partial y}\iint_S \frac{l(x', y')}{y - y'}\left[1 + \frac{\sqrt{(x - x')^2 + (y - y')^2}}{x - x'}\right] dx'\, dy'.\end{aligned} \tag{21}$$

When this equation is approximated by

$$w(x, y, 0) \approx \frac{1}{8\pi}\frac{\partial}{\partial y}\iint_S \frac{l(x', y')}{y - y'}\left[1 + \frac{|y - y'|}{x - x'}\right] dx'\, dy', \tag{22}$$

the downwash can be written as the sum of two terms

$$\begin{aligned}w(x, y, 0) &\approx \frac{1}{8\pi}\frac{\partial}{\partial y}\iint_S \frac{l(x', y')}{y - y'} dx'\, dy' + \frac{1}{4\pi}\int_{x_{LE}(y)}^{x_{TE}(y)} l(x', y)\frac{dx'}{x - x'}\\ &\approx \alpha_{i0}(y) + w_{2D}(x, y).\end{aligned} \tag{23}$$

The Standard Method introduces some modifications to equation (23), but they are negligible for wings of aspect ratio 6; we, therefore, ignore them here (they are of importance only for wings of small aspect ratio).

For a swept wing, the Standard Method derives an approximate value of the downwash by splitting the vorticity vector again into a spanwise component and a chordwise component; spanwise means here parallel to the leading edge. (For a tapered wing a mean sweep angle is chosen.) The downwash induced by the spanwise vorticity is again approximated by the downwash of a system of infinite kinked vortices for which the strength does not vary along the span and is determined by the chordwise load distribution at the station under consideration. The downwash from the chordwise vorticity (which includes the trailing vortices behind the wing) is again approximated by half the downwash far behind the wing. (For this contribution to the downwash Küchemann[2] has proposed the use of $2n_s\alpha_{i0}$ which, for wings of large aspect ratio, is equal to α_{i0}. In Ref. 1 the use of $2n(y)\alpha_{i0}$ has been suggested, but it is shown below (*see* Section 4.4) that this does not necessarily improve matters. In this Report, we have used $2n_s\alpha_{i0} = \alpha_{i0}$.)

We have mentioned in Section 2 that Küchemann has proposed to approximate the downwash induced by a distribution of infinite kinked vortices, of constant strength along the span, by the term given in equation (12). He has further suggested that, for a wing of finite span, the downwash from the spanwise vortices near the tip is similar to that near the centre of a swept forward wing. For a wing of finite span, it has therefore been suggested that for $\lambda(y)$ in equation (12) the relation

$$\lambda(y) = \sqrt{1 + \left(2\pi\frac{y}{c}\right)^2} - 2\pi\frac{y}{c} - \left\{\sqrt{1 + \left(2\pi\frac{s-y}{c}\right)^2} - 2\pi\frac{s-y}{c}\right\} \tag{24}$$

should be used, where s is the semispan and c the local wing chord.

A load distribution which near the centre section is constant along the span produces at the centre section, $y = 0$, an infinite downwash in the plane $z = 0$, but finite values for $z \neq 0$. The relation (12) has been suggested as an approximation to the finite downwash at the surface of a wing with finite thickness. In this Report, we want to compare only values of the downwash in the plane $z = 0$; we therefore exclude comparisons at the station $y = 0$.

When we use relation (7) between $\gamma(\xi, y)$ and $l(\xi, y)$ we obtain for the approximate values of the downwash on a swept wing the equation:

$$w(\xi, y) = \frac{1}{4\pi\cos\phi}\int_0^1 l(\xi', y)\frac{d\xi'}{\xi - \xi'} + \frac{\tan(\lambda(y)\phi)}{4\cos\phi}l(\xi, y) + \alpha_{i0}(y). \tag{25}$$

We note also that for a swept wing where the bound vortices are unswept at the centre section, as *e.g.* for a plane wing at an angle of incidence, the following modification to equation (25) has been suggested in Ref. 2:

$$w(\xi, y) = \frac{1}{4\pi\cos\phi_v(y)}\int_0^1 l(\xi', y)\frac{d\xi'}{\xi - \xi'} + \frac{\tan(\lambda(y)\phi)}{4\cos\phi_v(y)}l(\xi, y) + \alpha_{i0}(y), \tag{26}$$

with

$$\cos\phi_v(y) = \frac{\cos\phi}{\cos(\lambda(y)\phi)}. \tag{27}$$

This relation implies that the term w_{2D} is derived from a system of vortices with a sweep angle ϕ_v.

As stated in the introduction, we have chosen four load distributions, (1) to (4) (*see* Table 1), and have computed for these the approximate downwash from equation (25). For the load distributions (1) and (2), which involve an elliptic spanwise variation of C_L, $\alpha_{i0} = \pi/2A$; for the load distributions (3) and (4), a formula for $\alpha_{i0}(\eta)$ is derived in the Appendix.

3.2. Discussion of Results for the Rectangular Wings

For the four load distributions considered in this Report, the values of the twodimensional contribution $w_{2D}(x, y)$ and values of $\alpha_{i0}(y)$ are quoted in Table 1, so that for the rectangular planform the values of $w(x, y)$ according to the approximate equation (23) is known. The exact values of $w(x, y)$ computed from equation (21) are given in Table 2.

We may mention that, for the rectangular planform and the load distributions (1) and (2), Ray and Miller[9] have computed values of the downwash by a more accurate method than the Sells program, the agreement between the results of the two methods is excellent except very close to the tip.

In Fig. 8, we have plotted some exact downwash distributions together with the corresponding approximate distributions. We learn from Fig. 8a that, for the load distribution (1), the difference between the approximate and the exact downwash over the inner part of the wing, $|\eta| \leqslant 0{\cdot}5$, is at most 7 per cent of the local downwash, but at the outboard station $\eta = 0{\cdot}9$, the maximum difference increases to 23 per cent. For the load distribution (3), the corresponding values are 4 per cent and 29 per cent.

We note from Fig. 8b that, for the load distributions (2) and (4), the difference between the exact and the approximate downwash is again small over the inner wing and larger on the outer wing. The exact downwash is zero at certain points of the wing so that we cannot express the difference as a percentage of the exact value.

The aim of a threedimensional wing theory is to estimate the threedimensional effects, *i.e.* the difference between the downwash on the finite wing and the local twodimensional downwash. For a general wing, the latter is the downwash of an infinite sheared wing with the sweep and the chordwise load distribution of the spanwise station under consideration. In the following we therefore examine the difference between the downwash on the wing, $w(x, y)$, and the twodimensional value, $w_{2D}(x, y)$. When we examine the error in the threedimensional effect, *i.e.* the term $w - w_{2D} - \alpha_{i0}$, then we have of course to remember that the error in the actual pressure distribution on the wing caused by the error of the camber shape is related to $w - w_{2D} - \alpha_{i0}$ measured in terms of w and not in terms of $w - w_{2D}$. In Fig. 9, we have plotted the ratio between the difference $w(x, y) - w_{2D}(x, y)$ and $\alpha_{i0}(y)$. In the Standard Method this ratio is taken as equal to one. We note that near the centre of pressure of the load distributions ($x_{CP} = 0{\cdot}25$ for the distributions (1) and (3), $x_{CP} = 0{\cdot}5$ for the distributions (2) and (4)) the approximate results are close to the exact results. The chordwise distributions of $(w(x, y) - w_{2D}(x, y))/\alpha_{i0}(y)$ for the load distributions (1) and (3) (and for the distributions (2) and (4)) are surprisingly similar even though the spanwise distributions of α_{i0} for the load distributions (3) and (4) (some values of α_{i0} are quoted in Fig. 8 and in Table 1) differ a great deal from the constant value of α_{i0} which corresponds to the distributions (1) and (2).

Since the downwash upstream of the wing tends to zero and downstream tends to $2\alpha_{i0}$, it is to be expected that the term $w(x, y) - w_{2D}(x, y)$ increases along the chord. The chordwise variation of $(w(x, y) - w_{2D}(x, y))/\alpha_{i0}(y)$ is stronger on the outboard part of the wing than on the inboard part. To explain this, we consider a single bound vortex at $x = 0{\cdot}25$, $-s < y < s$ of strength $\Gamma(y)$. The related trailing vortex sheet induces at x, y the downwash

$$w(x, y) = w(x = 0{\cdot}25, y) + \frac{1}{4\pi}\int_{-s}^{s} \frac{\partial\Gamma}{\partial y'} \frac{(x - 0{\cdot}25)\, dy'}{(y - y')\sqrt{(x - 0{\cdot}25)^2 + (y - y')^2}}. \tag{28}$$

Values of $2w(x, y)/w(x = \infty, y)$ are plotted in Fig. 10 for the elliptic distribution $\Gamma(y) = \sqrt{s^2 - y^2}$ and for the distribution $\Gamma(y) = \text{const}$. We note the similarity of the curves for the two rather different distributions of $\Gamma(y)$.

For the load distribution (1) (or (2)) where the chordwise distribution is of the same type across the span, we can use the results derived for an isolated bound vortex (equation (28) and Fig. 10) and determine by integration with respect to x the value of the downwash, w_{STRV}, induced by the streamwise vorticity component related to $l(x, y)$. For the load distribution (1) and $\eta = 0{\cdot}5$ and $\eta = 0{\cdot}9$, we have found that $|w - w_{2D} - w_{STRV}|$ is less than 0·05, whilst $w - w_{2D} - \alpha_{i0} = 0{\cdot}21$ for $\eta = 0{\cdot}9$ and $\xi = 1$. These results and the general similarity between the curves of Fig. 10 and those of Fig. 9 suggest that, for the load distributions considered, the difference between the exact downwash and the downwash computed by the approximate equation (23) is due mainly to an inaccurate approximation of the part of the downwash which is induced by the chordwise vorticity and is due less to an inaccurate approximation of the part of the downwash which is induced by the spanwise vorticity. The figures suggest that for a rectangular wing we may improve the Standard Method by modifying the term which is related to the chordwise vorticity by taking instead of $\alpha_{i0}(\eta)$ a term of the form

$$\alpha_{i0}(\eta)[1 + f(\eta; A)g(x)],$$

so that equation (23) would be replaced by the approximation

$$w(x, y) = w_{2D}(x, y) + \alpha_{i0}(y)[1 + f(\eta, A)g(x)]. \tag{29}$$

Even though a comparison of Figs. 9a and 9b shows that the function $(w - w_{2D})/\alpha_{i0}$ is somewhat dependent on the type of chordwise load distribution, one may expect that, with the same function $g(x)$, equation (29) would

give an improvement on equation (23). Such an improvement was demonstrated by Sells,[10] when he solved the inverse problem of calculating the load distribution of a rectangular wing of given shape. Sells has used for $g(x)$ the function

$$g(x) = -0{\cdot}5 + 2{\cdot}5x - x^2. \tag{30}$$

One can expect some benefit from varying the function $f(\eta, A)$ with the aspect ratio A of the wing. Sells[10] has suggested the function

$$f(\eta, A) = \frac{1}{1 + A(1 - |\eta|)}. \tag{31}$$

Some further guidance for the variation of $f(\eta, A)$ may be obtained from the distribution of $2w(x, y)/w(x = \infty, y)$ given by equation (28) for the distribution $\Gamma(y) = \text{const.}$; this reads

$$\frac{2w(x, y)}{w(x = \infty, y)} = 1 + \frac{1 + \eta}{2} \frac{(x - x_{CP})/s}{\sqrt{\left(\frac{x - x_{CP}}{s}\right)^2 + (1 - \eta)^2}} + \frac{1 - \eta}{2} \frac{(x - x_{CP})/s}{\sqrt{\left(\frac{x - x_{CP}}{s}\right)^2 + (1 + \eta)^2}}. \tag{32}$$

We have mentioned above that the values of $w - w_{2D}$ differ somewhat from those for w_{STRV}. This is of course due to the fact that the spanwise vortices are not infinitely long and that their strength varies along the span. We have to remember that the results discussed refer only to load distributions where the chordwise distributions are of the same type across the span. For load distributions where the type of chordwise distribution varies fairly rapidly along the span, we may expect that the twodimensional downwash is not such a good approximation to the downwash from the spanwise vortices.

3.3. Discussion of the Downwash Distribution on the 45 degree Swept Wings

For the swept wings, some exact downwash distributions are plotted in Fig. 11 (*see* also Table 3) together with the approximate results from equations (25) and (24). If we compare Fig. 11 with the corresponding figure for the unswept wing, Fig. 8, then we note that the approximate method represents the sweep effect over the inner wing fairly well.

To examine the threedimensional effects in more detail, we have again plotted the difference $w(\xi, y) - w_{2D}(\xi, y)$, *see* Figs. 12 to 14, where for a spanwise station y

$$w_{2D}(\xi; y; 0) = \frac{1}{4\pi \cos \phi} \int_0^1 l(\xi'; y) \frac{d\xi'}{\xi - \xi'} \tag{33}$$

is the downwash of an infinite sheared wing with the sweep angle ϕ and a load distribution which is uniform across the span and varies chordwise as the distribution $l(\xi; y)$ of the station considered.

Fig. 12 shows that, for the inboard part of the wing, the additional downwash for the swept wing is larger than for the unswept wing and that the mean value is fairly well predicted by the approximate method; but the chordwise distribution of the additional downwash is not so well represented.

The difference between the exact and the approximate values for $w - w_{2D}$, at the inboard station $\eta = 0{\cdot}1$, *i.e.* $y/c = 0{\cdot}3$, Fig. 12, shows a strong resemblance to the corresponding term for the wing of infinite aspect ratio, *see* Figs. 5 and 1. We have therefore determined the difference

$$\begin{aligned} F(\xi, \eta) &= (w - w_{2D})_{A=6} - \frac{C_L(y, A = 6)}{C_L(A = \infty)} (w - w_{2D})_{A=\infty} \\ &= w(\xi, y; A = 6) - \frac{C_L(y; A = 6)}{C_L(A = \infty)} w(\xi, y; A = \infty), \end{aligned} \tag{34}$$

i.e. the difference between the downwash on the finite wing and the downwash on a swept wing of infinite aspect ratio with uniform load distribution across the span which is the same as the chordwise load distribution of the finite wing at the spanwise station η under consideration. For the unswept wing the function $F(\xi, \eta)$ is,

of course, the same as $w - w_{2D}$. We have plotted some values of the function $F(\xi, \eta) = w - w(A = \infty)$ in Fig. 15. According to the approximate method, the values of the function $F(\xi, \eta)$ for the inboard part of the wing, $0 < |y| < 0{\cdot}5$, are expected to be approximately equal to $\alpha_{i0}(\eta)$, both for the swept wings and the unswept wings. We have therefore plotted in Fig. 16 values of the ratio between $F(\xi, \eta)$ and $\alpha_{i0}(\eta)$.

Let us consider first the results for the inner part of the swept wings with the load distributions (3) and (4), plotted in Figs. 15a and 16. We note that the values of the function $F(\xi, \eta) = w - w(A = \infty)$ for $\phi = 45$ degrees are much smaller than α_{i0}, in contrast to the values for $\phi = 0$, shown in Fig. 9. For $|\eta| \leqslant 0{\cdot}5$, the ratio between the values of $F(\xi, \eta; \phi = 45$ degrees) and those of $F(\xi, \eta; \phi = 0)$ varies between 0·31 and 0·38.

The fact that the values of F for $\phi = 45$ degrees are consistently smaller than those for $\phi = 0$ is mainly due to the fact that on the swept wing the trailing vortices are staggered (*i.e.* they start at different x-values). This does not affect the downwash far downstream, *i.e.* $w(x = \infty, y) = 2\alpha_{i0}(y)$, but it has an effect on the downwash at the wing. To demonstrate this, we have determined the downwash from the trailing vortices which originate from one swept bound vortex at $\xi = 0{\cdot}25$, $-s < y < s$ of strength $\Gamma(y)$. In Fig. 17, we have plotted $2w(\xi, \eta)/w(\xi = \infty, y)$ for the two cases $\Gamma(y) = \sqrt{s^2 - y^2}$ and $\Gamma(y) = \text{const.}$ For $\eta = 0{\cdot}5$, we have added the curves from Fig. 10 for the unswept bound vortex. A comparison of the corresponding curves in Figs. 10 and 17 shows that the trailing vortices produce a smaller downwash on the swept wing than on the unswept wing. For the constant $\Gamma(y)$ distribution, the ratio between the values of $w(\xi, \eta)$ for $\phi = 45$ degrees and $\phi = 0$ is about 0·3 for $\eta = 0$ and 0·4 for $\eta = 0{\cdot}5$. These values thus explain the dependence of the function $F(\xi, \eta; \phi)$ on the angle of sweep for the load distributions (3) and (4). The curves in Fig. 17, for $\Gamma(y) = \text{const.}$, suggest also that, as for the unswept wing, the downwash from the chordwise vortices increases with ξ and with $|\eta|$ (*see* also Table 1 for $\alpha_{i0}(\eta)$).

We consider now the values of the function $F(\xi, \eta)$ for the load distributions (1) and (2). The trailing vortex sheet which originates from a single swept bound vortex with the load distribution $\Gamma(y) = \sqrt{1 - \eta^2}$ produces near $\xi = 0{\cdot}25$ an upwash which is logarithmically infinite at $\xi = 0{\cdot}25$. This infinity disappears, of course, when we deal with a chordwise distribution of bound vortices. When we consider a chordwise distribution of bound vortices for which the strength varies as $\sqrt{(1 - \xi)/\xi}$ and use the values of $2w(\xi, \eta)/w(\xi = \infty, \eta)$ given in Fig. 17 for $\Gamma(y) = \sqrt{1 - \eta^2}$, then we can compute values of that part of the downwash which is produced by the streamwise vorticity (the chordwise and trailing vortices), w_{STRV}, of the load distribution (1). Some values of w_{STRV} are plotted in Fig. 18.

Before we discuss the results given in Fig. 18, let us draw some general conclusions from Fig. 17. We have mentioned already that the trailing vortex sheet which originates from a single swept bound vortex of strength $\Gamma(y) = \sqrt{1 - \eta^2}$ produces an upwash near $\xi = 0{\cdot}25$ (the position of the bound vortex), the magnitude of which increases with the angle of sweep and with increasing values of $|\eta|$. This fact has several consequences with respect to the downwash w_{STRV} from the streamwise vorticity of the load distributions (1) and (2): (i) the reduction in the downwash from the streamwise vortices due to the sweep of the spanwise vortices is larger for the elliptic spanwise load distribution than for the constant spanwise distribution, (ii) for the elliptic spanwise load distribution, the variation of the downwash w_{STRV} with ξ is stronger for the swept wing than for the unswept wing, (iii) for the elliptic spanwise load distribution and larger values of η, an upwash is produced at the values of ξ where the strength of the spanwise vortices is large, which does not happen for the constant spanwise load distribution (for $\xi > 0{\cdot}6$ say, the downwash of the trailing vortices originating from a single bound vortex increases with $|\eta|$ and this effect reduces to some degree the effect of the increasing magnitude of the upwash with increasing $|\eta|$). The dependence of the downwash from the streamwise vorticity, w_{STRV}, on the angle of sweep and the type of load distribution explains to a large degree the variation of the function $F(\xi, \eta) = w - w(A = \infty)$ with ξ and η, with the angle of sweep and with the type of load distribution.

Fig. 18 shows that the values of $F(\xi, \eta)$ and w_{STRV} differ somewhat and that the difference increases with the angle of sweep and with $|\eta|$. This difference is produced by the spanwise decrease of the strength of the spanwise vortices. We note that, for the swept wing with load distribution (1), the spanwise variation of the spanwise vortices produces an upwash. To explain this, we compare, at a point ξ, η, the load distribution of a section normal to the leading edge with the chordwise distribution at $\eta = \text{const.}$ and find that the values of γ forward of the point considered are reduced and those rearward are increased. The twodimensional downwash related to the load distribution of the section normal to the leading edge is smaller than the downwash for the load distribution of the section $|\eta| = \text{const.}$ For wings of given aspect ratio, this effect becomes larger with increasing values of ϕ.

In the Standard Method, the tip of a swept wing is treated as if it had an effect on the downwash similar to that of the centre of a swept forward wing. Some justification for this may be derived from Fig. 15 where it is shown that the behaviour of $F(\xi, \eta)$ on the outboard part of the wing is somewhat similar to that of $w - w_{2D}$ for swept forward wings of infinite aspect ratio with the centre section at the tip of the finite wing, *see* Fig. 4.

In the Standard Method, no explicit account is taken of the fact that the downwash at the wing, induced by the streamwise vortices, depends on the angle of sweep. Thus, for a swept wing and an unswept wing with the same load distribution $l(\xi, \eta)$, the total downwash is expected to differ by $(1/\cos\phi - 1)w_{2D}(\xi, \eta; \phi = 0)$ and a term proportional to the local load $l(\xi, \eta)$; for a wing of constant chord, the Standard Method assumes that the factor to $l(\xi, \eta)$ in the second term changes sign at mid semispan, $\eta = 0{\cdot}5$.

To show how far the latter term does arise in practice, and how it varies along the span, we have plotted in Fig. 19 the term

$$k(\xi, \eta) = [w(\xi, \eta) - w_{2D}(\xi, \eta)]_{\phi=45^\circ} - [w(\xi, \eta) - w_{2D}(\xi, \eta)]_{\phi=0}. \tag{35}$$

The figure shows that the distribution of $k(\xi, \eta)$ over the outer wing is similar to that on the inner wing with the sign reversed. We are not surprised that the chordwise distribution of $k(\xi, \eta)$ does not resemble strongly the distribution of $l(\xi, \eta)$. For the part of the wing near the centre section, the term $k(\xi, \eta)$ is mainly produced by the central kink of the spanwise vortices and we have seen in Figs. 1 and 5, for the wing with infinite aspect ratio, that, at least for $\eta \neq 0$, the term $w - w_{2D}$ does not vary as strongly along the chord as the load distribution, $l(\xi, \eta)$.

Finally, we have plotted in Fig. 20 the mean value

$$\bar{k}(\eta) = \int_0^1 k(\xi, \eta)\, d\xi$$

$$= \Delta\alpha(\eta; \phi) - \Delta\alpha(\eta; \phi = 0), \tag{36}$$

derived from the exact values of w together with the approximate term from equation (25), $\tan(\lambda(y)\phi)C_L(\eta)/4\cos\phi$. We may note that for the present examples the approximate value of $\bar{k}$ at the centre section has the value $k(\eta = 0) = 2{\cdot}1$; the exact value (derived from the downwash in $z = 0$) is logarithmically infinite. Fig. 20 shows that over the inner part of the wing the exact value of $\bar{k}$ varies in a way similar to the approximate curve; the similarity is stronger for the load distribution (3) than for the load distribution (1). We have mentioned above, *see* Fig. 17, that, by ignoring the fact that the trailing vortices are staggered, the approximate method derives for the swept wing too large a downwash from the trailing vortices. This error is partly cancelled, at least over the inner wing, by the fact that the approximate downwash equation (12) produces for the spanwise vortices a smaller value of $\Delta\alpha$ than the downwash from equation (9), *see* Fig. 7. The use of the exact equation (9) for the spanwise vortices with the approximate value $\alpha_{i0}(\eta)$ for the downwash from the trailing vortices would thus increase the error in $\bar{k}(\eta)$, at least for the calculated examples.

4. The Load Distribution on Uncambered Wings at an Angle of Incidence

4.1. A Modified Approximate Downwash Equation

The Standard Method deals also with the task of determining the load distribution on a wing of given shape, in particular with the task of determining the spanwise C_L distribution. The method is based on equation (26). We have seen for the wing of infinite aspect ratio with uniform spanwise load distribution that the downwash given by the approximate equation (12) differs appreciably from the exact values, in particular near the trailing edge. We know that in inviscid flow the slope of the wing near the trailing edge is decisive in determining the circulation past a section. We would, therefore, like to assess the importance of this difference. In the following, we want to examine how the C_L distribution derived by Küchemann's method would change if we were to use instead of equation (12) a different downwash equation.

We therefore retain Küchemann's approach and approximate the downwash, produced by the spanwise vorticity of a load distribution which varies along the span, by the downwash produced by a distribution which is constant along the span and has the same chordwise distribution as the varying distribution has at the station considered.

A procedure of similar simplicity to Küchemann's method can be obtained from an approximation of the form:

$$w(\xi, y, 0) = \frac{1}{2\pi}\int_0^1 \gamma(\xi', y)\frac{d\xi'}{\xi - \xi'} + f(y, \phi)\gamma(\xi, y) + [g(y, \phi) - (\xi - \xi_{CP})h(y, \phi)]\int_0^1 \gamma(\xi', y)\, d\xi', \tag{37}$$

where the functions $f(y, \phi)$, $g(y, \phi)$, $h(y, \phi)$ do not depend on ξ. Equation (37) is an approximation to the values of the downwash given by equation (9). A possible set of values for the functions f, g, h have been derived from the exact values of w, computed for $\gamma = 2\sqrt{(1 - \xi)/\xi}$ and $\gamma = 8\sqrt{\xi(1 - \xi)}$ for $y/c \geq 0{\cdot}1$. These values have

been extrapolated to $y = 0$. Some values are given in Table 4. A comparison of the approximate values for the downwash from equation (37) with the exact ones and with the values from equation (12) (which corresponds to $f(y, \phi) = \frac{1}{2}\tan(\lambda(y)\phi)$, $g \equiv 0, h \equiv 0$) is made in Fig. 5. Equation (37) can still give a poor approximation near the leading edge; for the first Birnbaum distribution, the exact $w(\xi, y \neq 0, 0)$ is finite for $\xi = 0$ whilst equation (37) gives an infinite value. To improve the approximation, we would at least have to substitute for $f(y, \phi)$ a function which depends also on ξ. With given downwash, the equation for the unknown $\gamma(\xi, y)$ would still be of the type studied by Carleman,[11] so that a solution in closed form could be obtained. But this procedure would be too complex for the present purpose.

4.2. Solution of the Approximate Downwash Equation (37) for Constant Downwash along the Chord

With the aim of determining the load distribution of an uncambered swept wing at an angle of incidence, we want to derive a solution of the downwash equation (37) for the case when $w(\xi, y, 0)$ is independent of ξ.

When $f(y, \phi)$ does not depend on ξ, then equation (37) is of the form

$$\frac{1}{2\pi}\int_0^1 \gamma(\xi')\frac{d\xi'}{\xi - \xi'} + \tfrac{1}{2}\tan\phi^*\gamma(\xi) = F(\xi) \tag{38}$$

where ϕ^* is defined by $\frac{1}{2}\tan\phi^* = f(y, \phi)$ and

$$F(\xi) = w(\xi, y, 0) - [g - (\xi - \xi_{CP})h]\int_0^1 \gamma(\xi', y)\,d\xi'.$$

The solution of this equation, for which the Kutta condition at $\xi = 1$ is satisfied, reads (*see* equations (3.4), (3.6), (3.10) of Ref. 12):

$$\gamma(\xi) = 2\sin\phi^*\cos\phi^* F(\xi) - 2\cos^2\phi^*\left(\frac{1-\xi}{\xi}\right)^{n^*}\frac{1}{\pi}\int_0^1 F(\xi')\left(\frac{\xi'}{1-\xi'}\right)^{n^*}\frac{d\xi'}{\xi - \xi'} \tag{39}$$

with

$$n^* = \tfrac{1}{2}\left(1 - \frac{\phi^*}{\pi/2}\right). \tag{40}$$

For $F(\xi) = A + B\xi$ (which implies that w is also linear in ξ), the solution is

$$\gamma(\xi) = 2[A + B(\xi + n^*)]\cos\phi^*\left(\frac{1-\xi}{\xi}\right)^{n^*}. \tag{41}$$

For this

$$\int_0^1 \gamma(\xi)\,d\xi = [2A + B(1 + n^*)]n^*\pi \tag{42}$$

and

$$\int_0^1 \xi\gamma(\xi)\,d\xi = [A + B\tfrac{2}{3}(1 + n^*)]n^*(1 - n^*)\pi \tag{43}$$

so that

$$\xi_{CP} = \frac{\int_0^1 \xi\gamma(\xi)\,d\xi}{\int_0^1 \gamma(\xi)\,d\xi} = \frac{1 - n^*}{2}\,\frac{A + B2\dfrac{1 + n^*}{3}}{A + B\dfrac{1 + n^*}{2}}. \tag{44}$$

When $w(\xi, y, 0) = 1$, then we obtain from equations (37) to (44):

$$A = 1 - [g + \xi_{CP}h] \int_0^1 \gamma(\xi)\, d\xi$$
$$= 1 - g[2A + B(1 + n^*)]n^*\pi - h[A + B\tfrac{2}{3}(1 + n^*)]n^*(1 - n^*)\pi,$$

and

$$B = h \int_0^1 \gamma(\xi)\, d\xi$$
$$= h[2A + B(1 + n^*)]n^*\pi.$$

From these equations we obtain

$$A = \frac{1 - (1 + n^*)n^*h\pi}{1 + 2n^*g\pi - 2n^{*2}h\pi[1 - \frac{1}{6}(1 - n^{*2})h\pi]} \tag{45}$$

and

$$B = \frac{2n^*h\pi}{1 + 2n^*g\pi - 2n^{*2}h\pi[1 - \frac{1}{6}(1 - n^{*2})h\pi]}. \tag{46}$$

When we insert equations (45) and (46) into equations (42) and (44) then we obtain the relations:

$$\int_0^1 \gamma(\xi)\, d\xi = \frac{2n^*\pi}{1 + 2n^*g\pi - 2n^{*2}h\pi[1 - \frac{1}{6}(1 - n^{*2})h\pi]} \tag{47}$$

and

$$\xi_{CP} = \frac{1 - n^*}{2}[1 + \tfrac{1}{3}n^*(1 + n^*)h\pi]. \tag{48}$$

With the values of f, πg and πh quoted in Table 4, we have evaluated n^*, from equation (40) with $\phi^* = \tan^{-1} 2f$, and calculated $\int_0^1 \gamma(\xi, y; \phi)\, d\xi$ and $\xi_{CP}(y; \phi)$. Some results are plotted in Figs. 21 to 23. It should be pointed out that the ratio $\int_0^1 \xi\gamma(\xi)\, d\xi / \int_0^1 \gamma(\xi)\, d\xi$ is the same as the centre of pressure if the sweep angle of the vorticity vector is constant along the chord. In the following, we shall make this assumption. For the particular case which we consider, when $w(\xi, \eta, 0) = 1$, which represents a plane wing at an angle of incidence, the centre of pressure is also the aerodynamic centre. We have, therefore, plotted the values from equation (48) as values for the position of the aerodynamic centre.

We have also plotted in Figs. 21 to 23 the values from equation (12), *i.e.*

$$\frac{1}{\pi} \int_0^1 \gamma_K(\xi)\, d\xi = 2n(y) = 1 - \lambda(y)\frac{\phi}{\pi/2} \tag{49}$$

and

$$(\xi_{ac})_K = \frac{1 - n(y)}{2} = \frac{1}{4}\left[1 + \lambda(y)\frac{\phi}{\pi/2}\right]. \tag{50}$$

Figs. 21 and 22 show that with increasing y the term $1/\pi \int_0^1 \gamma(\xi, y)\, d\xi$ approaches the value of unity for the sheared wing at a slower rate when equation (37) is used than when the downwash equation (12) is used, this is the case whether $\lambda(y)$ is obtained from equation (14) or from equation (18). For $\phi = 45$ degrees and $y > 1$ we obtain from equation (37),

$$\frac{1}{\pi} \int_0^1 \gamma(\xi, y)\, d\xi = 1 - \frac{1}{8y} + 0\left(\frac{1}{y^2}\right) \tag{51}$$

and from equations (12) and (14)

$$\frac{1}{\pi}\int_0^1 \gamma(\xi, y)\, d\xi = 1 - \frac{1}{32y} + 0\left(\frac{1}{y^2}\right). \tag{52}$$

Fig. 23 shows that the chordwise centre of the vorticity distribution $\gamma(\xi, y)$ approaches the value of the sheared wing at a faster rate when $\gamma(\xi, y)$ is derived from equation (37) than when it is derived from equation (12).

To obtain from the vorticity distribution $\gamma(\xi, y)$ the load distribution $l(\xi, y)$, we use the same approximate procedure as Küchemann and approximate the angle of sweep of the vorticity vector by a value $\phi_v(y)$ which is taken as constant along the chord. Küchemann's suggestion for ϕ_v, equation (27), was to be an approximation to the sweep of the curve of the aerodynamic-centre position. The use of a function $\phi_v(y)$ constant along the chord is only a crude approximation; therefore, Küchemann has suggested the use of the simpler expression given in equation (27) instead of ϕ_v derived from the aerodynamic-centre position. A crude relation between $\gamma(\xi, \eta)$ and $l(\xi, \eta)$ seems justified for the present purpose, where we want only to explain, in Section 4.3, some differences in the spanwise C_L distribution computed by the Standard Method and a more exact method. We do not intend to derive here a general improvement to the Standard Method, because the results of Section 3.3 suggest that it is not likely that, for a general load distribution, one can devise a simple method for determining a reasonably accurate approximation to the downwash from the chordwise and trailing vortices.

Using the approximate relation

$$l(\xi, y) = \cos \phi_v(y) 2\gamma(\xi, y), \tag{53}$$

we obtain for the lift coefficient $C_L(y)$ the relation

$$C_L(y) = 2 \cos \phi_v(y) \int_0^1 \gamma(\xi, y)\, d\xi.$$

$\gamma(\xi)$ in equation (47) has been derived for the special case $w(\xi, y) = \alpha_e(y) = 1$. Thus we obtain for the sectional lift slope

$$a(y) = \frac{C_L(y)}{\alpha_e(y)} = \frac{4n^*(y)\pi \cos \phi_v(y)}{1 + 2n^* g(y)\pi - 2n^{*2} h(y)\pi[1 - \frac{1}{6}(1 - n^{*2})h\pi]}. \tag{54}$$

For the infinite sheared wing (for which $n^* = 0{\cdot}5$, $g = h = 0$, $\phi_v = \phi$) equation (54) gives the well-known result

$$a_\infty = 2\pi \cos \phi. \tag{55}$$

If we were to use the aerodynamic-centre position to determine $\cos \phi_v(y)$, then we would find that the downwash equation (37) leads (for $y > 0{\cdot}1$) to slightly smaller values of $\cos \phi_v$ than equation (12). In the following, we use with both downwash equations the same function for $\cos \phi_v / \cos \phi$, namely the one used in the Standard Method, $1/\cos(\lambda\phi)$, with $\lambda(y)$ from equation (18); this means that for the values of $a(y)/a_\infty$ we somewhat moderate the difference between the two downwash equations.

Values of a/a_∞ derived from the downwash equation (37) are plotted in Fig. 24 together with the values of the Standard Method, $2n/\sin \pi n$. The curve derived from equation (37) has not been extrapolated to $y = 0$, because the procedure of this Report cannot give reliable values for $y = 0$, since the downwash equation (37) is derived from values in $z = 0$ for vortices of constant strength and sweep angle for which the downwash in $y = 0$, $z = 0$ is infinite. We shall examine in the next section how important the difference of the values for a/a_∞ may be when one computes the spanwise C_L distribution.

4.3. The Spanwise Lift Distribution of an Uncambered 45 degree Swept Wing of Infinite Span at an Angle of Incidence; Comparison of Various Results

The case considered in this section differs from the one of the previous section in that we have to include also the effect of trailing vorticity.

Hui[6] has determined the load distribution for an uncambered 45 degree sweptback wing of infinite aspect ratio at an angle of incidence by solving the integral equation of lifting-surface theory, equation (21), by an

iteration procedure. Values of the lift coefficient $C_L(y)$, obtained by Hui, are plotted in Fig. 25. We have also plotted the values obtained by Küchemann (taken from Fig. 14 of Ref. 5). We notice that Hui's values are everywhere lower than Küchemann's values. We are here not interested in the differences in the values near $y = 0$, where it is known that Hui's values are not reliable, but we are interested in the values at $y > 1$ say.

There existed some uncertainty about the accuracy of Hui's results, since he has satisfied the boundary condition at relatively few spanwise stations on the outer wing. To determine the accuracy we have used Sells' program[3] and have calculated for a load distribution, similar to Hui's, the downwash at certain spanwise stations. For this purpose, we have taken the computed values of $l(\xi, y)$, $C_L(y)$, $\xi_{ac}(y)$, kindly given to us by Hui. We have found that it is possible to approximate Hui's values of $l(\xi, y)$ (except for $y = 0$) by

$$l(\xi, y) = \frac{4}{\pi} C_L(y) \left[(1 - 2\xi_{ac}) \sqrt{\frac{1 - \xi}{\xi}} + 2(4\xi_{ac} - 1)\sqrt{\xi(1 - \xi)} \right] + f(y)F(\xi), \tag{56}$$

where

$$\int_0^1 F(\xi)\, d\xi = 0$$

and

$$\int_0^1 \xi F(\xi)\, d\xi = 0.$$

Based on Hui's results, we have determined numerical values for the functions $f(y)$ and $F(\xi)$, modified Hui's values for $C_L(y)$, as shown by curve II in Fig. 25, and similarly derived smooth values for $\xi_{ac}(y)$. With these smooth values of $l(\xi, y)$, we have computed by Sells' program[3] the downwash at the spanwise stations $y = 1, 2, 3$. (For these calculations we have used equation (56) also for the neighbourhood of the centre section, because we wanted to ensure that the derivatives of $l(\xi, y)$ are smooth functions and a local error in $l(\xi, y)$ has no important effect on the downwash sufficiently far away.) The results, plotted in Fig. 26, suggest that the values of C_L, given by curve II of Fig. 25, for $y \geqslant 1$ say, are correct to about 1 per cent and, therefore, that the values from the Standard Method are too high.

Part of this error is probably a consequence of the difference between the values of the sectional lift slope derived from the original downwash equation, (12), and from the modified equation, (37), shown in Fig. 24.

We have added in Fig. 25 the values of a/a_∞ derived from equation (37). To examine whether the difference between C_L/C_{L_∞} and a/a_∞, for $y > 1$, can be explained by the downwash induced by the chordwise and trailing vortices, we have derived approximate values for w_{STRV}. For this purpose, we have computed the downwash produced by a trailing vortex sheet starting from one bound vortex at $x = |y| \tan \phi$, $-\infty < y < \infty$ of strength

$$\Gamma(y) = \Gamma_\infty C_L(y)/C_{L_\infty} = \pi \cos \phi C_L(y)/C_{L_\infty}$$

with $C_L(y)/C_{L_\infty}$ given by curve II of Fig. 25. The chordwise distribution of the downwash for the spanwise stations $y = 1{\cdot}5$ and $y = 3$ is plotted in Fig. 27. The figure shows that $\alpha_{i0}(y) = \frac{1}{2}w(\xi = \infty, y)$ is an underestimate for the downwash from the trailing vortices. To derive an approximate value for the downwash from the streamwise vorticity of the load distribution $l(\xi, y)$ of equation (56), we have considered a chordwise distribution of bound vortices of strength $\Gamma(y)(2/\pi)\sqrt{(1 - \xi)/\xi}$ (the fact that we have ignored the difference between $l(\xi, y)$ from equation (56) and $(2/\pi)C_L(y)\sqrt{(1 - \xi)/\xi}$ implies of course that the related downwash is in error for small values of y). Approximate values for the downwash from the streamwise vortices are given in Fig. 28; we quote also values of $\alpha_{i0}(y)$ and values for the difference between a/a_∞ and C_L/C_{L_∞}. We note that the magnitude of w_{STRV} is comparable to the values of $a/a_\infty - C_L/C_{L_\infty}$. (The agreement is somewhat improved, if we take account of the fact that the total downwash computed for the load distribution of equation (56) differs somewhat from one, *see* Fig. 26.)

4.4. The Spanwise Lift Distribution of Finite Wings

The wing of infinite span is a rather special case, so that it is difficult to draw a conclusion about the error in $C_L(y)$ for the plane swept wing of finite span from the results for the wing of infinite span. This is due to the different systems of trailing vortices; the trailing vortices on the finite wing are, at least for most of the outer

part of the wing, of opposite sign and of greater strength than those for the wing with infinite span. The effect of ignoring the stagger of the trailing vortices varies with the aspect ratio of the wing and the spanwise station considered. We can, therefore, not expect to obtain a generally applicable estimate about the error in the C_L distribution derived by the Standard Method.

In the present Report, we examine only the C_L distribution of the plane wings of constant chord and aspect ratio 6 at an angle of incidence. The fact that we do not yet have a solution for the thin lifting swept wing, which is correct at the centre section and close to the tip, need not be too important for the present purpose.

Using an approximation to the load distribution by a vortex lattice, Carr–Hill (unpublished work) has written a computer program for determining an approximation to the load distribution of a wing of given shape. Sells (unpublished work) has used this program and has derived a first approximation $l^{(1)}(x, y)$ to the load distribution of a plane wing of constant chord, aspect ratio 6, swept by 45 degrees. Using his computer program,[3] Sells has then computed the downwash related to $l^{(1)}(x, y)$ and thus derived values for the error in the downwash, $\Delta w(x. y)$, at the control stations. By means of the Carr–Hill program, a modification of $l^{(1)}(x, y)$ can be found and the accuracy of $l^{(2)}(x, y) = l^{(1)}(x, y) + \Delta l(x, y)$ can be checked by computing the downwash. Sells has used various arrangements of the chordwise and spanwise control stations. He found that two steps of the iteration were sufficient to produce the spanwise distributions of the lift coefficient and the chordwise position of the aerodynamic centre within an accuracy sufficient for the present purpose. (The various symbols in Figs. 30 and 31 refer to different arrangements of control stations; one particular symbol refers to one set of control stations.)

We have already mentioned in Section 3.2 that, for wings of rectangular planform, Sells[10] has written a program to derive the load distribution for a wing of given shape, where he uses also an iterative method but with a different technique for determining an approximate load distribution for a given downwash distribution. For a plane rectangular wing of aspect ratio 6, the spanwise C_L distribution is given in Ref. 10.

In Figs. 29 and 30, we compare the results obtained by Sells with those from the Standard Method. Fig. 29 demonstrates the known fact that the Standard Method gives, for the unswept wing, values of C_L which are everywhere too high.

For the special case of a plane rectangular wing, Brebner[13] has shown that one can interpret the change in chordwise load distribution near the tip as becoming similar to that on wings of small aspect ratio. When the sectional lift slope, a, is locally modified, the Standard Method produces a C_L distribution which is close to the exact one.

We can derive the 'small-aspect-ratio effect' from the modified downwash equation (29). If we were to use equation (29) with

$$g(x) = a + bx + cx^2, \tag{57}$$

then we would obtain for the plane rectangular wing at an angle of incidence, $\alpha = 1$, the load distribution

$$l(x, y) = 4\sqrt{\frac{1-x}{x}}[1 - \alpha_{i0}(y) - \alpha_{i0} f(y)(a + \tfrac{1}{2}b + \tfrac{3}{8}c)] - 4\sqrt{x(1-x)}\alpha_{i0} f(b + \tfrac{1}{2}c) - 4x\sqrt{x(1-x)}\alpha_{i0} fc \tag{58}$$

with

$$C_L = 2\pi[1 - \alpha_{i0} - \alpha_{i0} f(a + \tfrac{3}{4}b + \tfrac{5}{8}c)], \tag{59}$$

$$x_{ac} = \frac{1}{4}\left[1 - \frac{\alpha_{i0} f(\frac{1}{4}b + \frac{5}{16}c)}{1 - \alpha_{i0} - \alpha_{i0} f(a + \frac{3}{4}b + \frac{5}{8}c)}\right], \tag{60}$$

where

$$\alpha_{i0}(y) = \frac{1}{8\pi}\int_{-s}^{s} \frac{dC_L(y')}{dy'}\frac{dy'}{y - y'}$$

differs, of course, from the α_{i0} derived with $f(y) \equiv 0$. For the function $g(x)$ given by equation (30) we obtain

$$x_{ac} = \frac{1}{4}\left[1 - \frac{\frac{5}{16}\alpha_{i0} f}{1 - \alpha_{i0}(1 + \frac{3}{4}f)}\right]. \tag{61}$$

This means that the aerodynamic centre is forward of the quarter chord similar to the position on a wing of small aspect ratio.

For a wing of 45 degree sweep, $A = 6$, Fig. 30 shows that the Standard Method gives an overestimate of the lift over the inboard part of the wing and an underestimate over the outboard part of the wing. The difference between the approximate and the exact values of the lift coefficient over the inner part of the span is somewhat similar to that shown in Fig. 25 for the wing of infinite aspect ratio. The fact that the Standard Method produces too low values for the lift coefficient over the outer part of the span can be explained by the fact (*see* for example Figs. 16 and 17) that the Standard Method assumes too large a contribution to the downwash from the trailing vortices of a swept wing. For the plane wing at an angle of incidence, the trailing vortices near the centre section may be of opposite sign to those on the outer wing, but their strength is so small that we can expect that ignoring the stagger of the trailing vortices produces too large a downwash, *i.e.* too small values of C_L for most of the span. It seems that one cannot generally improve matters by using instead of $\alpha_{i0}(y)$ (or $2n\alpha_{i0}(y)$ as in Ref. 2) the term $2n(y)\alpha_{i0}(y)$ (as suggested in Ref. 1) since this would still further increase the downwash from the streamwise vorticity near the wing tips.

It is also doubtful whether one obtains for a wing of given shape an improved estimate of the $C_L(y)$ distribution if one replaces the sectional lift slope of the Standard Method by the term derived from the modified downwash equation (37) (*i.e.* from equations (54), (27), (18); *see* Fig. 24), because the error in $a(y)$ has generally, at least inboards, an effect of opposite sign to the error in the downwash from the chordwise and trailing vortices. For the outer part of the wing, it is certainly not worthwhile to introduce a better estimate for the sectional lift slope of a swept forward wing without an improvement in the estimate of the downwash from the trailing vortices.

To examine how well the Standard Method estimates the type of chordwise load distribution, we have plotted in Fig. 31 the chordwise position of the aerodynamic centre, $\xi_{ac}(y)$, derived by the Standard Method and the values derived from the load distributions $l^{(2)}(x, y)$, computed by Sells. The agreement is good for the inner part of the span. For the outer part of the span, the aerodynamic centre is further forward than for the central part of a swept forward wing of infinite aspect ratio (which corresponds to the estimate of the Standard Method). This means a 'small-aspect-ratio effect' is again present near the tips of a swept wing, similar to the one mentioned above for the rectangular wing.

When we modify the sectional lift slope $a(y)$ near the tips of a swept wing to represent the small-aspect-ratio effect, then, on the outer wing, the difference between the exact $C_L(y)$ and the approximate $C_L(y)$ is larger than without the modification, as shown in Fig. 30, in contrast to the beneficial effect of the modification for an unswept wing shown in Fig. 29. The discrepancy is of course affected by the poor estimate of the downwash from the chordwise and trailing vortices for a swept wing. This means again that we should refrain from modifying the sectional lift slope of the Standard Method without improving the estimate of the downwash from the trailing vortices.

With the aim of giving some further examples for the magnitude of the possible error in the C_L values derived by the Standard Method, we have considered the warped wings discussed in Section 3. We have determined the $\Delta C_L(y)$ distributions of the wings which have the warp $z(x, y)$ for which

$$-\frac{\partial z(x, y)}{\partial x} = \Delta w(x, y)$$

$$= w_{\text{exact}}(x, y) - w_{\text{approx}}(x, y) \tag{62}$$

with w_{approx} given by equation (25).

For determining the $\Delta C_L(y)$ distributions we have used the approximate method, *i.e.* equation (25). (We have used equation (25) and not equation (26), *i.e.* used $\phi_v = \phi$ because the load distributions (1) to (4) are such that at the centre section $\phi_v = \phi$.) The unknown load distribution $\Delta l(\xi, y)$ is written as the sum of two terms

$$\Delta l(\xi, y) = \Delta l_I(\xi, y) + \Delta l_{II}(\xi, y). \tag{63}$$

The first term is the solution of the equation for the 'bound' (spanwise) vorticity (*see* equations (7) and (12)):

$$\frac{1}{4\pi \cos \phi} \int_0^1 \Delta l_I(\xi', y) \frac{d\xi'}{\xi - \xi'} + \frac{\tan(\lambda(y)\phi)}{4 \cos \phi} \Delta l_I(\xi, y) = \Delta w(\xi, y) \tag{64}$$

with $\lambda(y)$ from equation (24). The solution of this equation is known, *see* equations (38) and (39). Using the relation

$$\int_0^1 \left(\frac{1-x'}{x'}\right)^n \frac{dx'}{x-x'} = \frac{\pi}{\sin \pi n} - \frac{\pi}{\tan \pi n}\left(\frac{1-x}{x}\right)^n, \tag{65}$$

it is found that the lift coefficient related to Δl_I is

$$\Delta C_{L_I}(y) = 4 \cos \phi \cos \lambda\phi \int_0^1 \Delta w(\xi, y)\left(\frac{\xi}{1-\xi}\right)^{n(y)} d\xi \tag{66}$$

with

$$n(y) = \frac{1}{2}\left[1 - \frac{\lambda(y)\phi}{\pi/2}\right]. \tag{67}$$

$\Delta l_{II}(\xi, y)$ is the load distribution which satisfies equation (12) for $w_K(\xi, y) = -\Delta\alpha_{i0}(y)$. Using the relation

$$\int_0^1 \left(\frac{1-x}{x}\right)^n dx = \frac{n\pi}{\sin n\pi}, \tag{68}$$

it is found that the lift coefficient related to $\Delta l_{II}(\xi, y)$ is

$$\Delta C_{L_{II}}(y) = -\Delta\alpha_{i0}(y) 4\pi n(y) \cos \phi, \tag{69}$$

where $\Delta\alpha_{i0}$ is related to the lift coefficient

$$\Delta C_L(y) = \Delta C_{L_I}(y) + \Delta C_{L_{II}}(y) \tag{70}$$

by equation (20). To obtain $\Delta C_L(y)$ we have thus to solve the equation

$$\Delta C_L(y) = \Delta C_{L_I}(y) - 4\pi n(y) \cos \phi \frac{1}{8\pi} \int_{-s}^{s} \frac{d\Delta C_L(y')}{dy'} \frac{dy'}{y-y'}. \tag{71}$$

(This equation differs somewhat from the corresponding relations of Ref. 2, (i) because we have ignored the effect of finite aspect ratio on $n(y)$, *i.e.* the difference between $n_0(y)$ and $n(y)$ of Ref. 2; (ii) because we have used equation (25) instead of equation (26). If we were to use equation (26) then ΔC_{L_I} and $\Delta C_{L_{II}}$ from equations (66) and (69) would be multiplied by $\cos \phi_v(y)/\cos \phi = \cos(\lambda\phi)$. The factor $\cos(\lambda\phi)$ is nearly one except close to the centre section and the tip.) Equation (71) has been solved by Multhopp's method (*see, e.g.* paragraph VIII.19 of Ref. 14).

Values of $\Delta C_{L_I}(y)/2\pi$ are plotted in Fig. 32 for the rectangular wings of Section 3.2 and in Fig. 33 for the swept wings of Section 3.3; we have divided ΔC_{L_I} by 2π since $C_L(\eta = 0) = 2\pi$ for the basic wings. To obtain values of ΔC_{L_I} close to the tip of the rectangular wings, we have used the exact values of $w(x, y)$ at $\eta = 0{\cdot}95$ and $\eta = 1$ given in Ref. 9 for the load distributions (1) and (2). For the load distributions (3) and (4), we have refrained from extrapolating ΔC_{L_I} towards the tip because we have an insufficient number of values and because ΔC_{L_I} varies so rapidly on the outer wing, due to the rapid variation of the basic C_L distribution. For the swept wings and load distributions (1) and (2), we have extrapolated ΔC_{L_I} towards $\eta = 0$ and $\eta = 1$, as shown in Fig. 33. (We have not chosen the logarithmically infinite value at $\eta = 0$ which would correspond to the infinite values of $w_{exact}(\xi, \eta = 0, z = 0)$ and $\Delta w(\xi, \eta = 0)$, because such infinite values would not arise for practical wings of given shape.)

The values of $\Delta C_L(\eta)$, computed from equation (71), are also plotted in Figs. 32 and 33.

Fig. 32 shows that, if we were to compute by the Standard Method the load distribution of the rectangular wing which has the exact downwash related to the load distributions (1) or (2), then we would obtain values of $C_L(\eta)$ which are everywhere too high. The error is thus of the same sign as for the plane wing at an angle of incidence, *see* Fig. 29. For the cambered wings, the error varies less across the span than for the plane wing; the maximum value of $\Delta C_L(\eta)/C_L(\eta = 0)$ is largest for the plane wing where it is about 0·08 near $\eta = 0{\cdot}9$.

For swept cambered wings, the C_L values derived by the Standard Method are too low for most of the wing, as is also the case for the plane wing at an angle of incidence, compare Figs. 30 and 33. The magnitude of the error over the outer wing is larger for the cambered wings; this feature depends of course on the type of spanwise loading.

5. Conclusion

The comparisons made in this Report between the downwash computed by the Standard Method and results from exact linear theory suggest that the Standard Method represents the effects of sweep and finite aspect ratio qualitatively fairly well, but that it does not give the details with sufficient accuracy. We have not been able to suggest a modification of the simple procedure of the Standard Method except for the design of the inboard part of such wings, where the effect of the chordwise and trailing vortices is relatively small.

In the preliminary stages of designing a swept wing, the Standard Method is thus useful for understanding the effects of changing the shape of a wing and for finding major errors in more elaborate computer programs; in the later stages, it seems essential to compute the downwash produced by a given load distribution by a more accurate procedure, for example by Sells' program.[3]

LIST OF SYMBOLS

A	Aspect ratio
c	Wing chord, taken as unity
s	Semispan
x, y, z	Rectangular coordinate system, z-axis normal to wing plane
ξ	$= x - \lvert y \rvert \tan \phi$
ξ_{ac}	Position of aerodynamic centre
ξ_{CP}	Position of centre of pressure
η	$= y/s$
V_0	Velocity of free stream, taken as unity
v_z	Component of perturbation velocity parallel to z-axis, positive upwards
w	$= - v_z$, downwash
w_{2D}	Downwash in twodimensional flow
$w_{STR\ V}$	Downwash induced by streamwise vorticity
$\alpha_{i0}(y)$	$= \frac{1}{2} w(x = \infty, y, z = 0)$
$\Delta\alpha$	*See* equation (16)
ϕ	Leading-edge sweep
ϕ_v	Angle of sweep of bound vortices
$l(x, y)$	$= - \Delta C_p(x, y)$, coefficient of pressure difference across the wing
$C_L(y)$	Local lift coefficient
ΔC_{L_I}	*See* Section 4.4, equation (66)
ΔC_L	*See* Section 4.4, equations (69) and (70)
a	Sectional lift slope
a_∞	Lift slope of infinite sheared wing
γ	Local strength of spanwise vorticity
Γ	Circulation
$n(y)$	$= \frac{1}{2}\left[1 - \lambda(y)\frac{\phi}{\pi/2}\right]$
$\lambda(y)$	Interpolation function, *see* equations (12), (14) and (18)
$F(\xi, \eta)$	*See* equation (34), difference between the downwash of a finite swept wing and of a swept wing of infinite aspect ratio with uniform load distribution across the span and with the same chordwise load distribution as at the spanwise station y of the finite wing
$k(\xi, \eta)$	*See* equation (35)
$\bar{k}(\eta)$	$= \int_0^1 k(\xi, \eta)\, d\xi$

REFERENCES

No.	*Author(s)*	*Title, etc.*
1	.. ..	Method for predicting the pressure distribution on swept wings with subsonic attached flow. Roy. Aero. Soc., Transonic Data Memorandum 6312 (1963).
2	D. Küchemann	A simple method for calculating the span and chordwise loading on straight and swept wings of any given aspect ratio at subsonic speeds. A.R.C., R. & M. 2935 (1952).
3	C. C. L. Sells	Calculation of the induced velocity field on and off the wing plane for a swept wing with given load distribution. A.R.C., R. & M. 3725 (1970).
4	J. A. Ledger	Computation of the velocity field induced by a planar source distribution, approximating a symmetrical non-lifting wing in subsonic flow. R.A.E. Technical Report 72176 A.R.C. 34383 (1972).
5	D. Küchemann	A simple method for calculating the span and chordwise loadings on thin swept wings. R.A.E. Report Aero 2392 A.R.C. 13758 (1950).
6	W. H. Hui	A new approach to subsonic lifting surface theory. A.R.C. 33067; F.M. 4243, January, 1970.
7	J. Weber	The shape of the centre part of a swept-back wing with a required load distribution. A.R.C., R. & M. 3098 (1957).
8	G. G. Brebner	The application of camber and twist to swept wings in incompressible flow. A.R.C., C.P. 171 (1952).
9	V. A. Ray and G. F. Miller	Numerical evaluation of the downwash integral for a lifting rectangular planform. N.P.L. Report Maths 90 (1970).
10	C. C. L. Sells	An iterative method for calculation of the loading on a thin unswept wing. A.R.C., R. & M. 3719 (1972).
11	T. Carleman	Sur la résolution de certaines équations intégrales. Arkiv för Matematik, Astronomi och Fysik, *16* (1922).
12	J. Weber	The calculation of the pressure distribution on the surface of thick cambered wings and the design of wings with given pressure distribution. A.R.C., R. & M. 3026 (1955).
13	G. G. Brebner, L. A. Wyatt and G. P. Ilott	Low speed wing tunnel tests on a series of rectangular wings of varying aspect ratio and aerofoil section. A.R.C., C.P. 916 (1965).
14	B. Thwaites	*Incompressible aerodynamics.* Oxford, Clarendon Press (1960).

APPENDIX

Induced Incidence for the Load Distributions (3) and (4) of Table 1

The induced incidence $\alpha_{i0}(y)$ is according to equation (20) given by

$$\alpha_{i0}(y) = \frac{1}{8\pi}\int_{-s}^{s} \frac{dC_L(y')c(y')}{dy'}\frac{dy'}{y-y'}.$$

For a wing of constant chord:

$$\alpha_{i0}(\eta) = \frac{1}{4\pi A}\int_{-1}^{+1} \frac{dC_L(\eta')}{d\eta'}\frac{d\eta'}{\eta-\eta'}. \tag{A-1}$$

For the load distributions (3) and (4) of Table 1

$$C_L = 2\pi \quad \text{for } 0 < |\eta| < 0{\cdot}8$$

$$C_L = 2\pi\sqrt{1-\left(\frac{|\eta|-0{\cdot}8}{0{\cdot}2}\right)^2}$$

$$= 10\pi\sqrt{-\eta^2+1{\cdot}6|\eta|-0{\cdot}6} \quad \text{for } 0{\cdot}8 < |\eta| < 1. \tag{A-2}$$

From equations (A-1) and (A-2) we obtain

$$\alpha_{i0}(\eta) = \frac{5}{2A}\int_{0{\cdot}8}^{1}\left[2-\frac{\eta+0{\cdot}8}{\eta+\eta'}-\frac{\eta-0{\cdot}8}{\eta-\eta'}\right]\frac{d\eta'}{\sqrt{-\eta'^2+1{\cdot}6\eta'-0{\cdot}6}}.$$

Evaluation of the integral gives for $|\eta| < 0{\cdot}6$:

$$\alpha_{i0}(\eta) = \frac{5}{2A}\left\{\pi - \frac{0{\cdot}8+\eta}{\sqrt{\eta^2+1{\cdot}6\eta+0{\cdot}6}}\left[\frac{\pi}{2}-\sin^{-1}\frac{0{\cdot}2}{0{\cdot}8+\eta}\right] - \right.$$
$$\left. - \frac{0{\cdot}8-\eta}{\sqrt{\eta^2-1{\cdot}6\eta+0{\cdot}6}}\left[\frac{\pi}{2}-\sin^{-1}\frac{0{\cdot}2}{0{\cdot}8-\eta}\right]\right\}$$

for $0{\cdot}6 < |\eta| < 1$:

$$\alpha_{i0}(\eta) = \frac{5}{2A}\left\{\pi - \frac{0{\cdot}8+\eta}{\sqrt{\eta^2+1{\cdot}6\eta+0{\cdot}6}}\left[\frac{\pi}{2}-\sin^{-1}\frac{0{\cdot}2}{0{\cdot}8+\eta}\right] + \right.$$
$$\left. + \frac{0{\cdot}8-\eta}{\sqrt{-\eta^2+1{\cdot}6\eta-0{\cdot}6}}\log\frac{|0{\cdot}8-\eta|}{0{\cdot}2+\sqrt{-\eta^2+1{\cdot}6\eta-0{\cdot}6}}\right\}.$$

For $A = 6$, values of $\alpha_{i0}(\eta)$ have been computed and are tabulated in Table 1.

TABLE 1

Load Distributions Considered

(1) $l(x, y) = 4\sqrt{\dfrac{1-\xi}{\xi}}\sqrt{1-\eta^2}$

$w_{2D} = \dfrac{\sqrt{1-\eta^2}}{\cos\phi}$

$\alpha_{i0} = \dfrac{\pi}{2A} = 0{\cdot}262$

(2) $l(x, y) = 16\sqrt{\xi(1-\xi)}\sqrt{1-\eta^2}$

$w_{2D} = \dfrac{2(2\xi-1)\sqrt{1-\eta^2}}{\cos\phi}$

$\alpha_{i0} = 0{\cdot}262$

(3) $l(x, y) = 4\sqrt{\dfrac{1-\xi}{\xi}}$ for $0 \leqslant |\eta| < 0{\cdot}8$

$l(x, y) = 4\sqrt{\dfrac{1-\xi}{\xi}}\sqrt{1-\left(\dfrac{|\eta|-0{\cdot}8}{0{\cdot}2}\right)^2}$ for $|\eta| > 0{\cdot}8$

$w_{2D} = \dfrac{1}{\cos\phi}$ for $0 \leqslant |\eta| < 0{\cdot}8$

$w_{2D} = \dfrac{1}{\cos\phi}\sqrt{1-\left(\dfrac{|\eta|-0{\cdot}8}{0{\cdot}2}\right)^2}$ for $|\eta| > 0{\cdot}8$

α_{i0} = see below.

(4) $l(x, y) = 16\sqrt{\xi(1-\xi)}$ for $0 \leqslant |\eta| < 0{\cdot}8$

$l(x, y) = 16\sqrt{\xi(1-\xi)}\sqrt{1-\left(\dfrac{|\eta|-0{\cdot}8}{0{\cdot}2}\right)^2}$ for $|\eta| > 0{\cdot}8$

$w_{2D} = \dfrac{2(2\xi-1)}{\cos\phi}$ for $0 \leqslant |\eta| < 0{\cdot}8$

$w_{2D} = \dfrac{2(2\xi-1)}{\cos\phi}\sqrt{1-\left(\dfrac{|\eta|-0{\cdot}8}{0{\cdot}2}\right)^2}$ for $|\eta| > 0{\cdot}8$

α_{i0} = see below.

η	0·05	0.1	0·2	0.3	0.5	0.7	0·8	0·9
α_{i0} for (3) and (4)	0·1750	0·1765	0·1826	0·1936	0·2436	0·3880	0·7020	1·0162

TABLE 2

Downwash on Rectangular Wing Computed by Sells' Program[3]

Load distribution	η \ ξ	0	0·0381	0·1464	0·3087	0·5	0·6913	0·8536	0·9619	1
(1)	0·05	1·233	1·238	1·251	1·268	1·287	1·304	1·317	1·325	1·328
	0·1	1·229	1·234	1·247	1·265	1·284	1·301	1·314	1·322	1·324
	0·2	1·213	1·218	1·232	1·250	1·270	1·287	1·300	1·308	1·311
	0·3	1·186	1·191	1·205	1·224	1·245	1·263	1·277	1·285	1·288
	0·5	1·092	1·098	1·115	1·139	1·163	1·185	1·200	1·210	1·213
	0·7	0·925	0·934	0·959	0·992	1·027	1·055	1·075	1·086	1·089
	0·8	0·792	0·805	0·840	0·886	0·931	0·966	0·989	1·001	1·005
	0·9	0·582	0·606	0·670	0·746	0·813	0·861	0·889	0·901	0·905
(2)	0·1	−1·772	−1·622	−1·183	−0·523	0·258	1·041	1·704	2·150	2·304
	0·3	−1·694	−1·550	−1·128	−0·493	0·258	1·012	1·649	2·077	2·226
	0·5	−1·528	−1·397	−1·011	−0·430	0·258	0·949	1·533	1·924	2·060
	0·7	−1·250	−1·140	−0·816	−0·325	0·259	0·845	1·337	1·667	1·780
	0·9	−0·786	−0·715	−0·498	−0·156	0·262	0·681	1·024	1·244	1·318
(3)	0·05	1·167	1·168	1·172	1·177	1·183	1·189	1·194	1·197	1·198
	0·1	1·168	1·170	1·173	1·178	1·184	1·190	1·196	1·199	1·200
	0·2	1·174	1·175	1·179	1·185	1·191	1·198	1·204	1·207	1·209
	0·3	1·183	1·185	1·190	1·196	1·204	1·212	1·219	1·223	1·225
	0·5	1·223	1·226	1·234	1·246	1·260	1·274	1·285	1·292	1·294
	0·7	1·333	1·342	1·365	1·402	1·443	1·480	1·508	1·524	1·530
	0·9	1·484	1·567	1·783	2·051	2·295	2·474	2·582	2·634	2·648
(4)	0·05	−1·834	−1·686	−1·251	−0·599	0·172	0·944	1·599	2·040	2·193
	0·1	−1·833	−1·684	−1·250	−0·597	0·173	0·945	1·601	2·042	2·195
	0·2	−1·829	−1·679	−1·245	−0·592	0·179	0·952	1·608	2·049	2·203
	0·3	−1·821	−1·671	−1·236	−0·582	0·190	0·964	1·622	2·063	2·217
	0·5	−1·788	−1·638	−1·199	−0·540	0·238	1·018	1·681	2·126	2·280
	0·7	−1·710	−1·555	−1·104	−0·423	0·384	1·192	1·876	2·334	2·492
	0·9	−1·348	−1·191	−0·711	0·065	1·025	1·986	2·765	3·252	3·412

TABLE 3

Downwash on 45 degree Swept Wing Computed by Sells' Program[3]

Load distribution	η \ ξ	0	0·0381	0·1464	0·3087	0·5	0·6913	0·8536	0·9619	1
(1)	0·05	2·600	2·595	2·551	2·451	2·320	2·191	2·093	2·039	2·023
	0·1	2·084	2·081	2·066	2·033	1·986	1·940	1·907	1·889	1·884
	0·2	1·727	1·728	1·731	1·732	1·732	1·732	1·733	1·735	1·735
	0·3	1·543	1·547	1·557	1·572	1·589	1·605	1·619	1·628	1·631
	0·5	1·229	1·237	1·259	1·291	1·329	1·365	1·396	1·416	1·423
	0·7	0·819	0·833	0·871	0·927	0·992	1·057	1·110	1·145	1·157
	0·8	0·519	0·538	0·592	0·672	0·765	0·856	0·930	0·977	0·993
	0·9	0·046	0·081	0·179	0·323	0·483	0·625	0·732	0·796	0·817
(2)	0·1	−2·143	−1·927	−1·308	−0·398	0·647	1·672	2·542	3·132	3·338
	0·3	−2·442	−2·248	−1·678	−0·816	0·212	1·254	2·147	2·752	2·962
	0·5	−2·346	−2·173	−1·665	−0·888	0·050	1·009	1·840	2·406	2·604
	0·7	−2·051	−1·915	−1·512	−0·884	−0·108	0·704	1·420	1·914	2·088
	0·9	−1·483	−1·421	−1·216	−0·857	−0·356	0·221	0·760	1·144	1·284
(3)	0·05	2·587	2·580	2·529	2·419	2·277	2·137	2·030	1·970	1·952
	0·1	2·088	2·082	2·060	2·015	1·955	1·896	1·852	1·827	1·819
	0·2	1·786	1·784	1·775	1·760	1·743	1·726	1·713	1·705	1·703
	0·3	1·682	1·681	1·678	1·672	1·666	1·660	1·656	1·654	1·653
	0·5	1·611	1·611	1·612	1·614	1·617	1·620	1·624	1·627	1·628
	0·7	1·609	1·611	1·619	1·632	1·652	1·678	1·704	1·723	1·730
	0·9	0·912	0·991	1·212	1·533	1·886	2·193	2·413	2·541	2·582
(4)	0·05	−1·873	−1·629	−0·940	0·036	1·089	2·042	2·803	3·323	3·507
	0·1	−2·169	−1·951	−1·328	−0·416	0·627	1·646	2·509	3·093	3·297
	0·2	−2·434	−2·225	−1·621	−0·717	0·348	1·413	2·318	2·927	3·139
	0·3	−2·544	−2·335	−1·729	−0·819	0·256	1·332	2·247	2·863	3·077
	0·5	−2·624	−2·414	−1·805	−0·889	0·194	1·280	2·203	2·824	3·039
	0·7	−2·636	−2·425	−1·812	−0·887	0·208	1·309	2·250	2·884	3·104
	0·9	−2·423	−2·266	−1·776	−0·945	0·163	1·383	2·482	3·241	3·508

TABLE 4

Coefficients in Equation (37)

y \ ϕ	f			πg			πh		
	30°	45°	60°	30°	45°	60°	30°	45°	60°
0	0·22	0·3	0·42	0·5	0·75	0·9	0·2	0·3	0·5
0·05	0·141	0·162	0·17	0·44	0·65	0·76	0·181	0·275	0·42
0·1	0·083	0·090	0·075	0·39	0·57	0·645	0·162	0·25	0·35
0·15	0·053	0·050	0·034	0·345	0·50	0·545	0·145	0·226	0·29
0·2	0·035	0·030	0·016	0·315	0·44	0·465	0·125	0·205	0·24
0·3	0·017	0·011	0·004	0·260	0·355	0·350	0·099	0·160	0·165
0·4	0·009	0·004	0	0·218	0·287	0·270	0·075	0·120	0·115
0·5	0·005	0·001		0·188	0·239	0·216	0·058	0·090	0·081
0·6	0·003	0		0·163	0·204	0·180	0·045	0·068	0·058
0·8	0·001			0·129	0·155	0·135	0·029	0·042	0·035
1·0	0			0·106	0·124	0·108	0·020	0·028	0·023
1·5				0·071	0·083	0·072	0·010	0·013	0·010
2·0				0·054	0·062	0·054	0·006	0·008	0·006

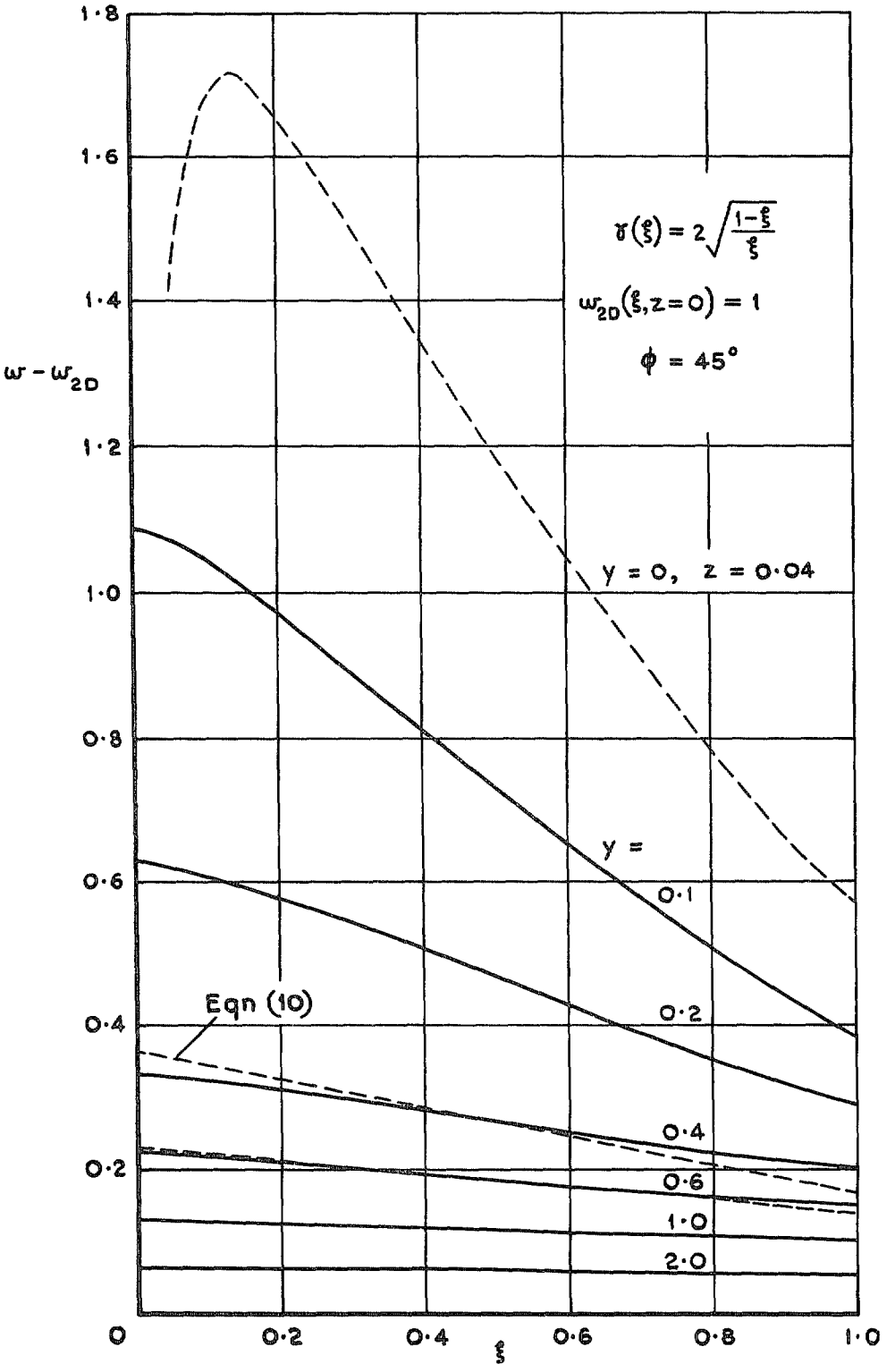

FIG. 1a. Additional downwash in $z = 0$.

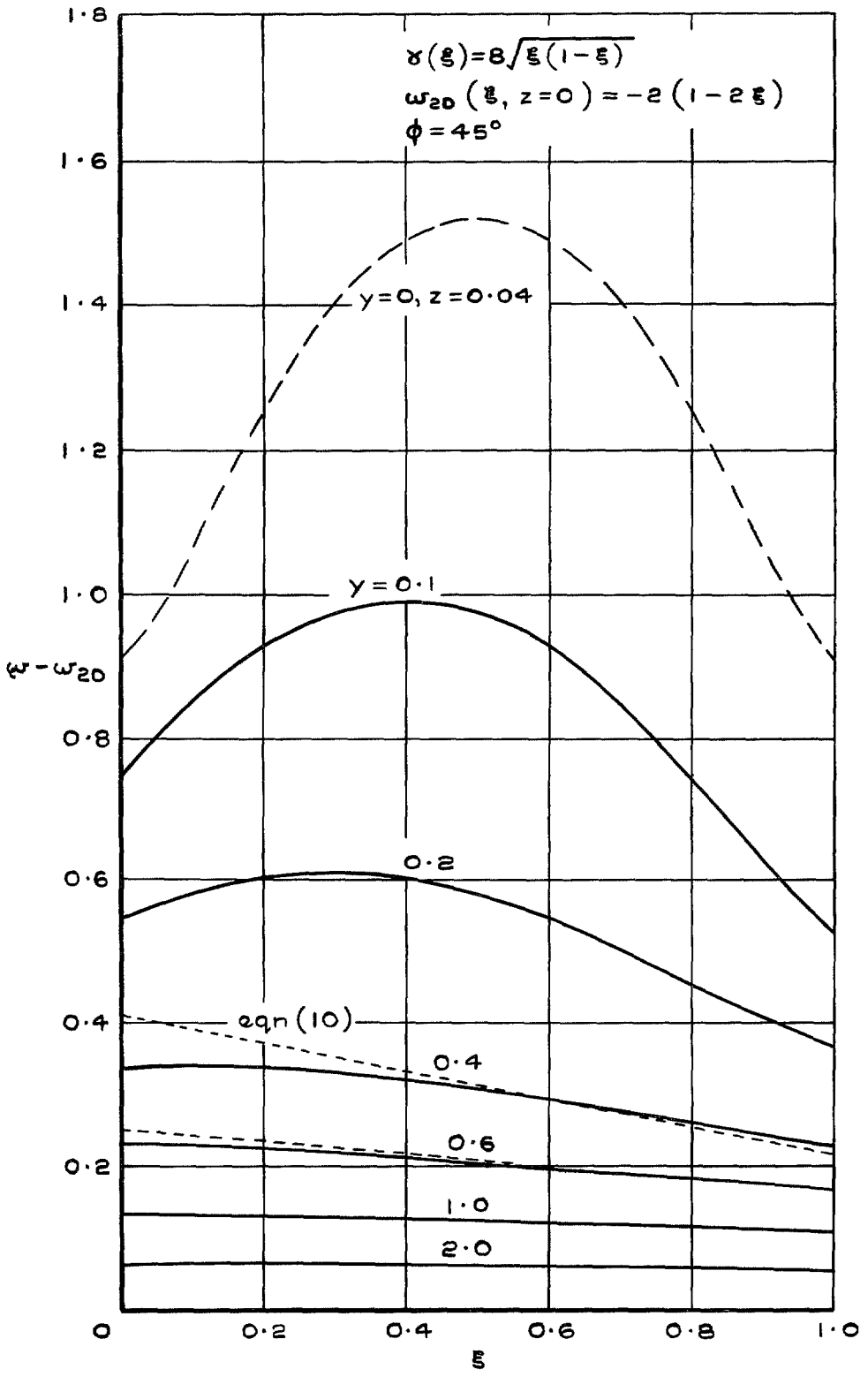

FIG. 1b. Additional downwash in $z = 0$.

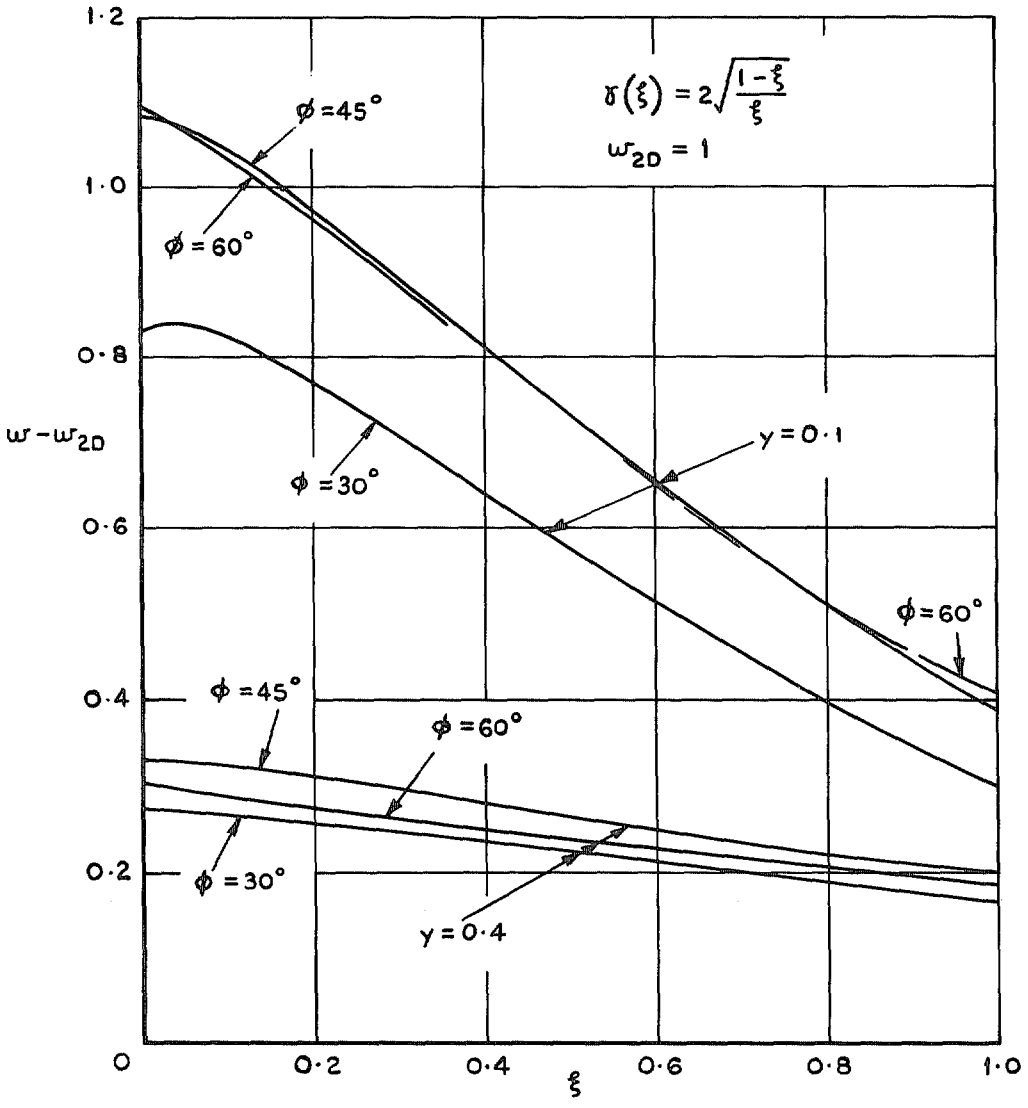

FIG. 2a. Additional downwash for various angles of sweep.

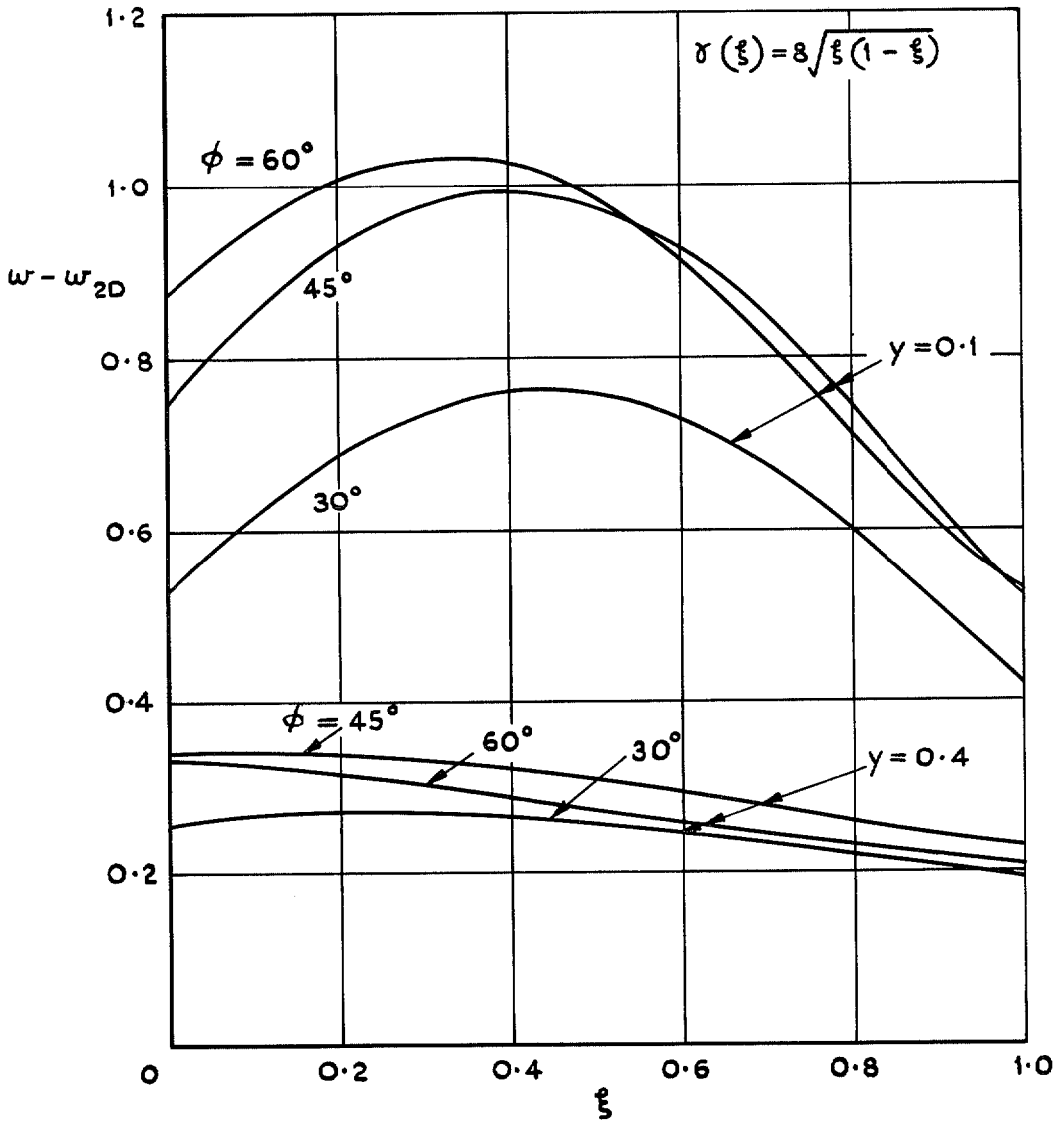

FIG. 2b. Additional downwash for various angles of sweep.

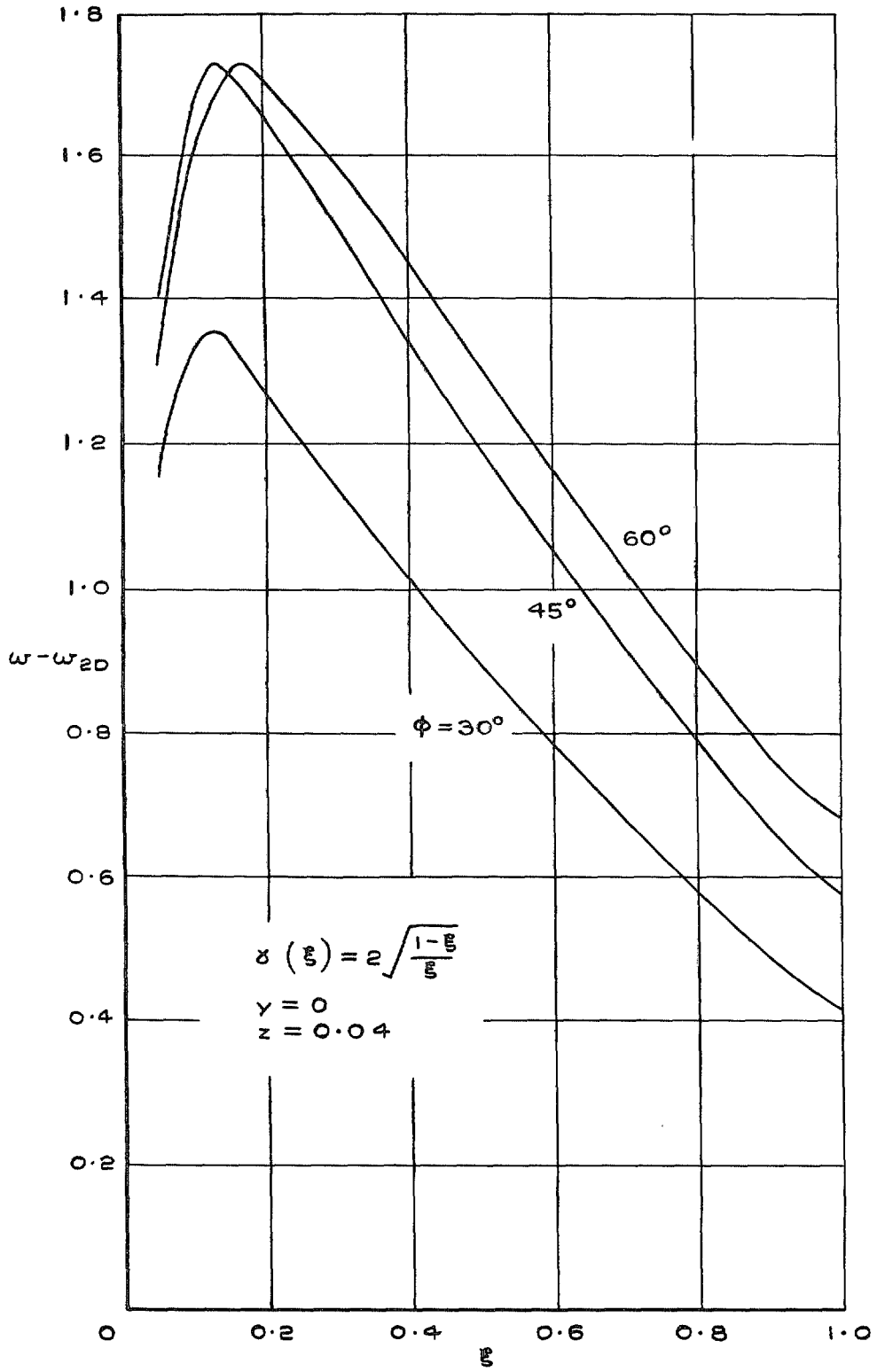

FIG. 3. Additional downwash at the centre section.

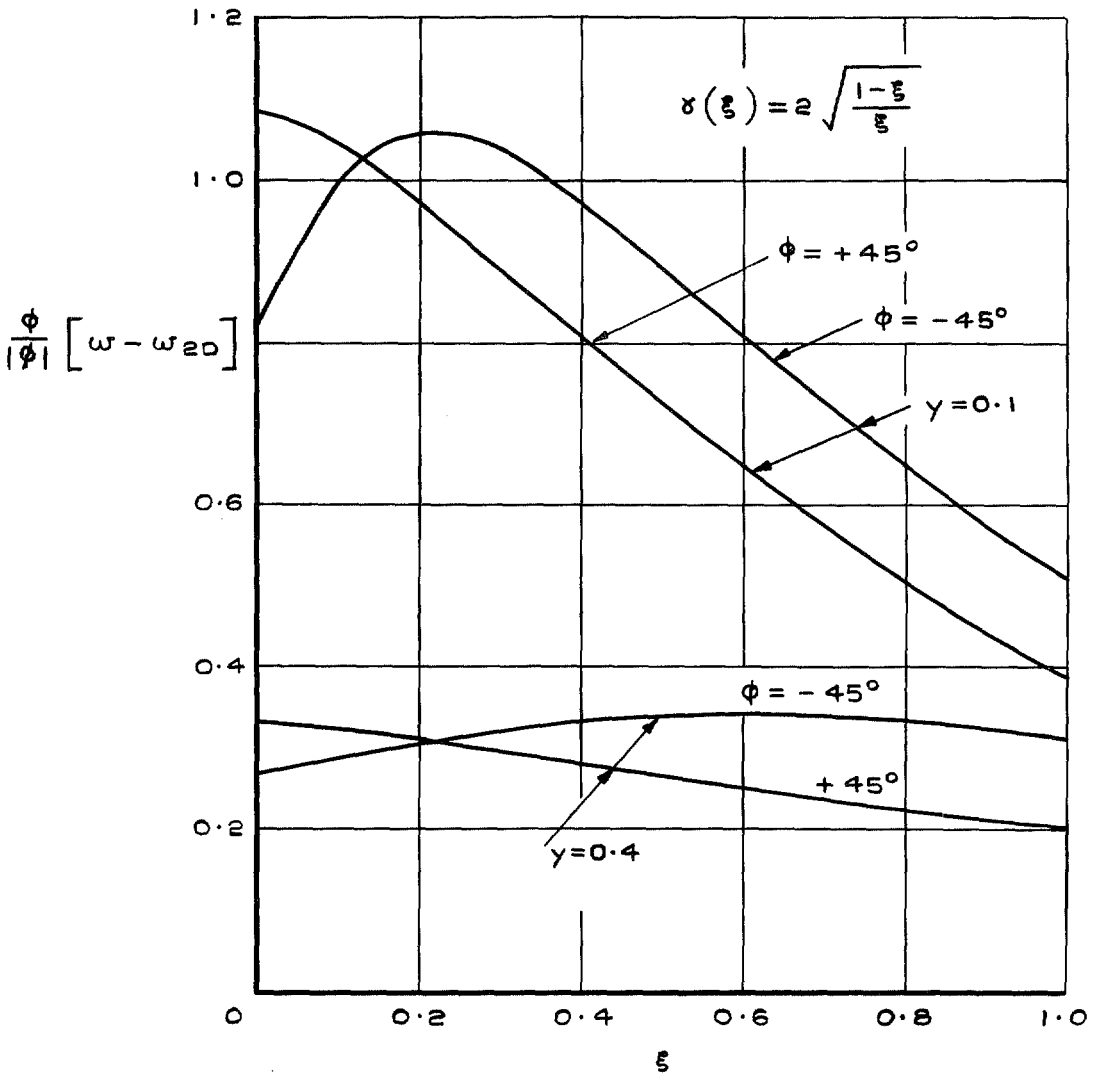

FIG. 4. Additional downwash for swept forward and swept back wings.

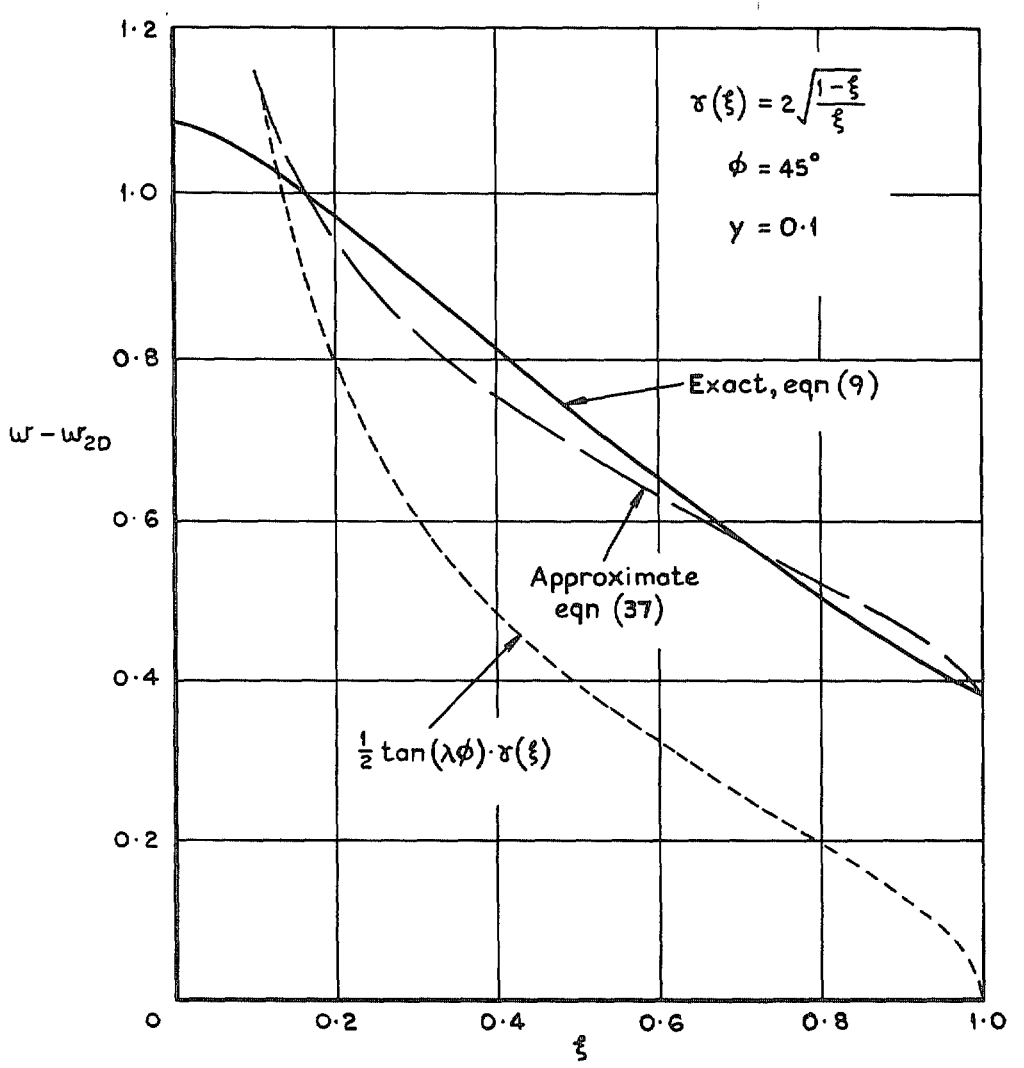

FIG. 5. Comparison of approximate values for the downwash with exact results.

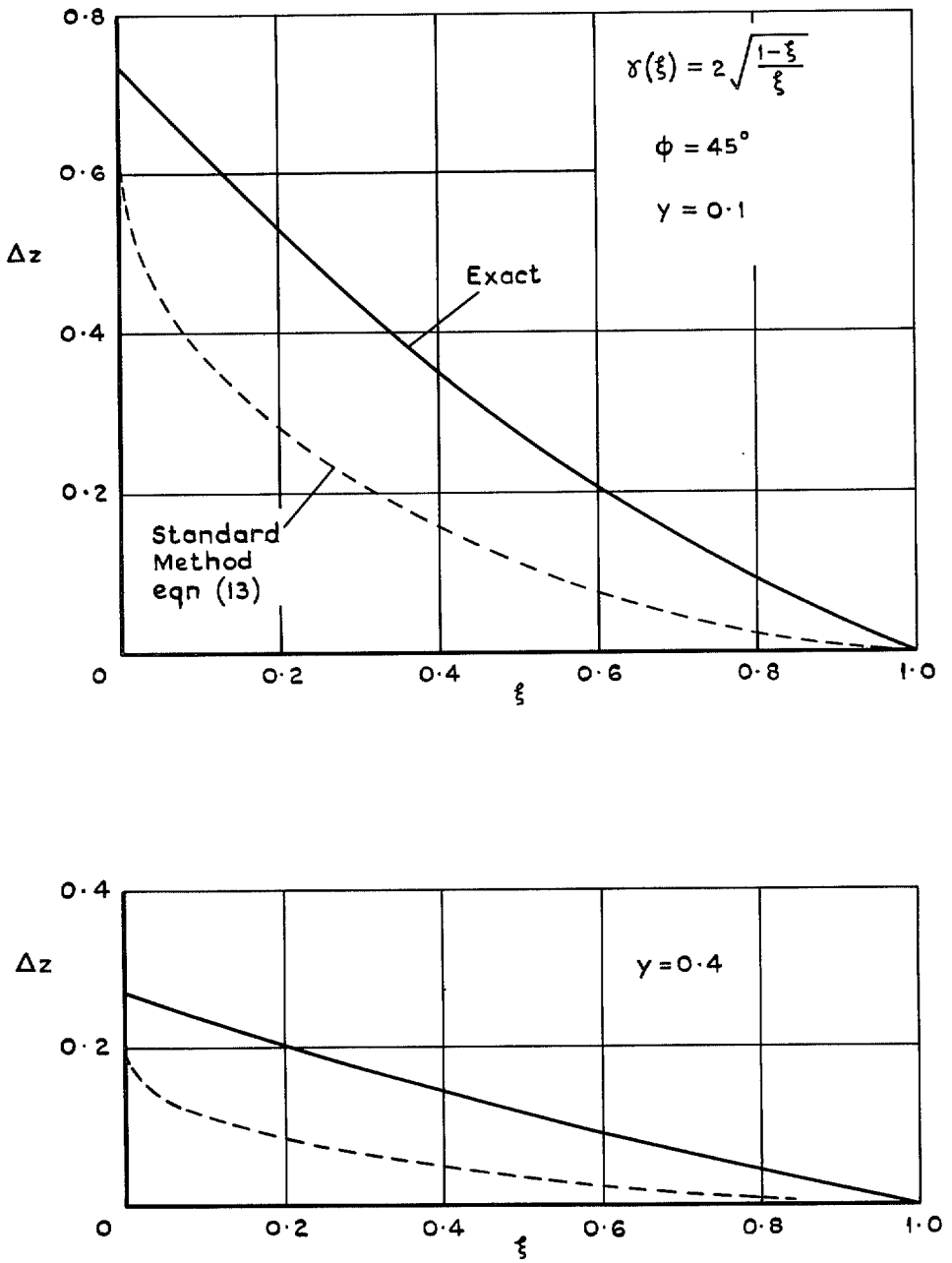

FIG. 6a. Comparison of wing shape.

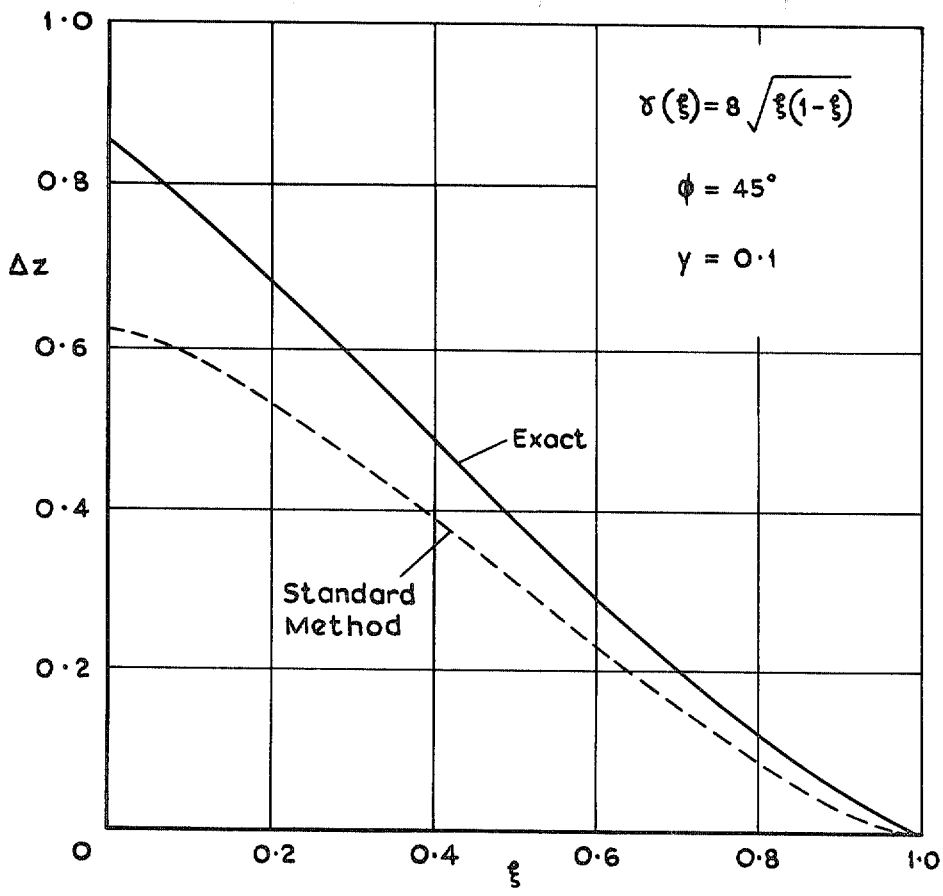

FIG. 6b. Comparison of wing shape.

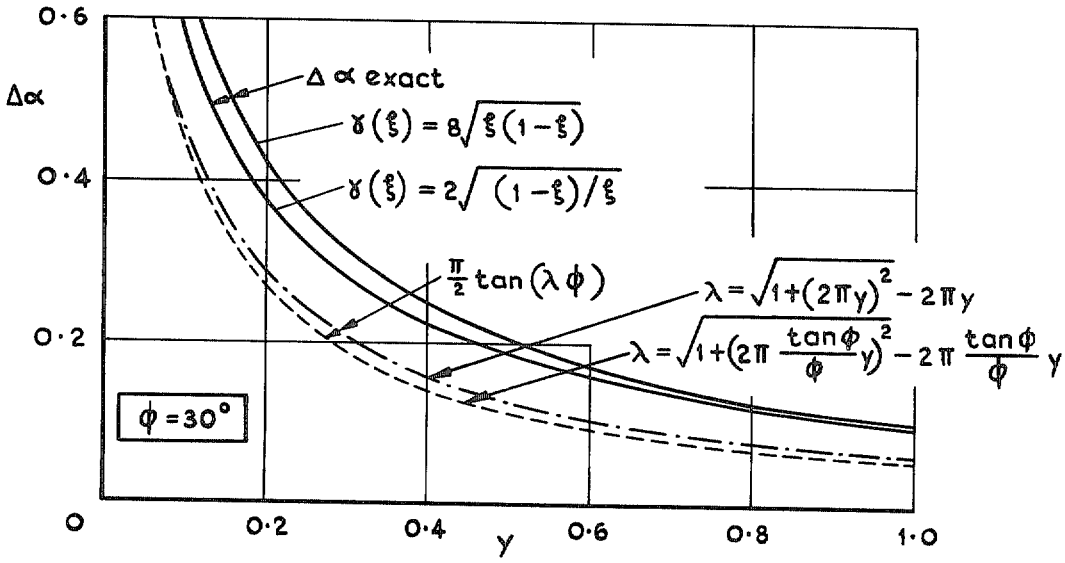

FIG. 7a. Spanwise twist distribution.

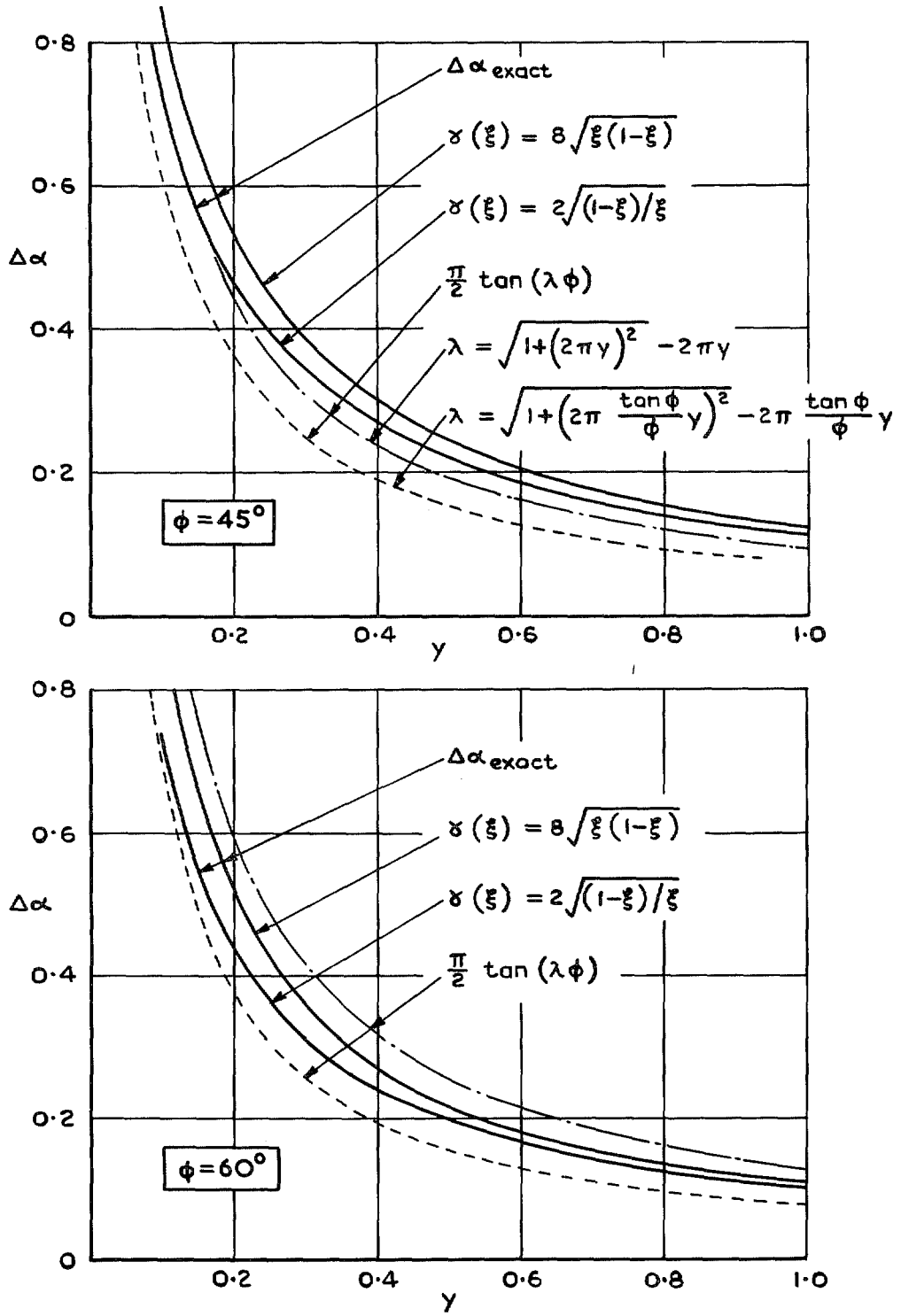

FIG. 7b. Spanwise twist distribution.

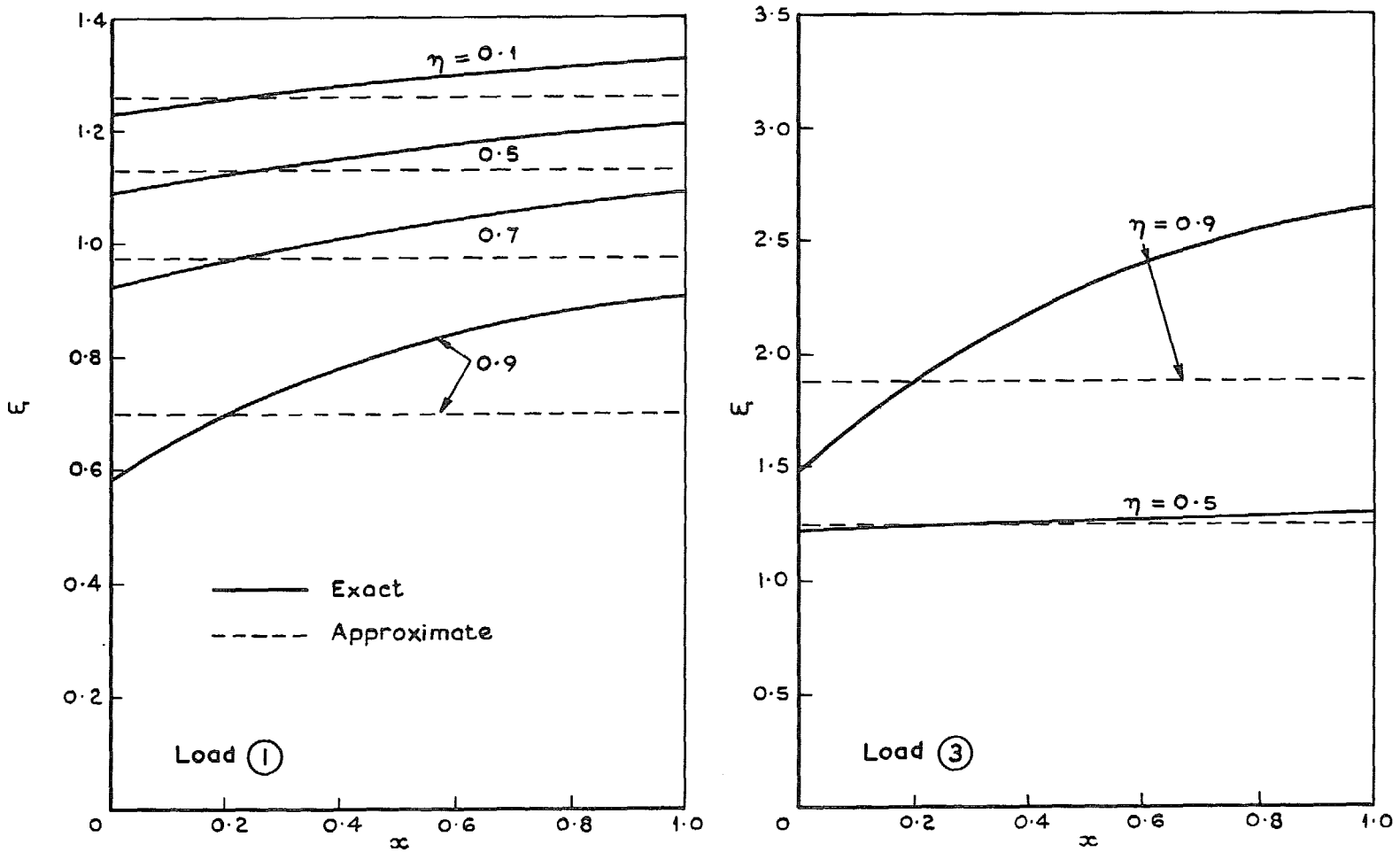

FIG. 8a. Downwash distributions for rectangular wings; $A = 6$.

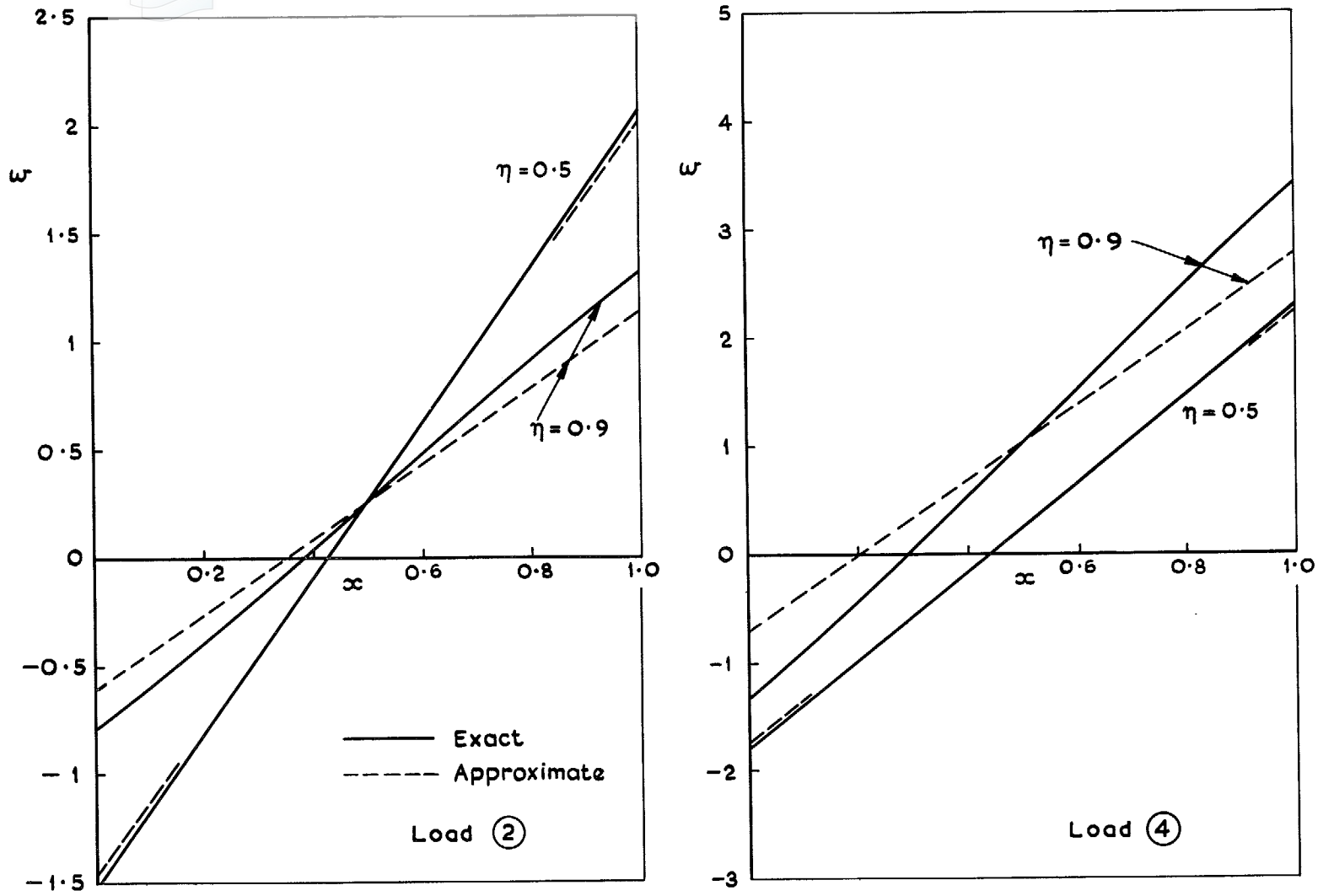

FIG. 8b. Downwash distributions for rectangular wings; $A = 6$.

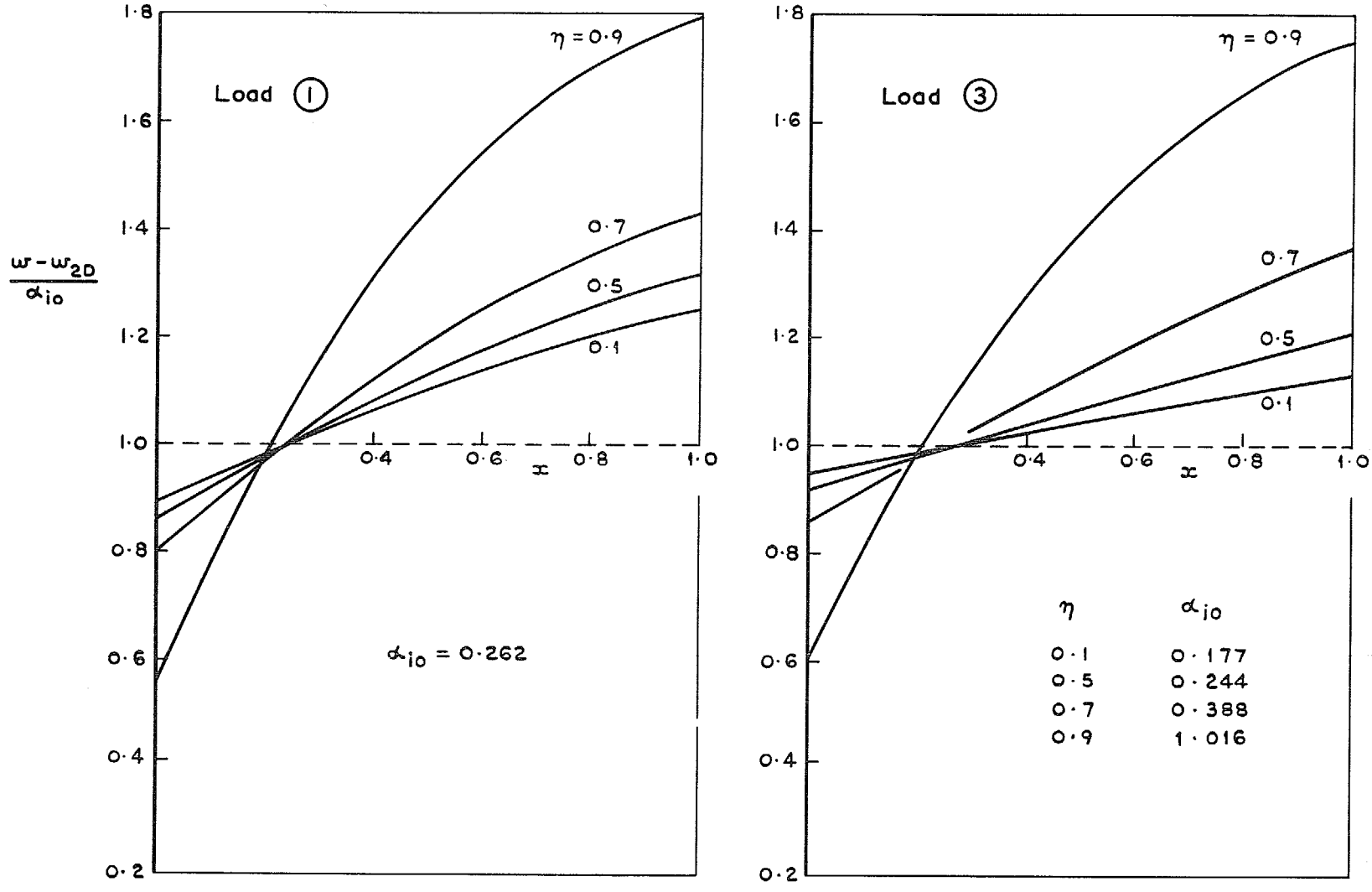

FIG. 9a. Threedimensional effect on downwash distributions for rectangular wings; $A = 6$.

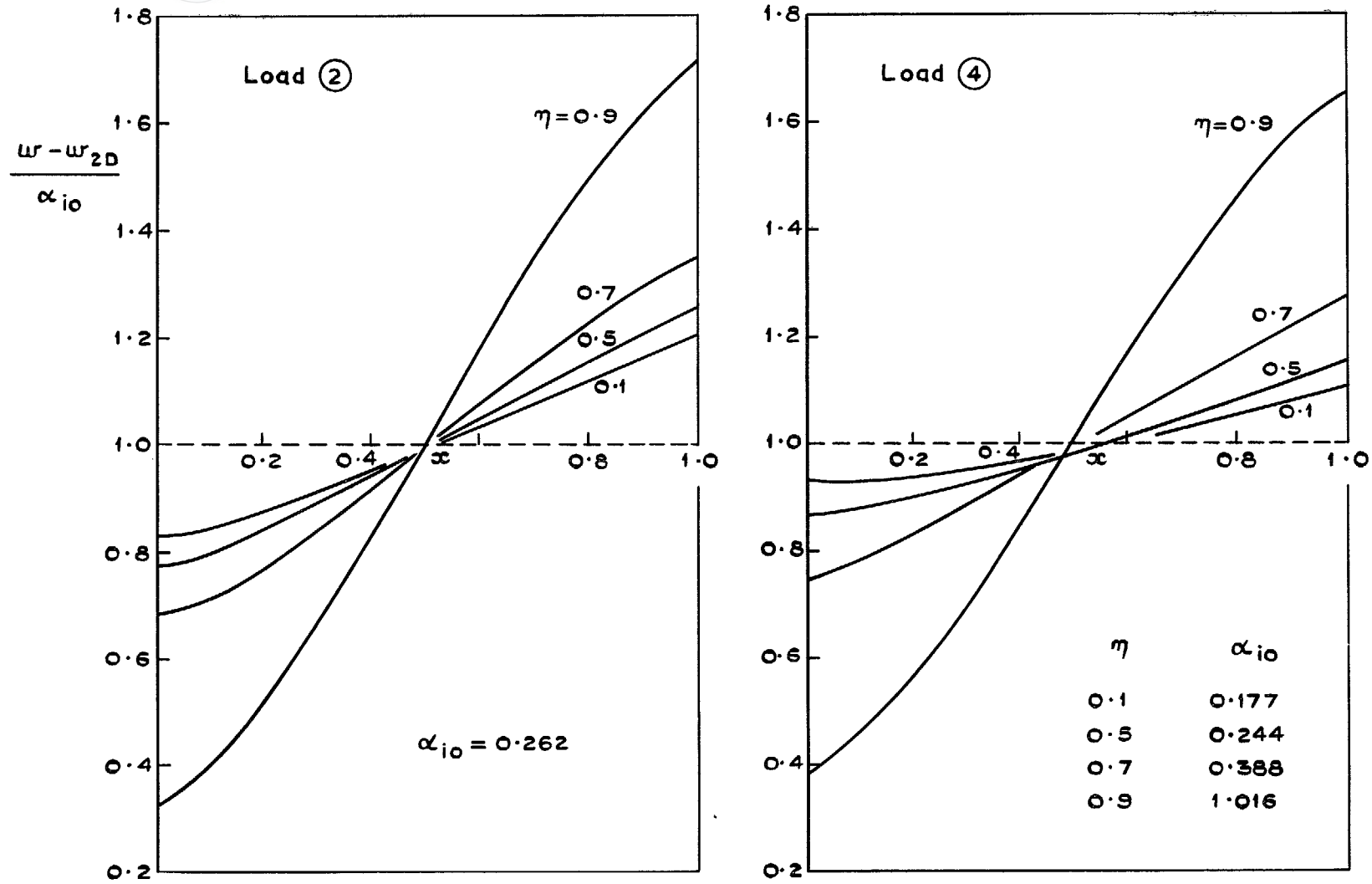

FIG. 9b. Threedimensional effect on downwash distributions for rectangular wings; $A = 6$.

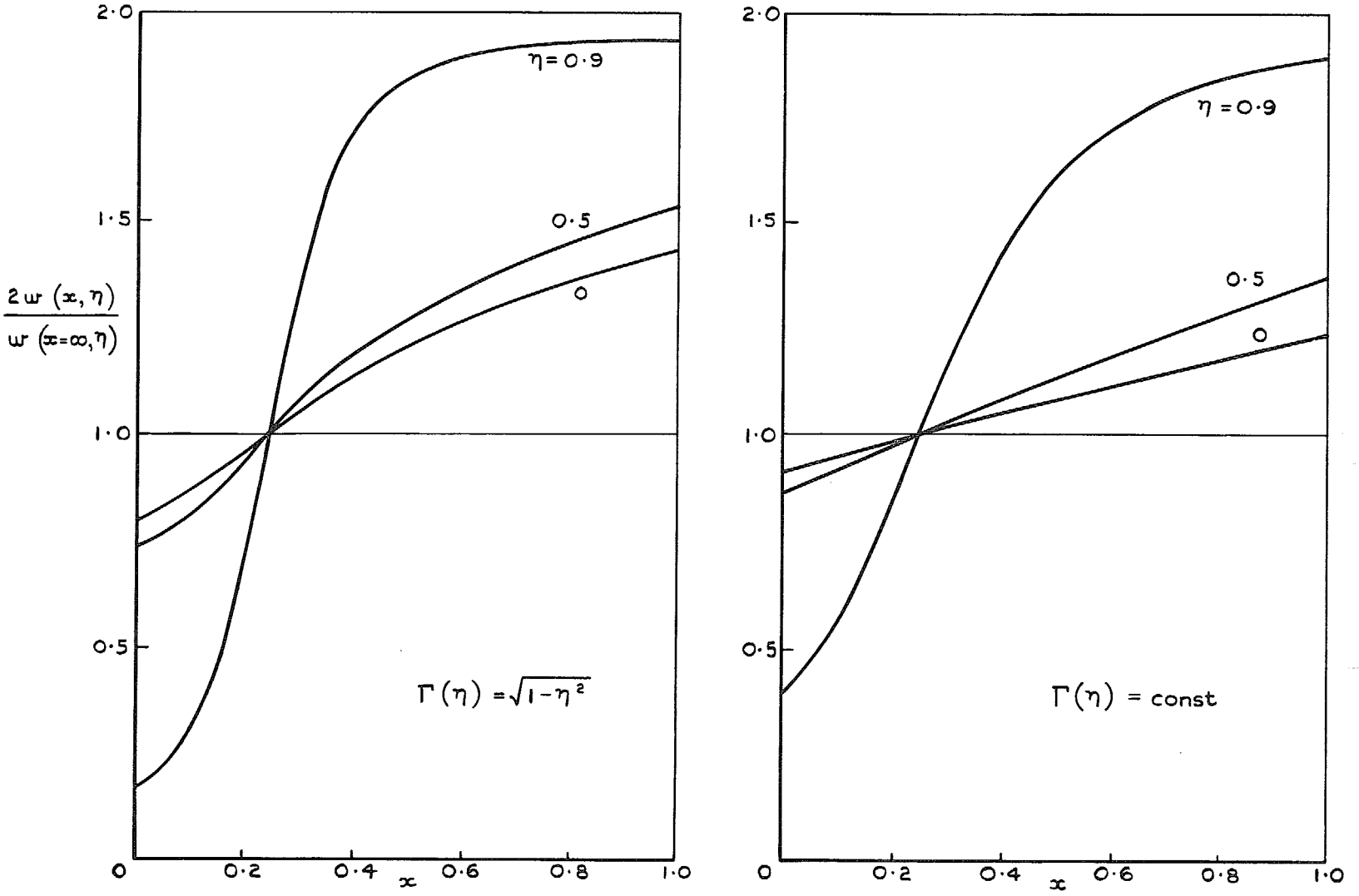

FIG. 10. Downwash induced by a trailing vortex sheet originating from an unswept bound vortex at $x = 0{\cdot}25$, $-3 < y < 3$ of strength $\Gamma(y)$.

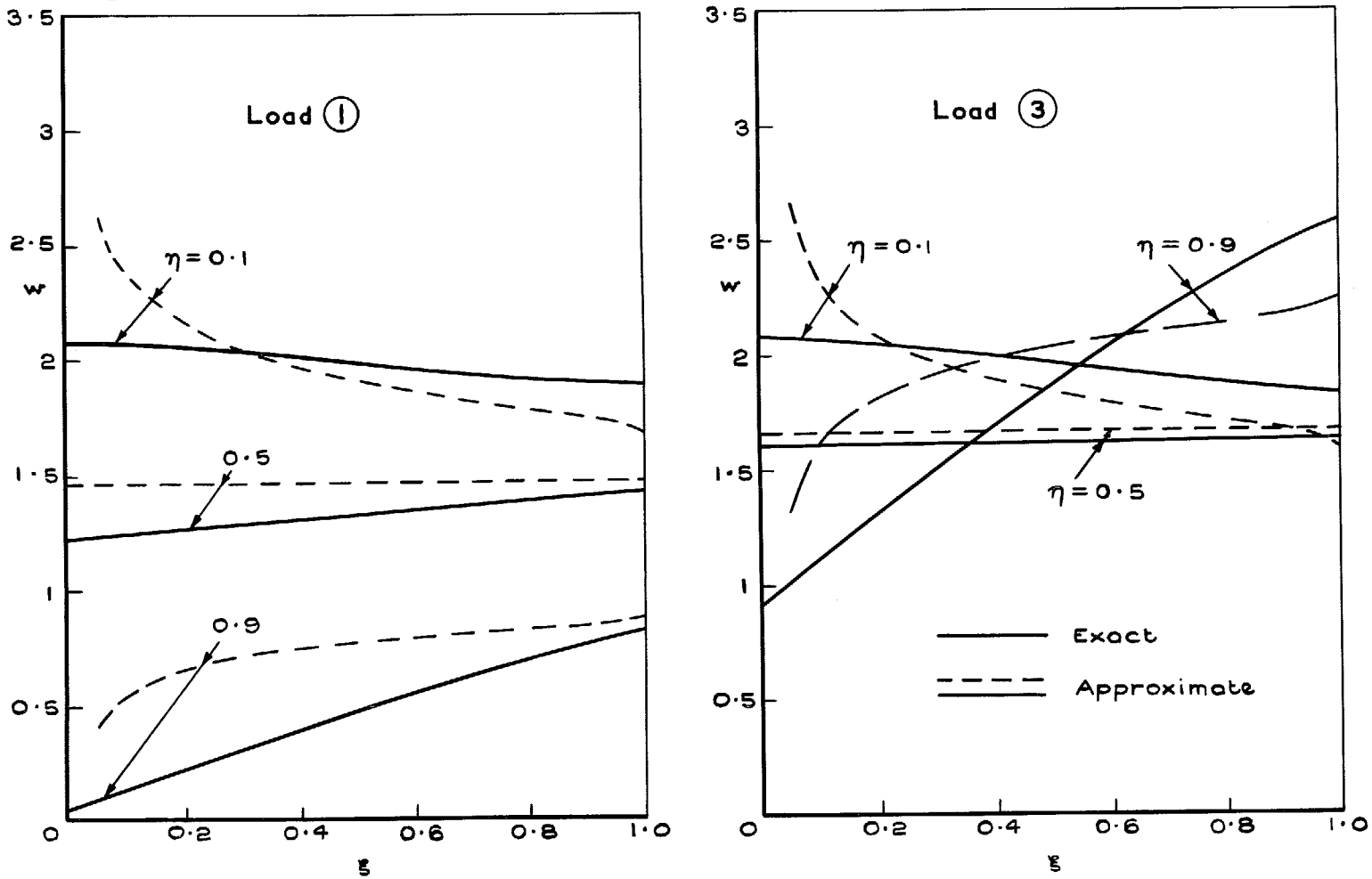

FIG. 11a. Downwash distributions for swept wings; $\phi = 45°$, $A = 6$.

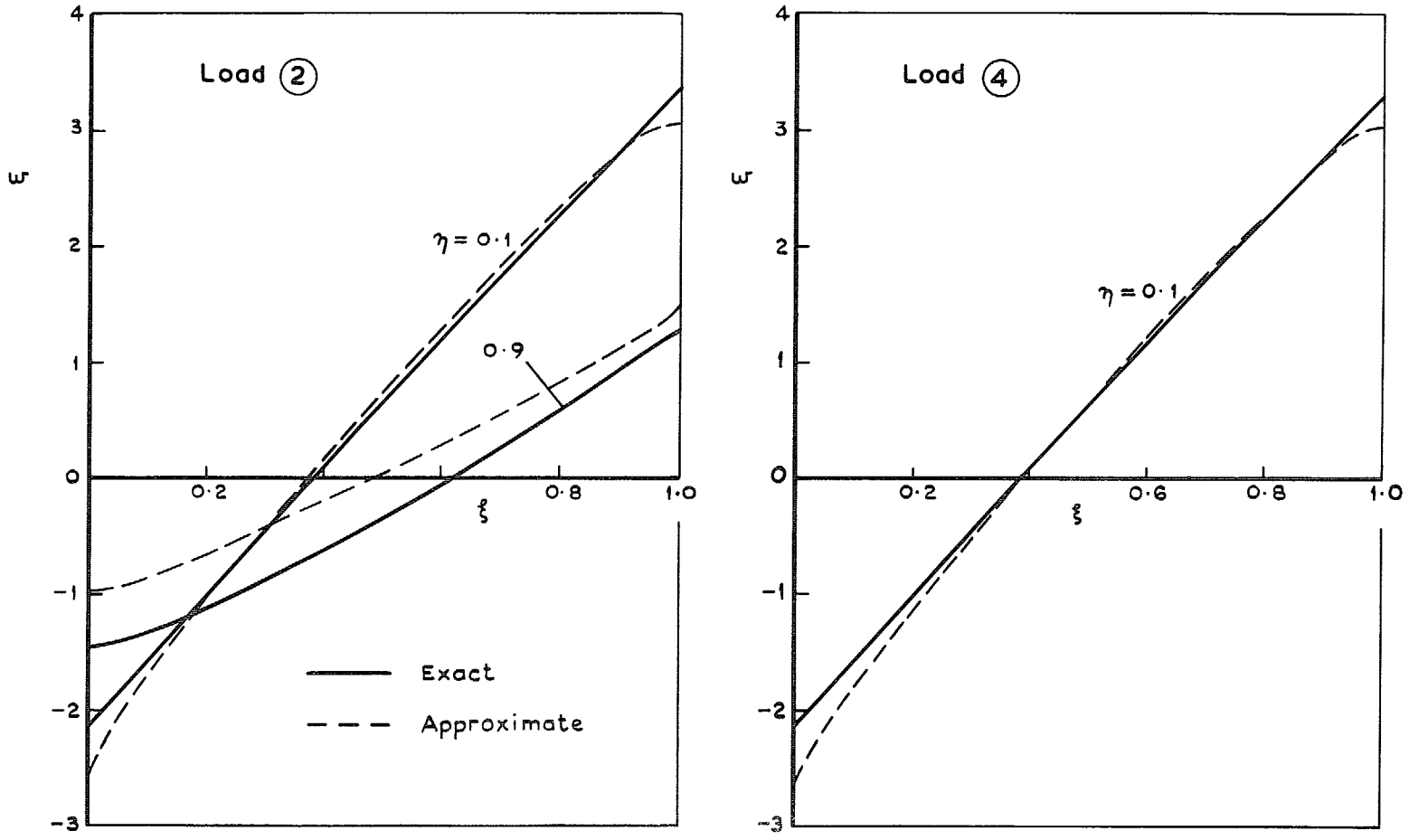

FIG. 11b. Downwash distributions for swept wings, $\phi = 45°$, $A = 6$.

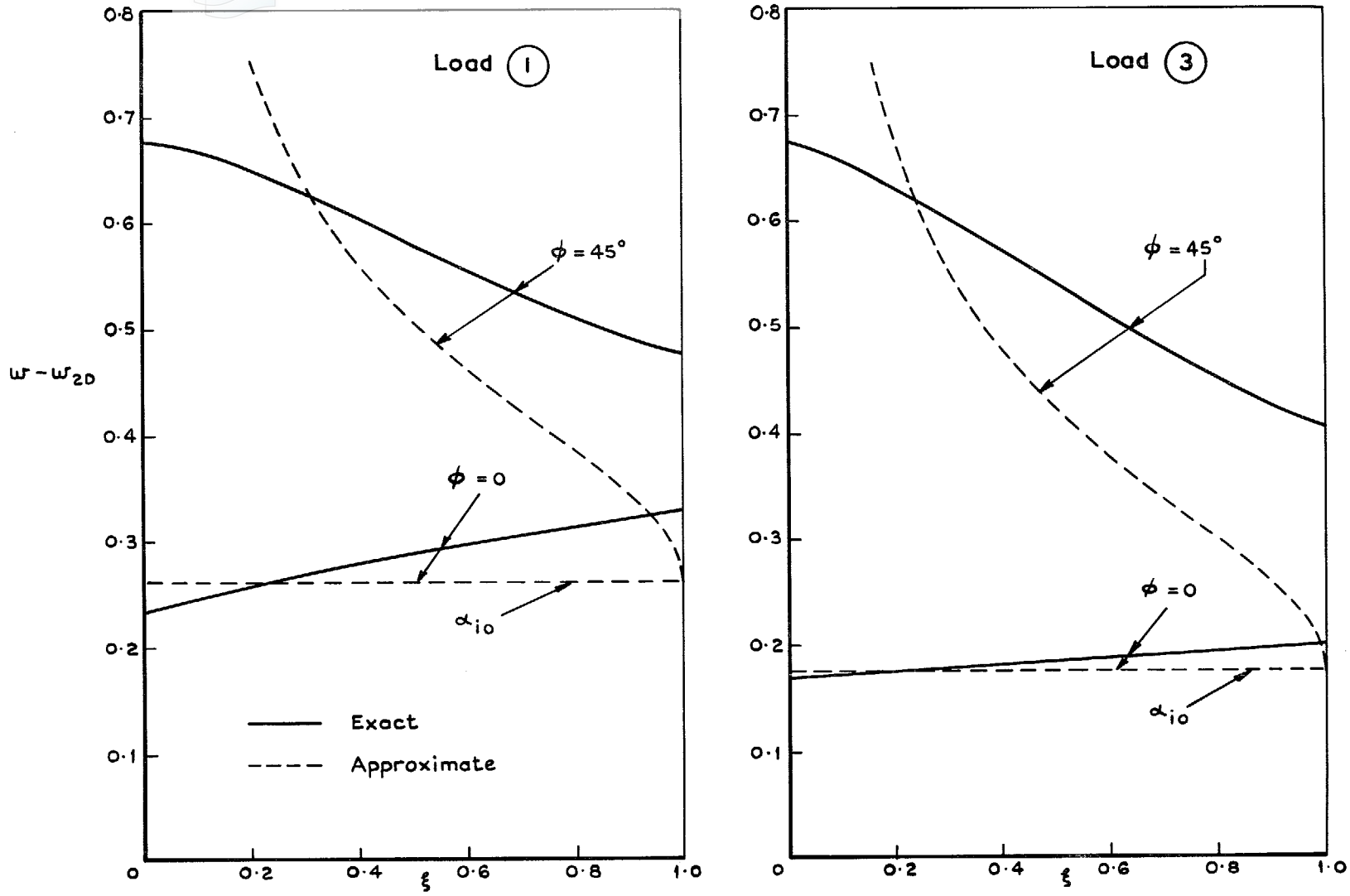

FIG. 12a. Threedimensional effect on downwash distributions at the inboard station $\eta = 0{\cdot}1$; $A = 6$.

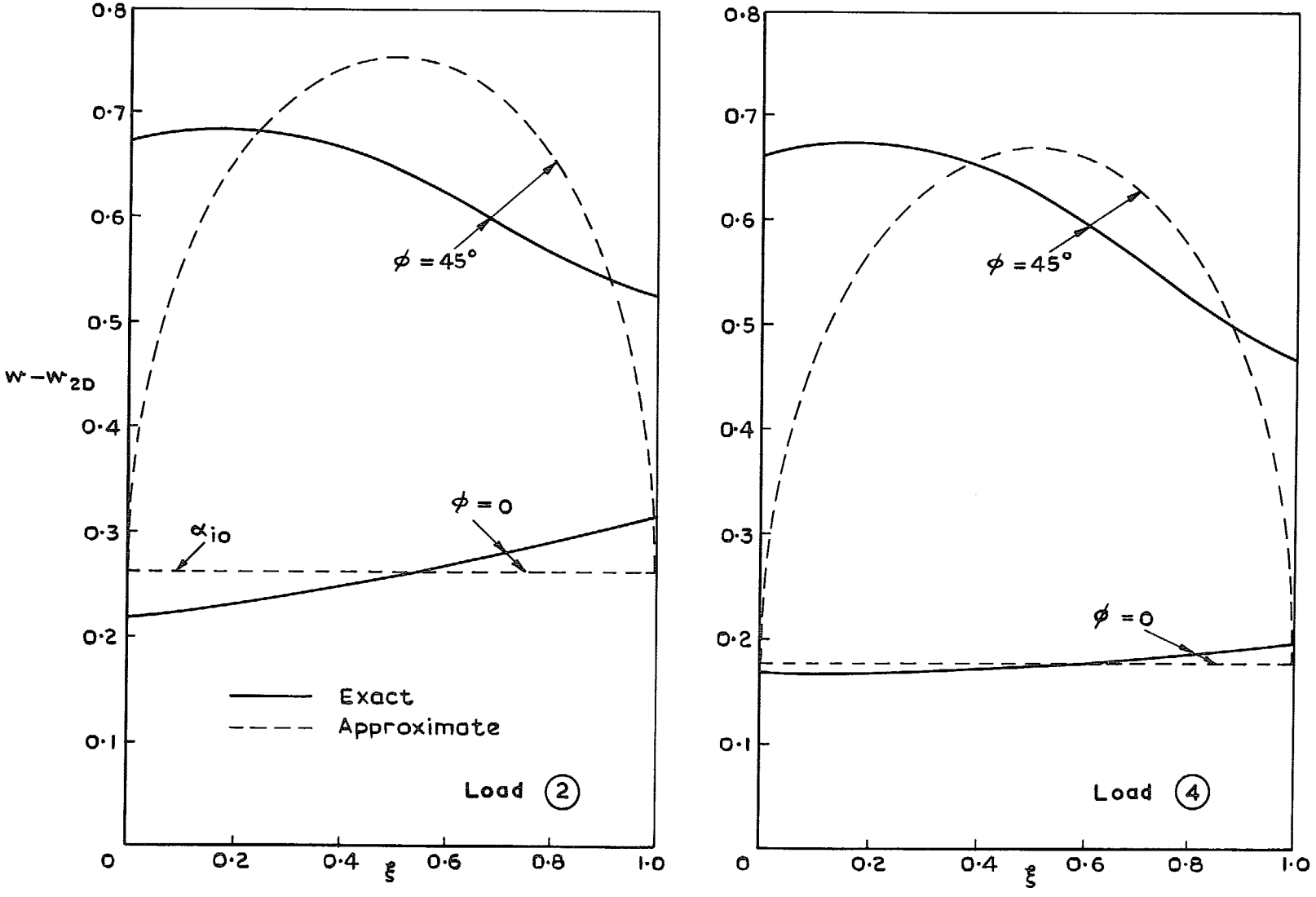

FIG. 12b. Threedimensional effect on downwash distributions at the inboard station $\eta = 0{\cdot}1$; $A = 6$.

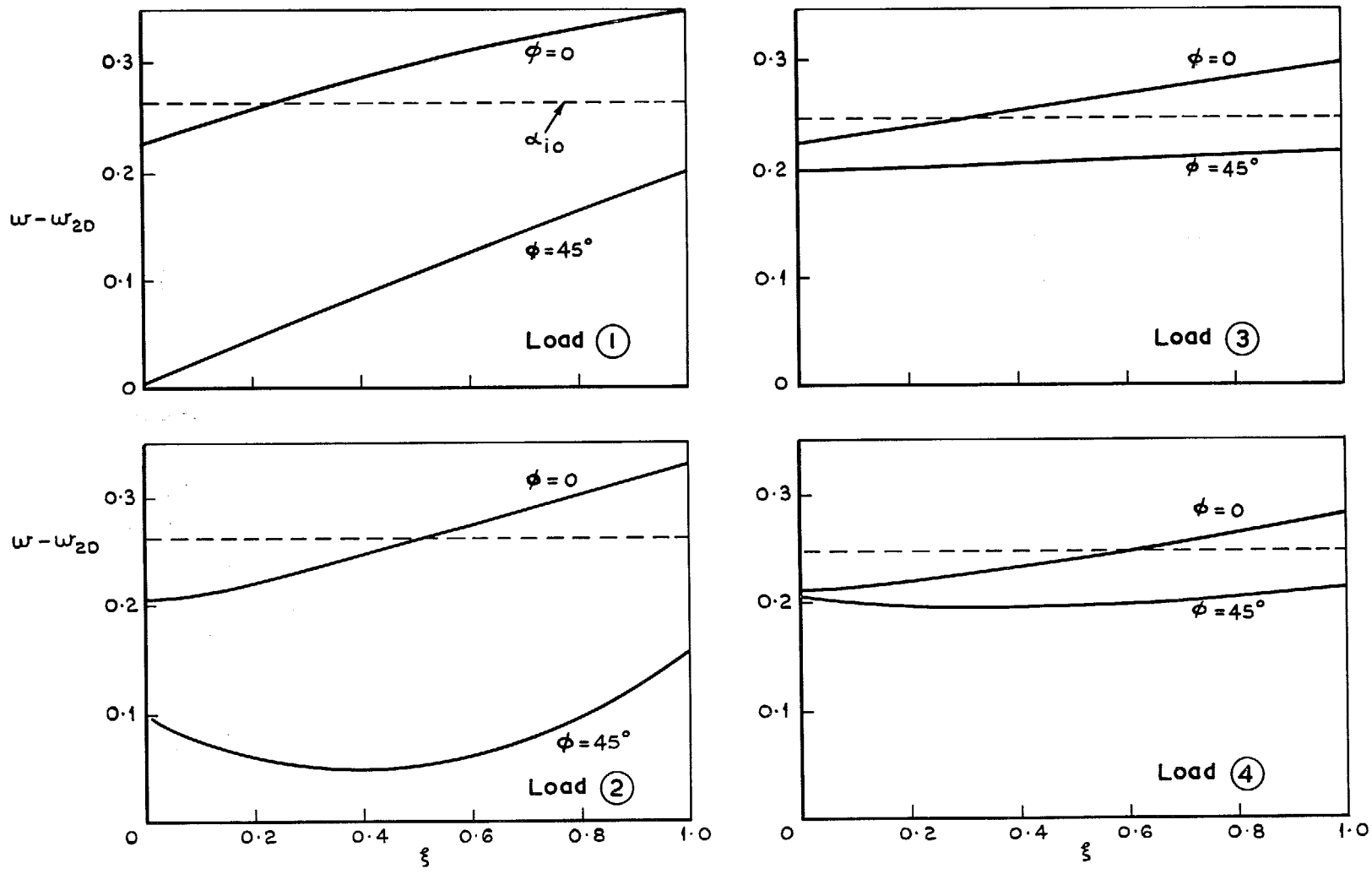

FIG. 13. Threedimensional effect on downwash distributions at midspan $\eta = 0{\cdot}5$; $A = 6$.

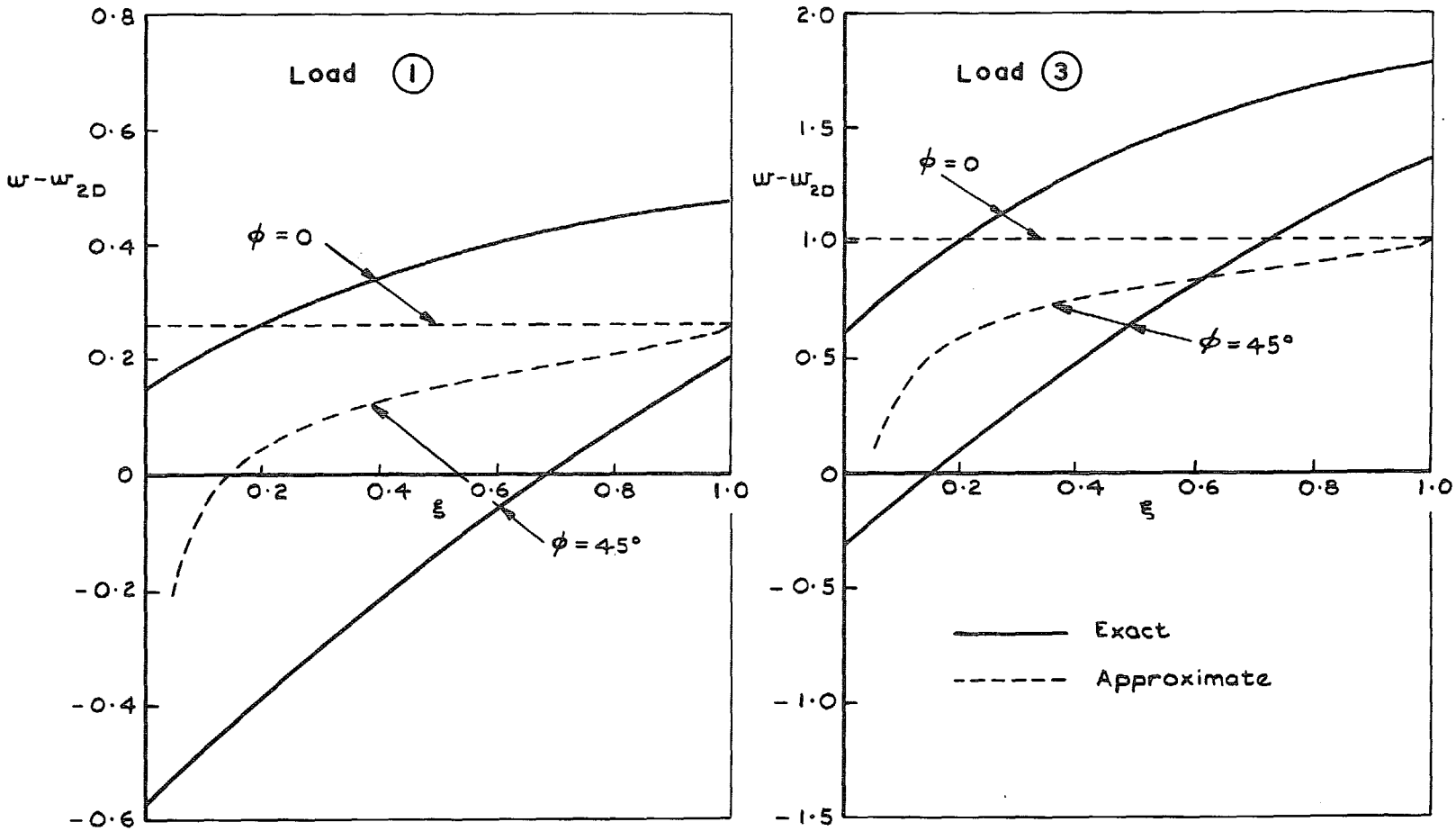

FIG. 14a. Threedimensional effect on the downwash distributions at the outboard station $\eta = 0{\cdot}9$; $A = 6$.

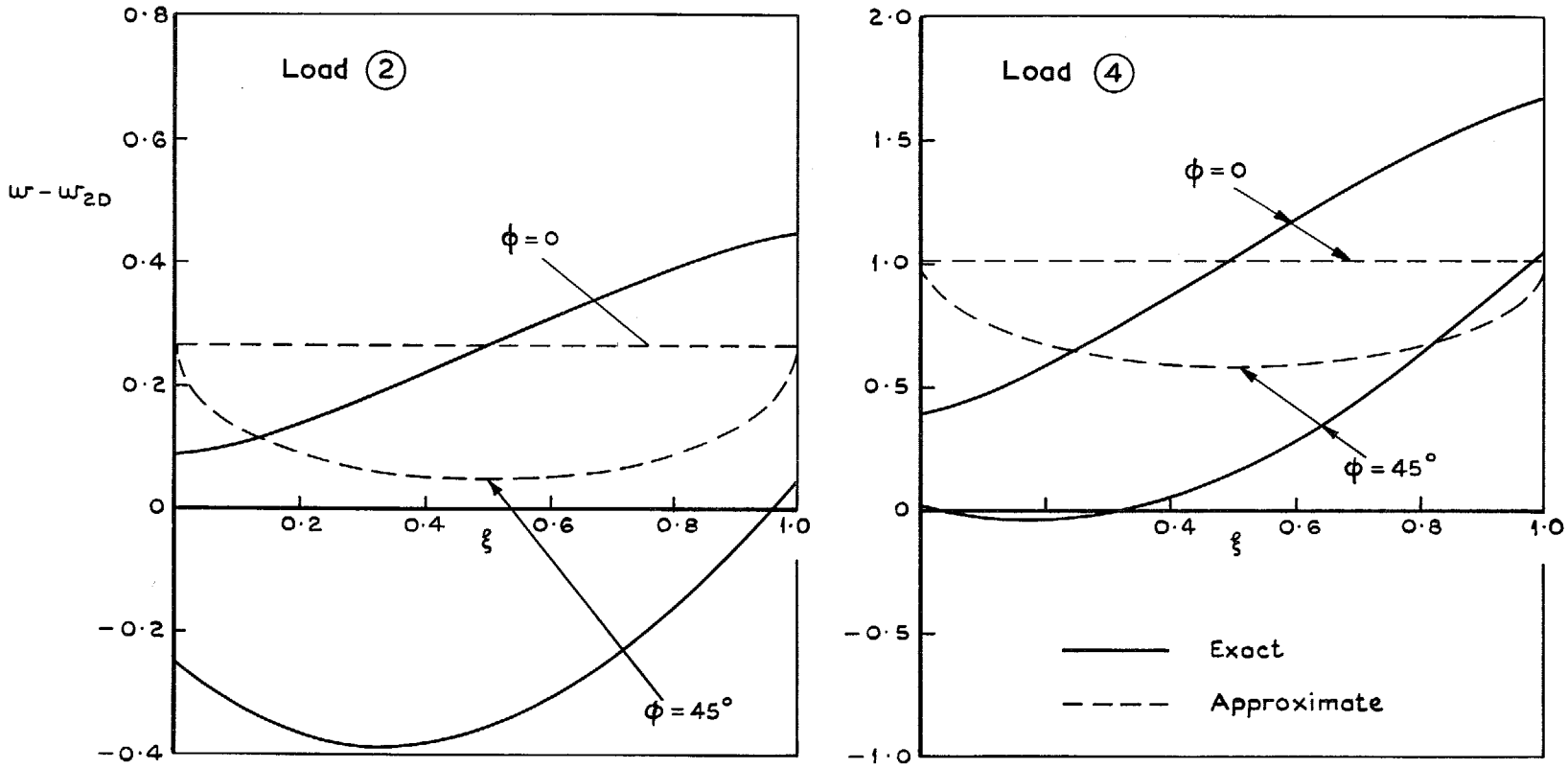

FIG. 14b. Threedimensional effect on the downwash distributions at the outboard station $\eta = 0{\cdot}9$; $A = 6$.

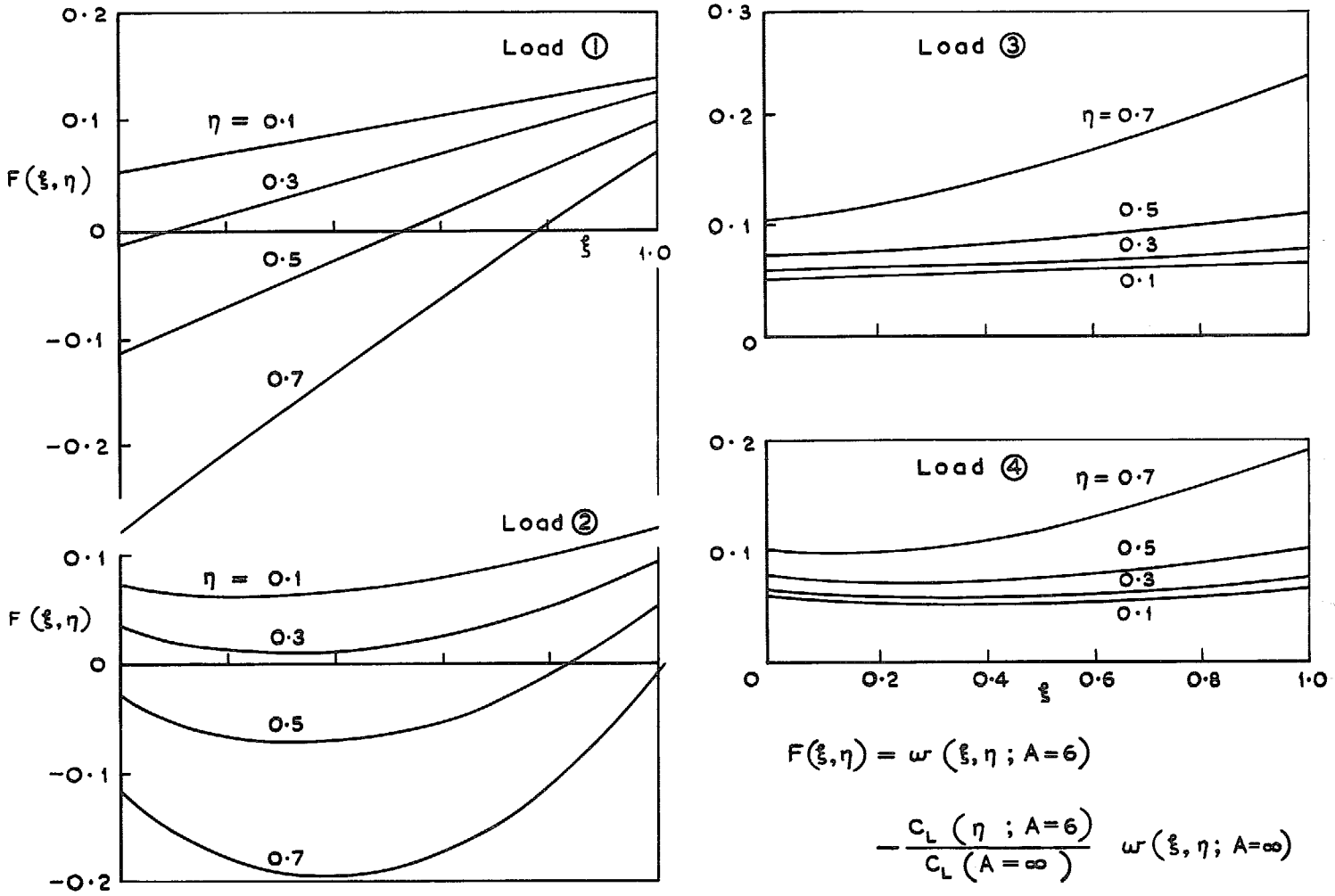

FIG. 15a. Difference between the downwash on a finite swept wing and on a swept wing of infinite aspect ratio; $\phi = 45°$, $A = 6$.

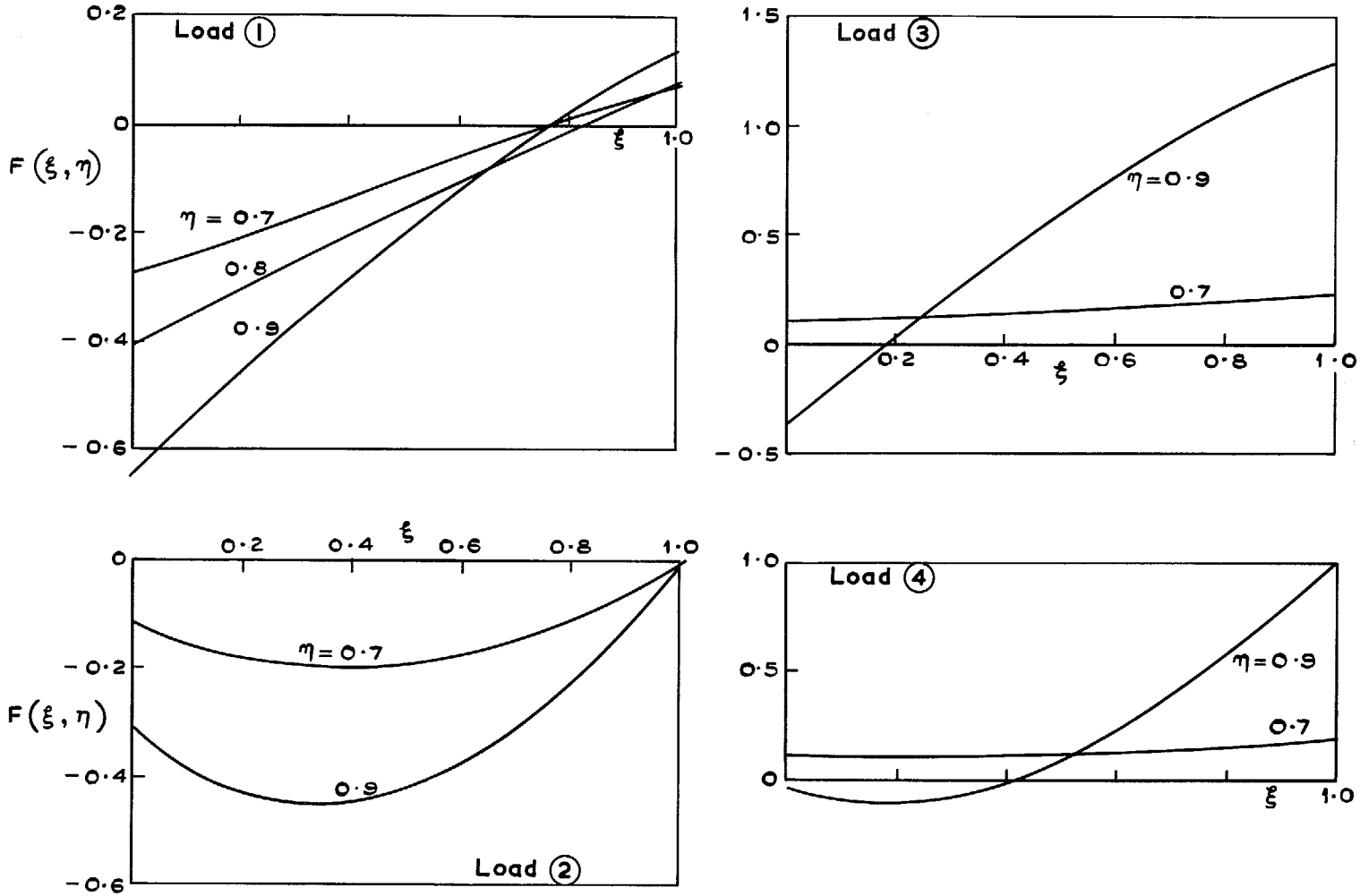

FIG. 15b. Difference between the downwash on a finite swept wing and on a swept wing of infinite aspect ratio; $\phi = 45°$, $A = 6$.

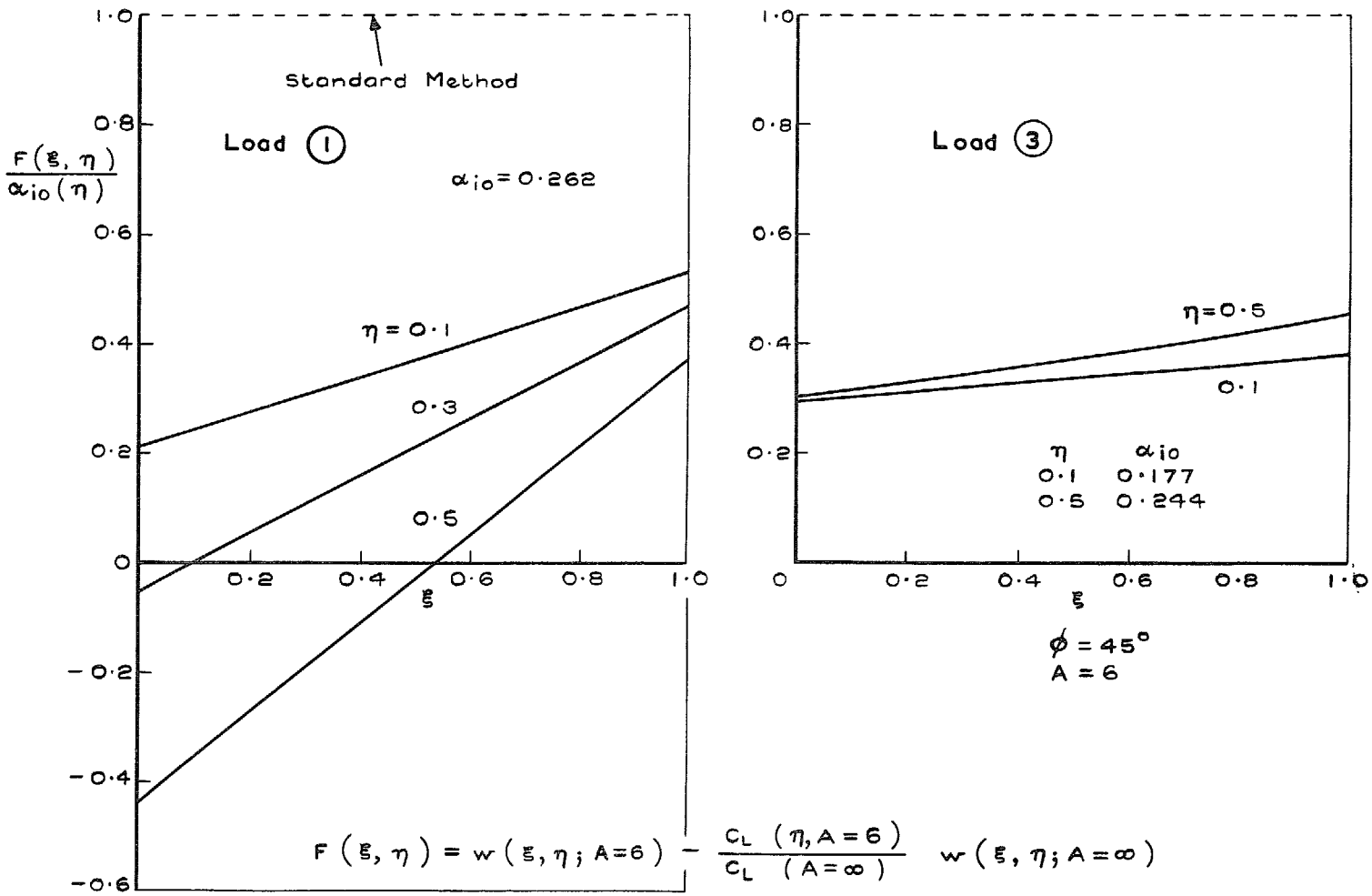

FIG. 16. Difference between the downwash on a finite swept wing and on a swept wing of infinite aspect ratio.

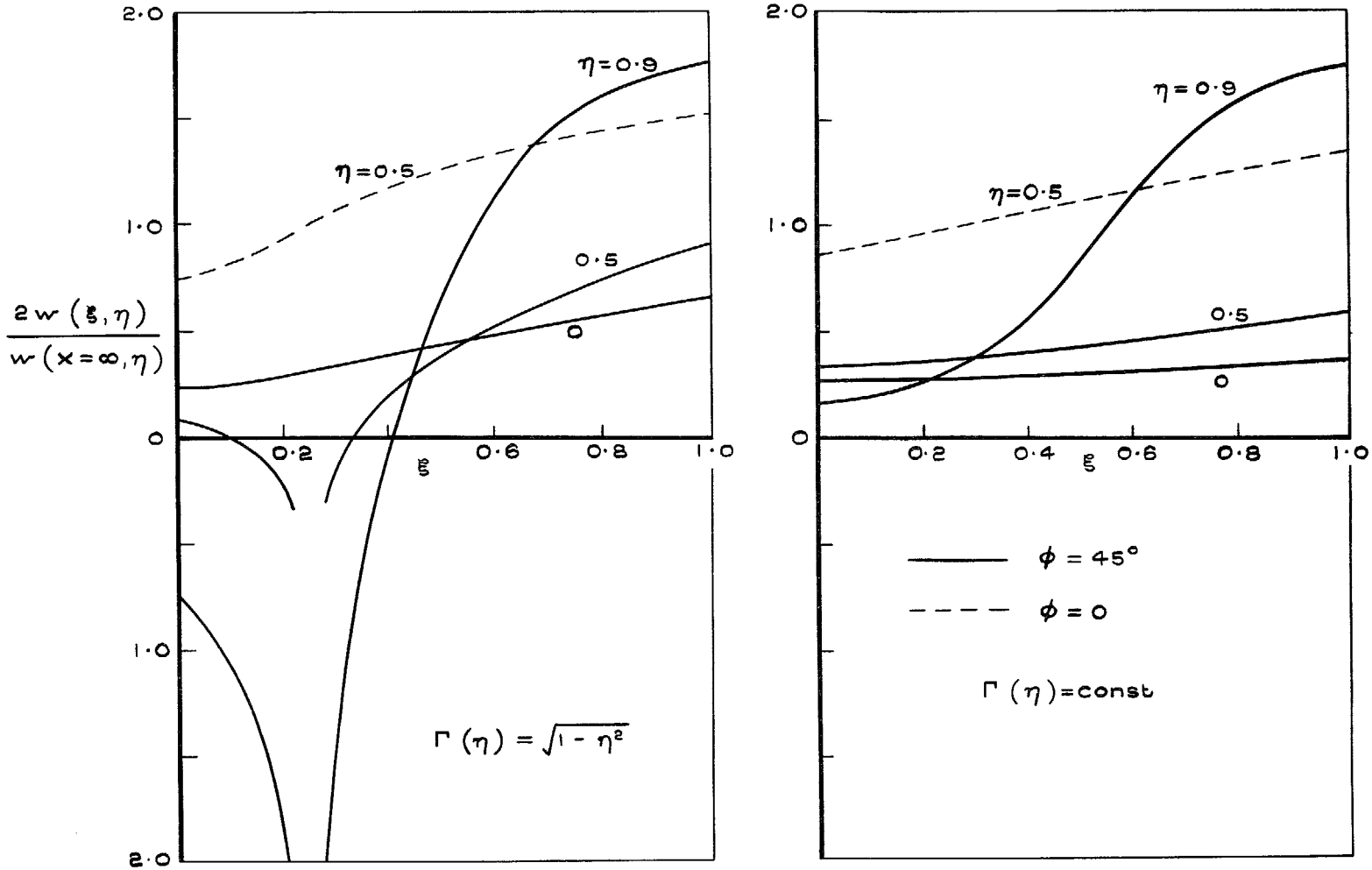

FIG. 17. Downwash induced by a trailing vortex sheet originating from a single swept bound vortex at $X = |y| \tan \phi + 0{\cdot}25$; $-3 < y < 3$ of strength $\Gamma(y)$.

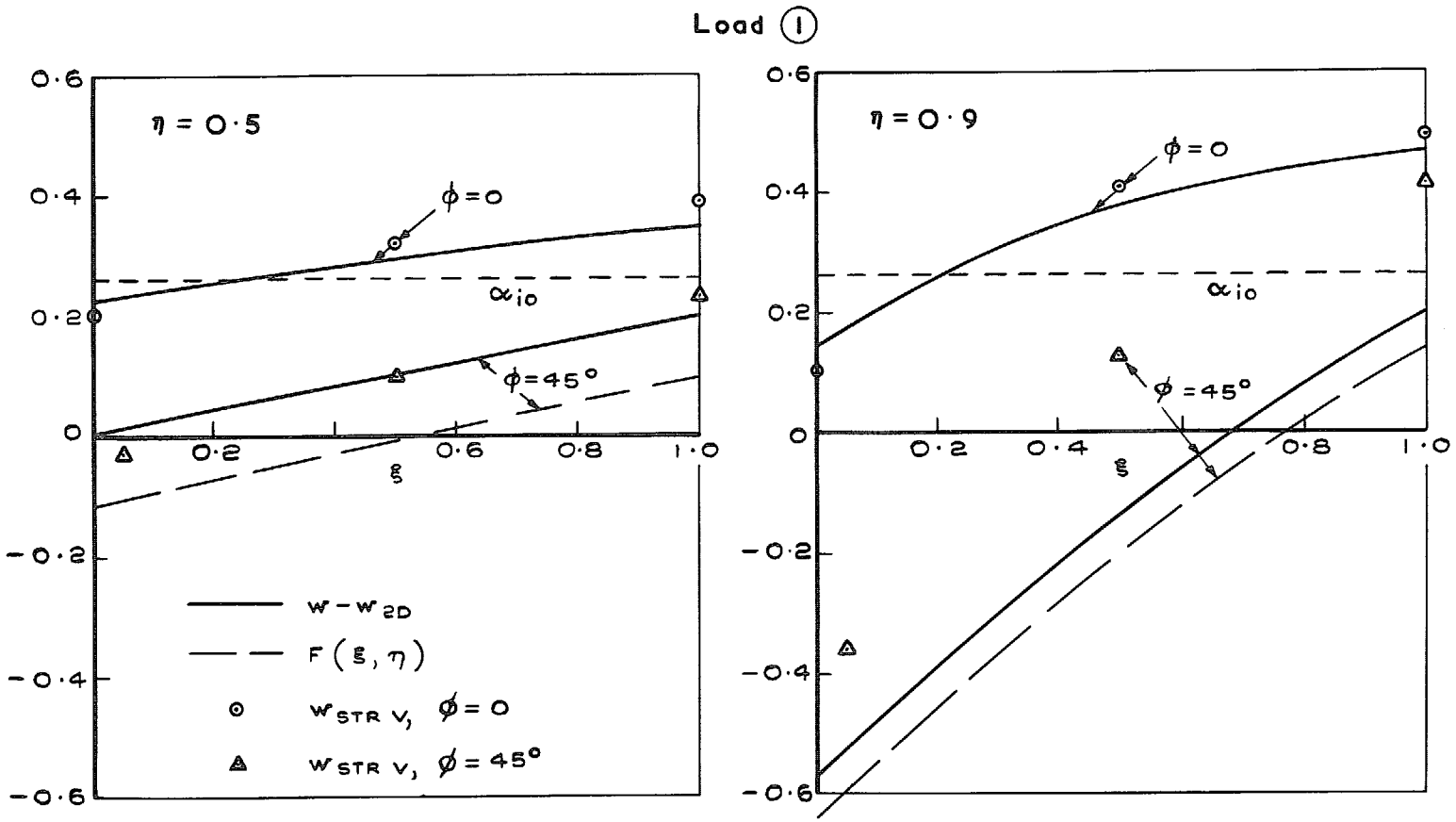

FIG. 18. Comparison of downwash from streamwise vorticity, w_{STRV}, with $F(\xi, \eta) = w - w(A = \infty)$ and with $w - w_{2D}$.

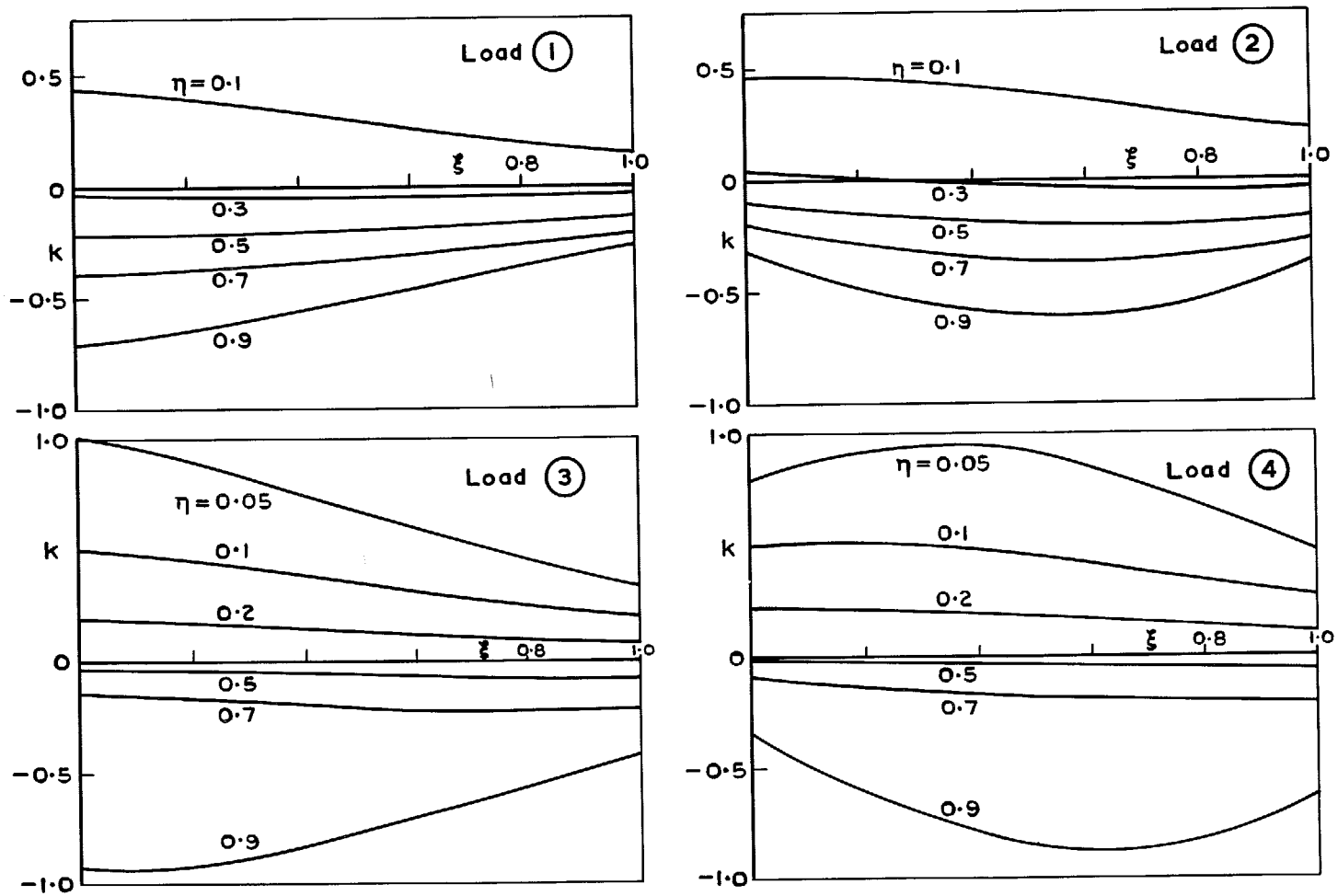

FIG. 19. The effect of sweep on the downwash distributions $k(\xi, \eta) = [w(\xi, \eta) - w_{2D}(\xi, \eta)]_{\phi=45°} - [w(\xi, \eta) - w_{2D}(\xi, \eta)]_{\phi=0}$.

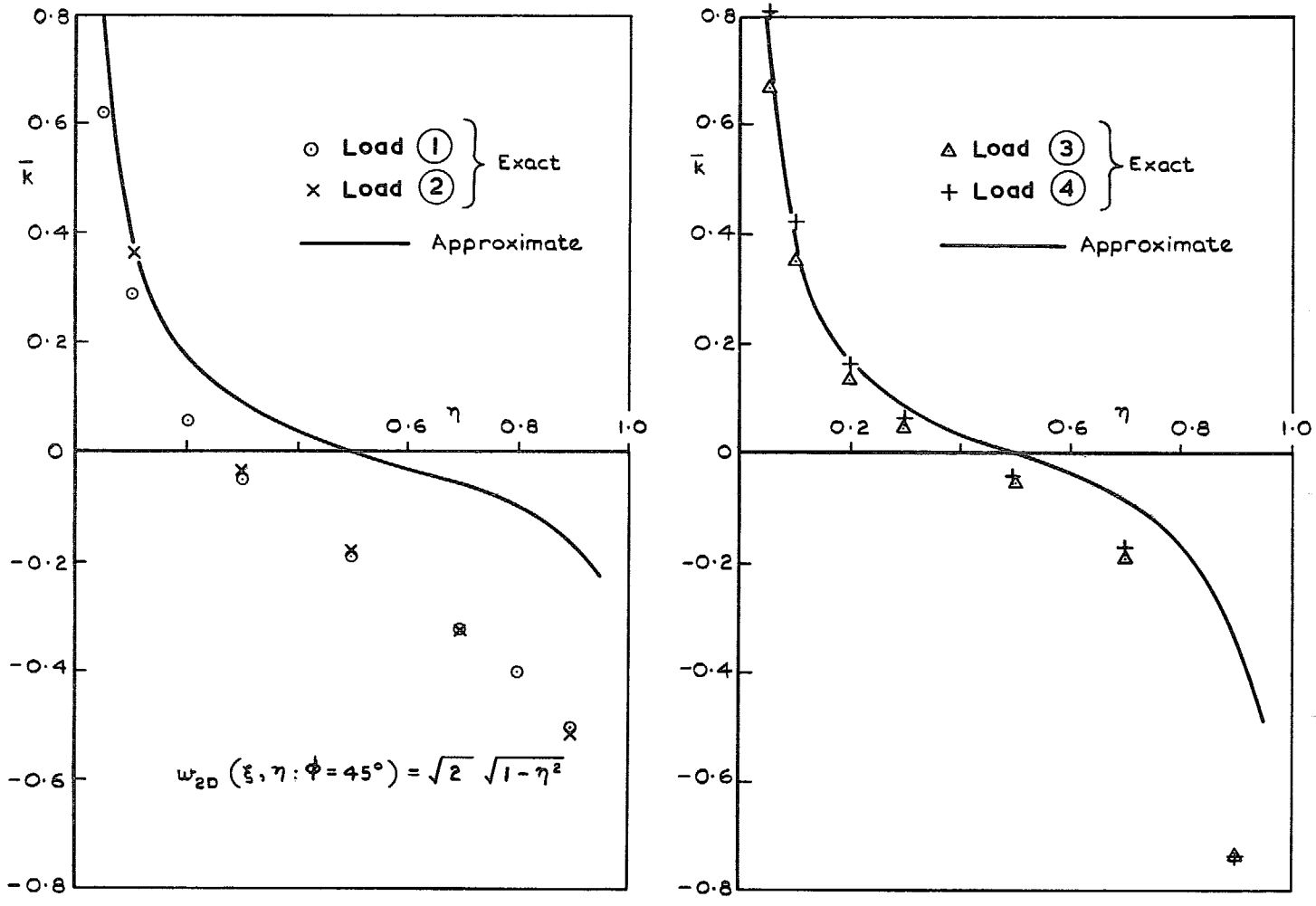

FIG. 20. The effect of sweep on the spanwise twist distribution $\bar{k}(\eta) = \int_0^1 k(\xi, \eta)\, d\xi = \int_0^1 \{[w - w_{2D}]_{\phi=45°} - [w - w_{2D}]_{\phi=0}\}\, d\xi$.

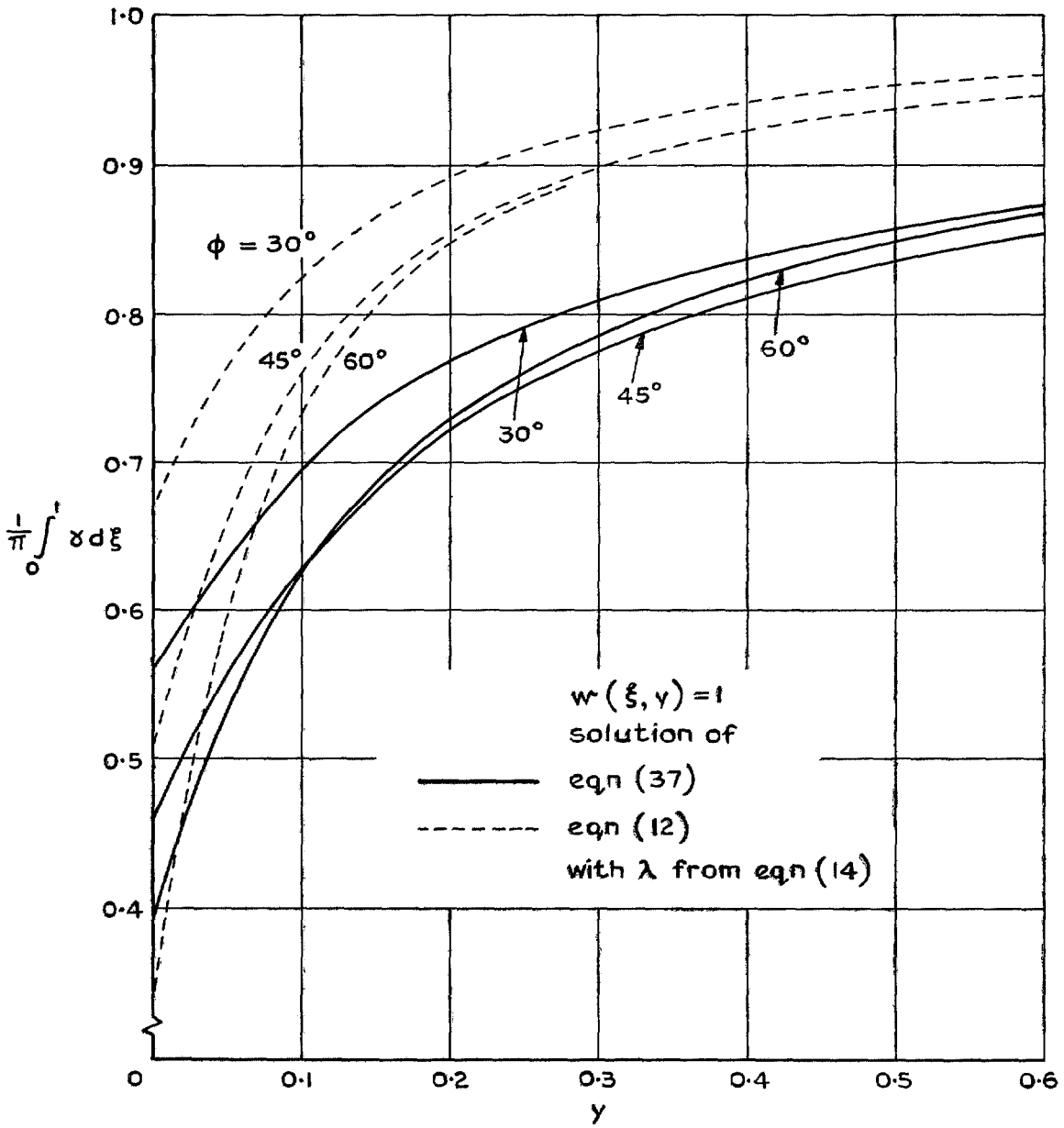

FIG. 21. Comparison of circulation derived from different downwash equations.

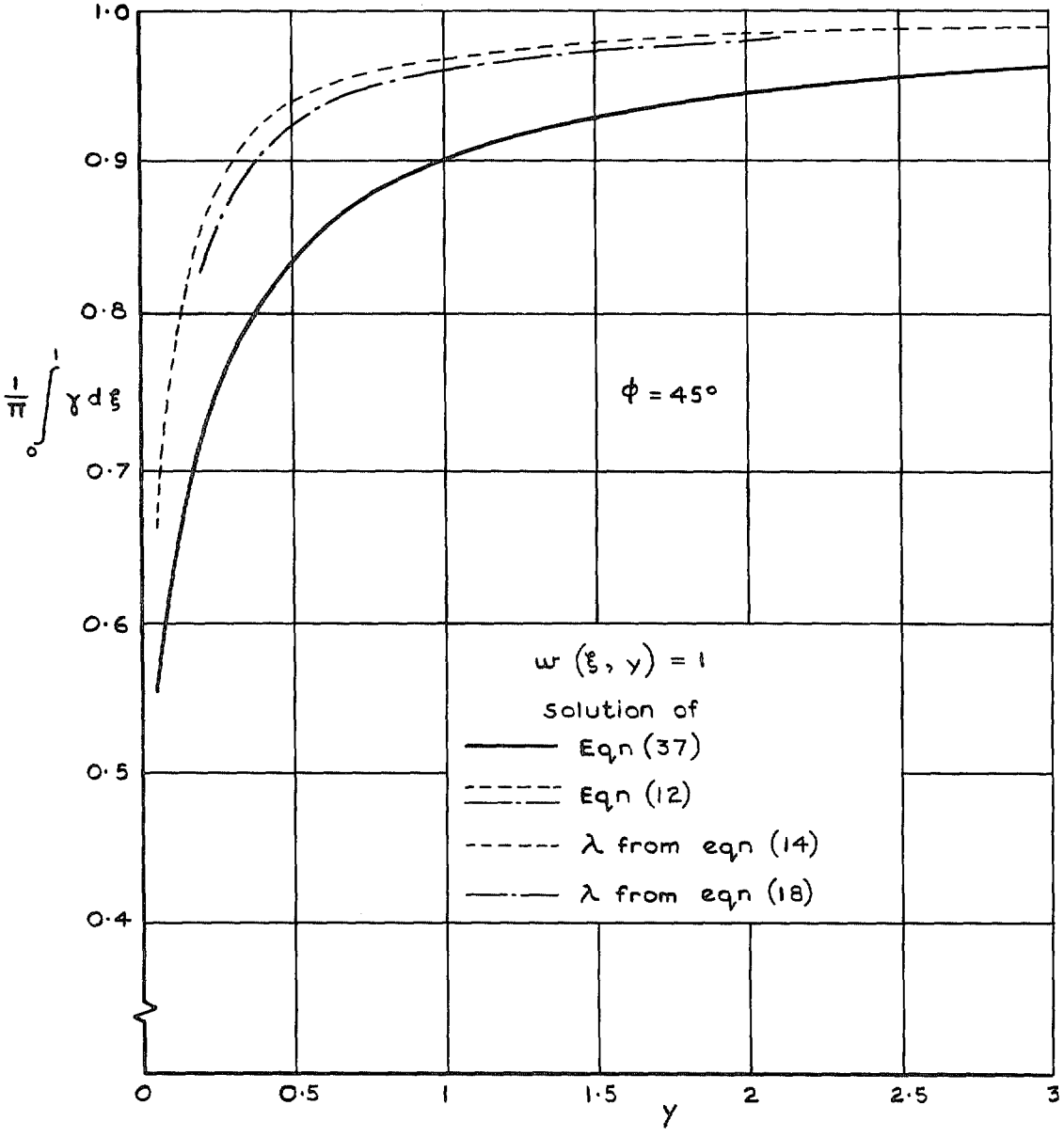

FIG. 22. Comparison of circulation derived from different downwash equations.

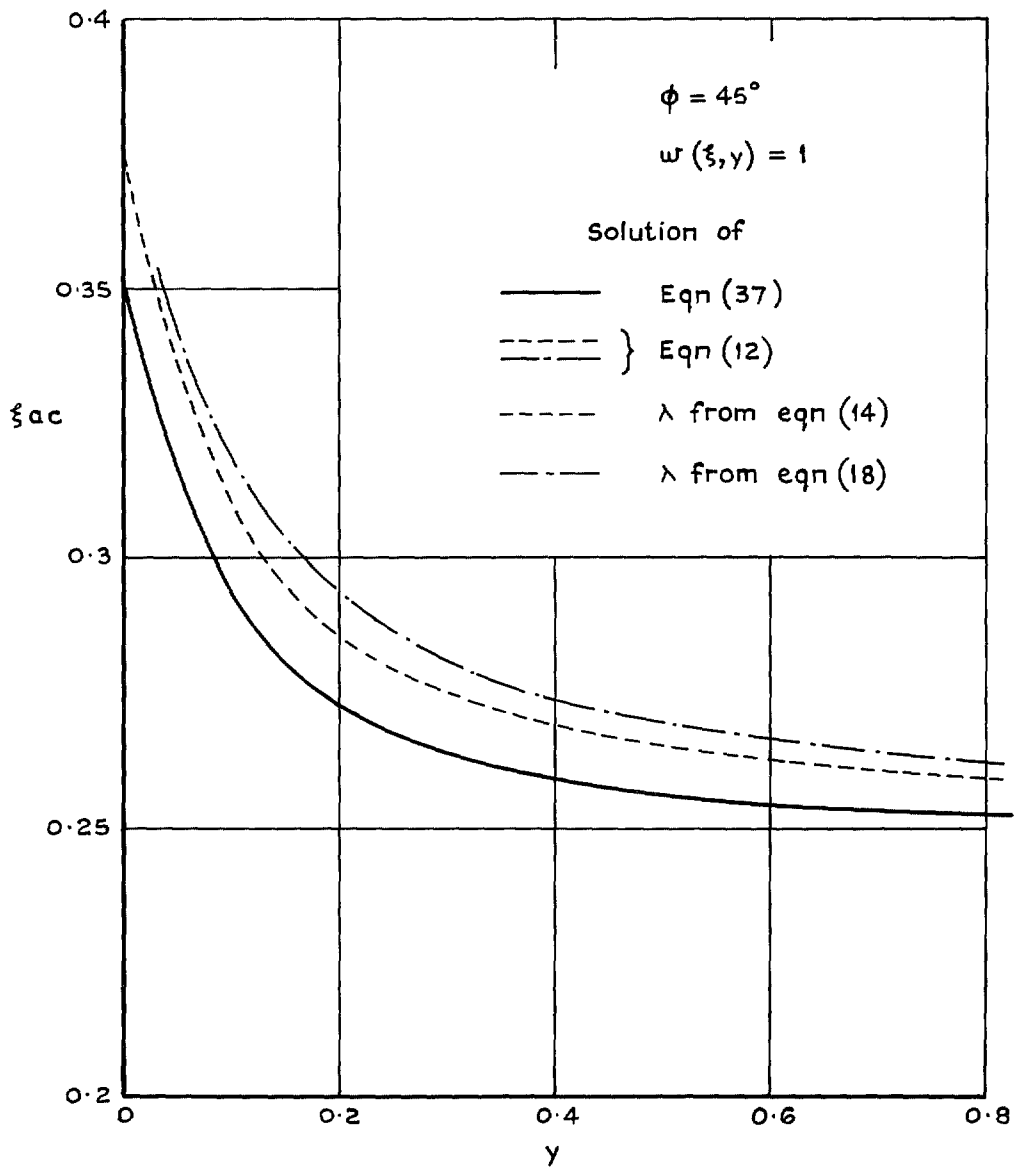

FIG. 23. Aerodynamic-centre position derived from different downwash equations.

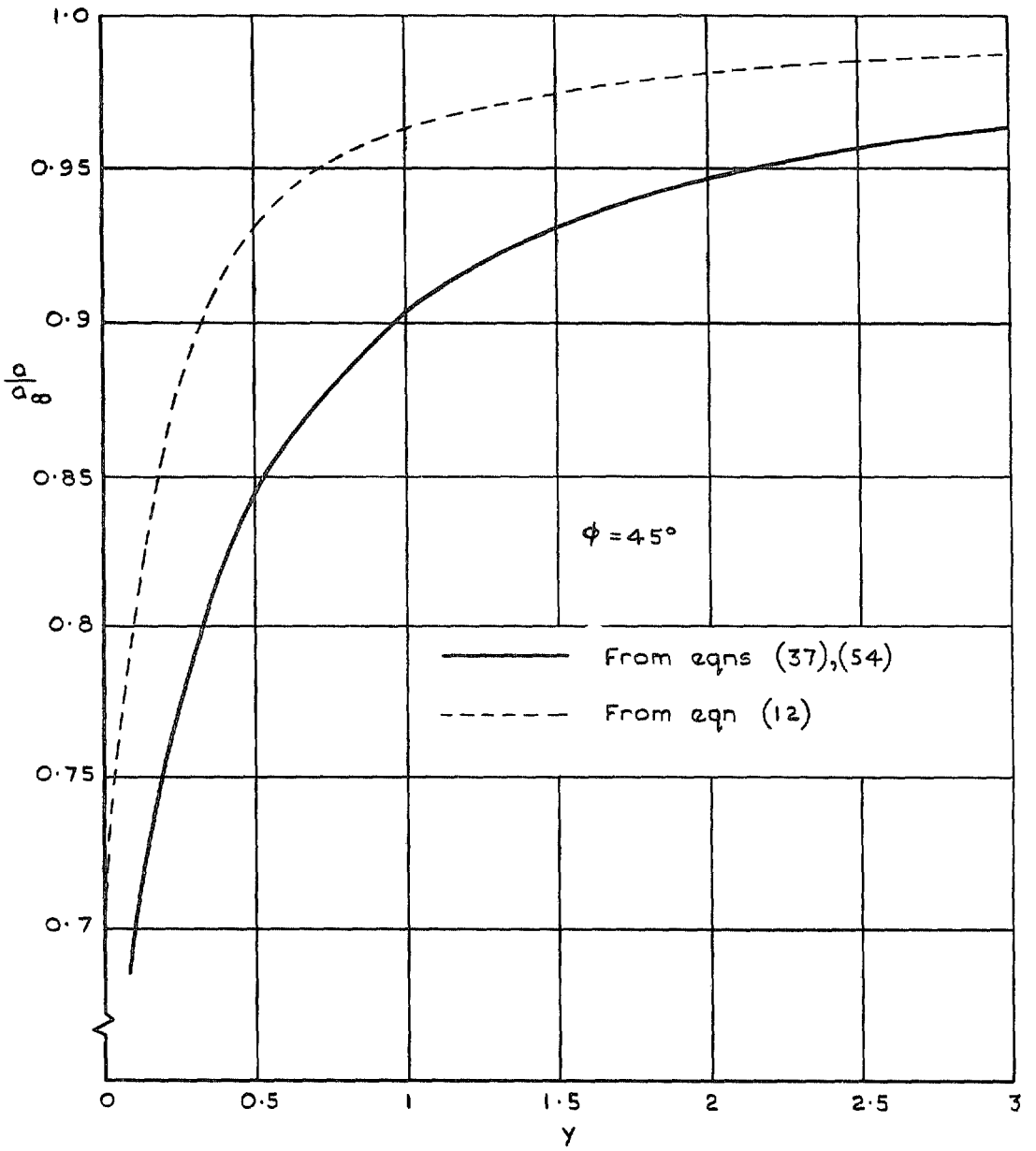

FIG. 24. Comparison of sectional lift slope derived from different downwash equations.

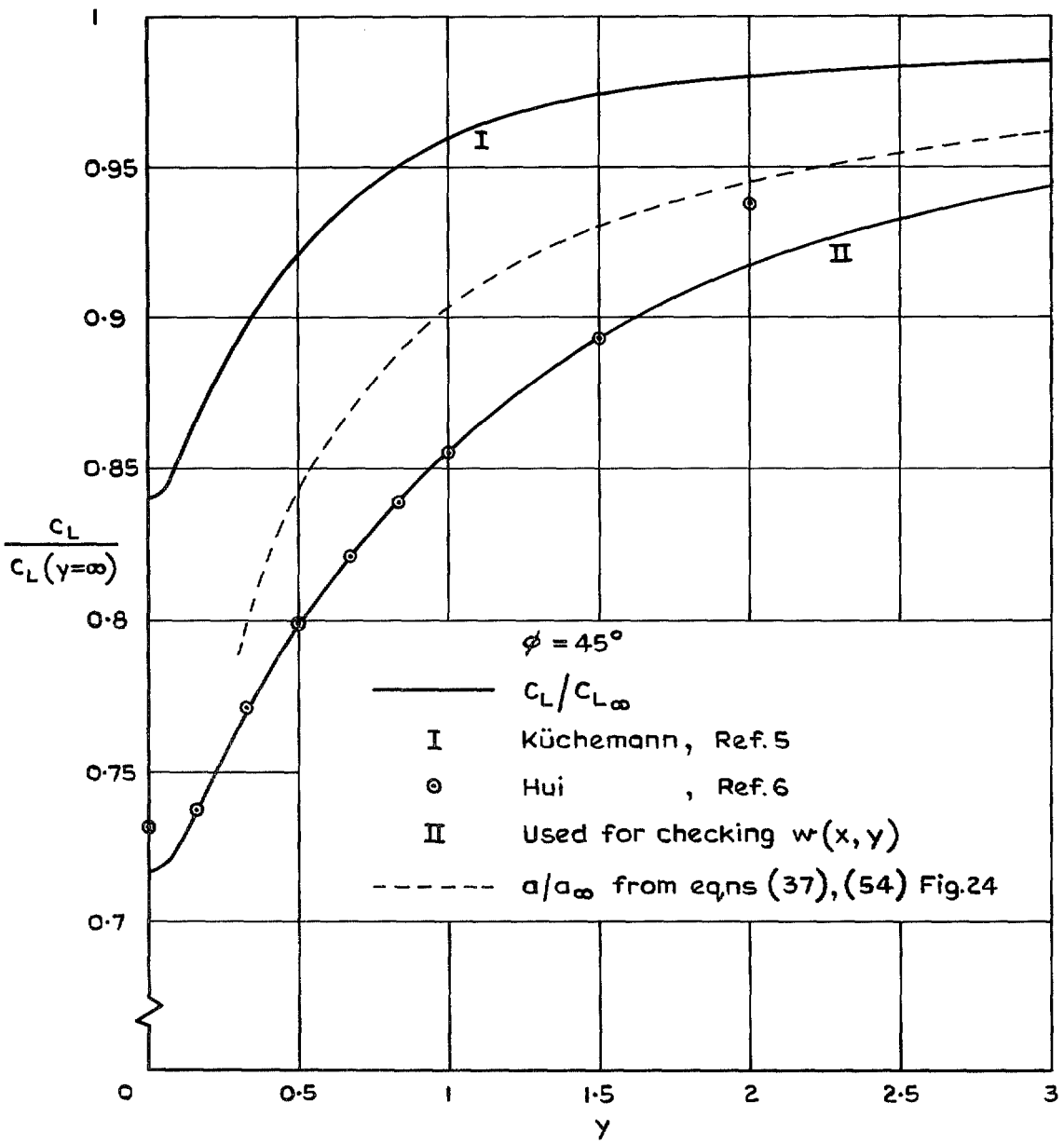

FIG. 25. Spanwise load distribution for a plane swept wing of infinite aspect ratio at an angle of incidence.

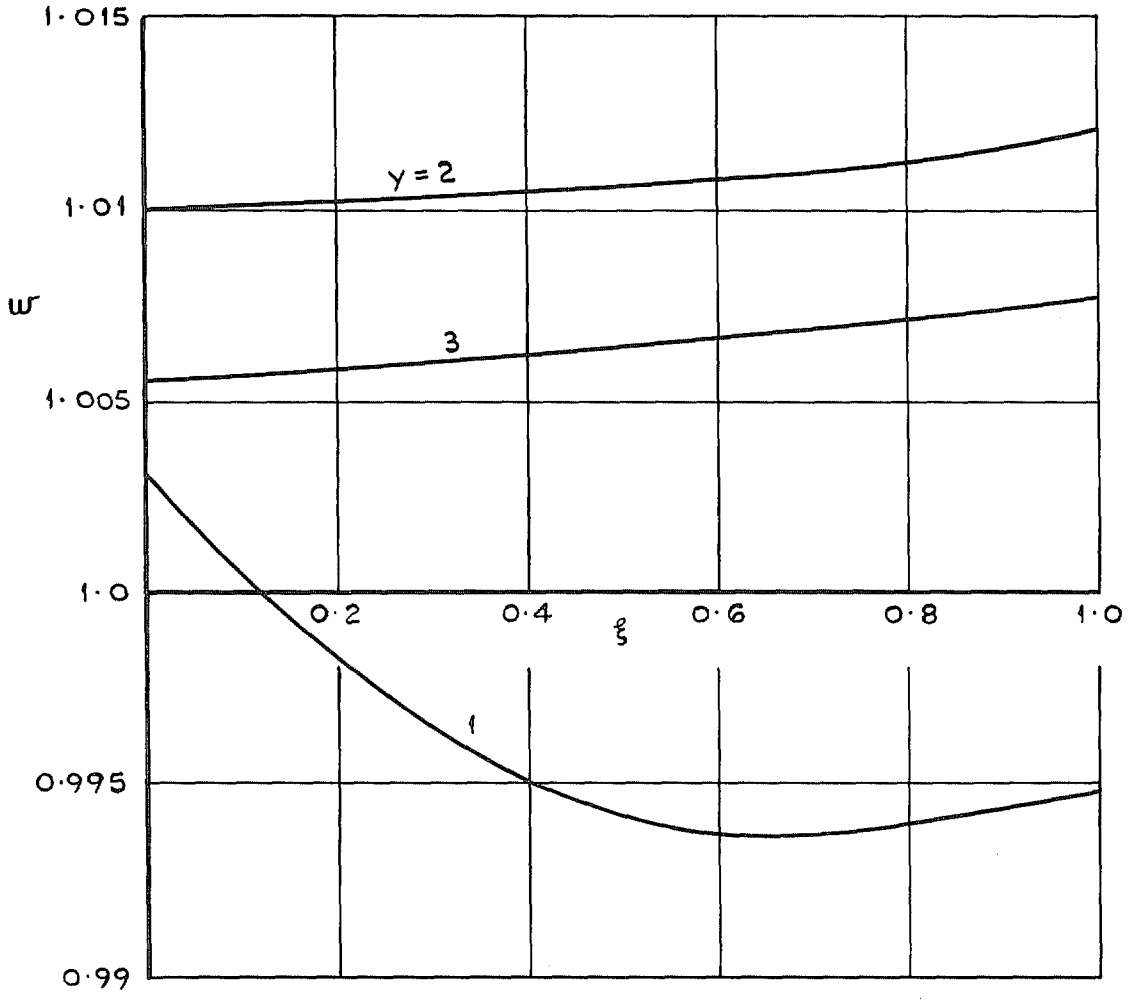

FIG. 26. Downwash related to the load distribution of equation (56) with $C_l(y)$ from curve II of Fig. 25.

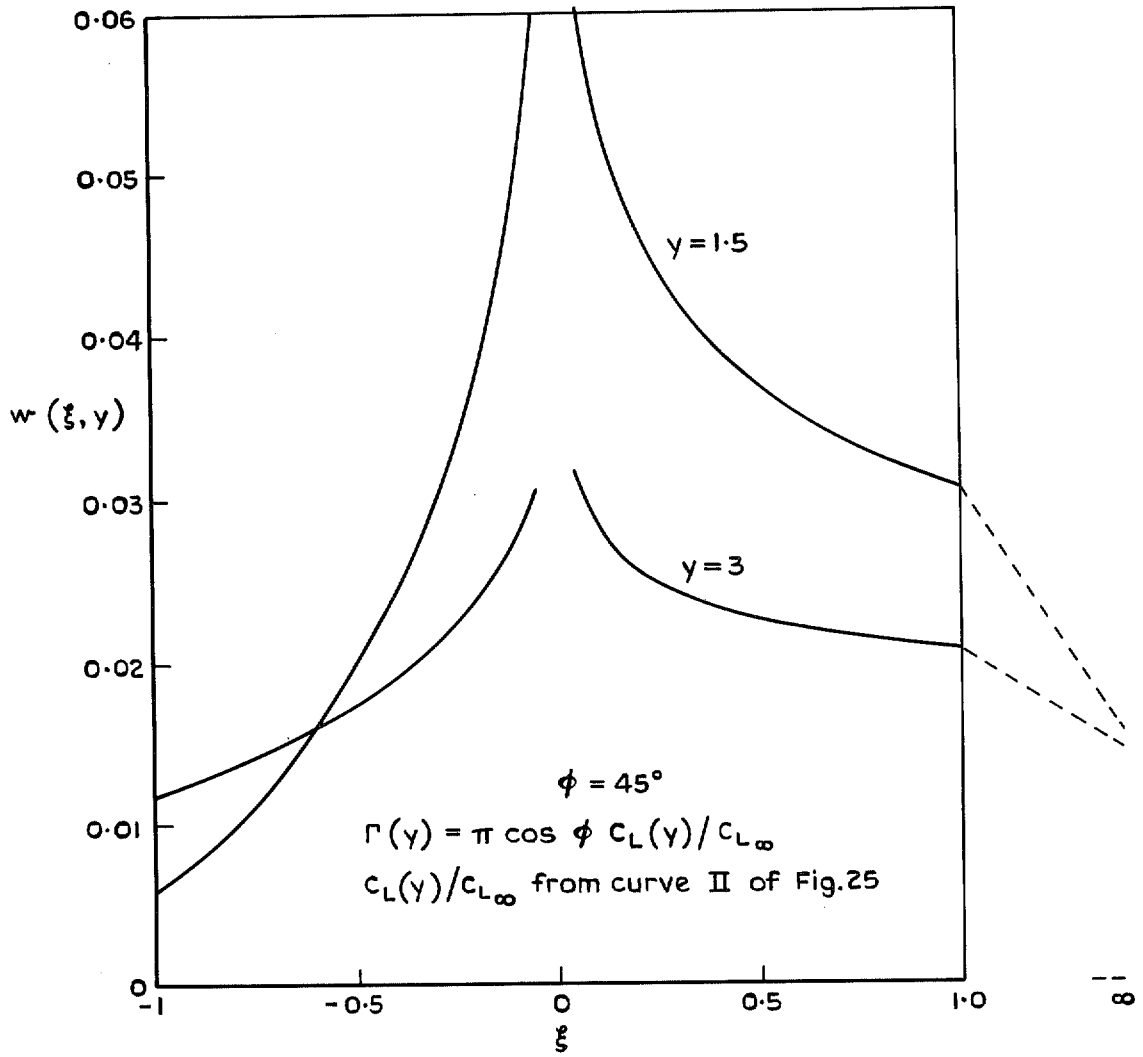

FIG. 27. Downwash induced by a trailing vortex sheet originating from a single swept spanwise vortex at $x = |y|, -\infty < y < \infty$ of strength $\Gamma(y)$.

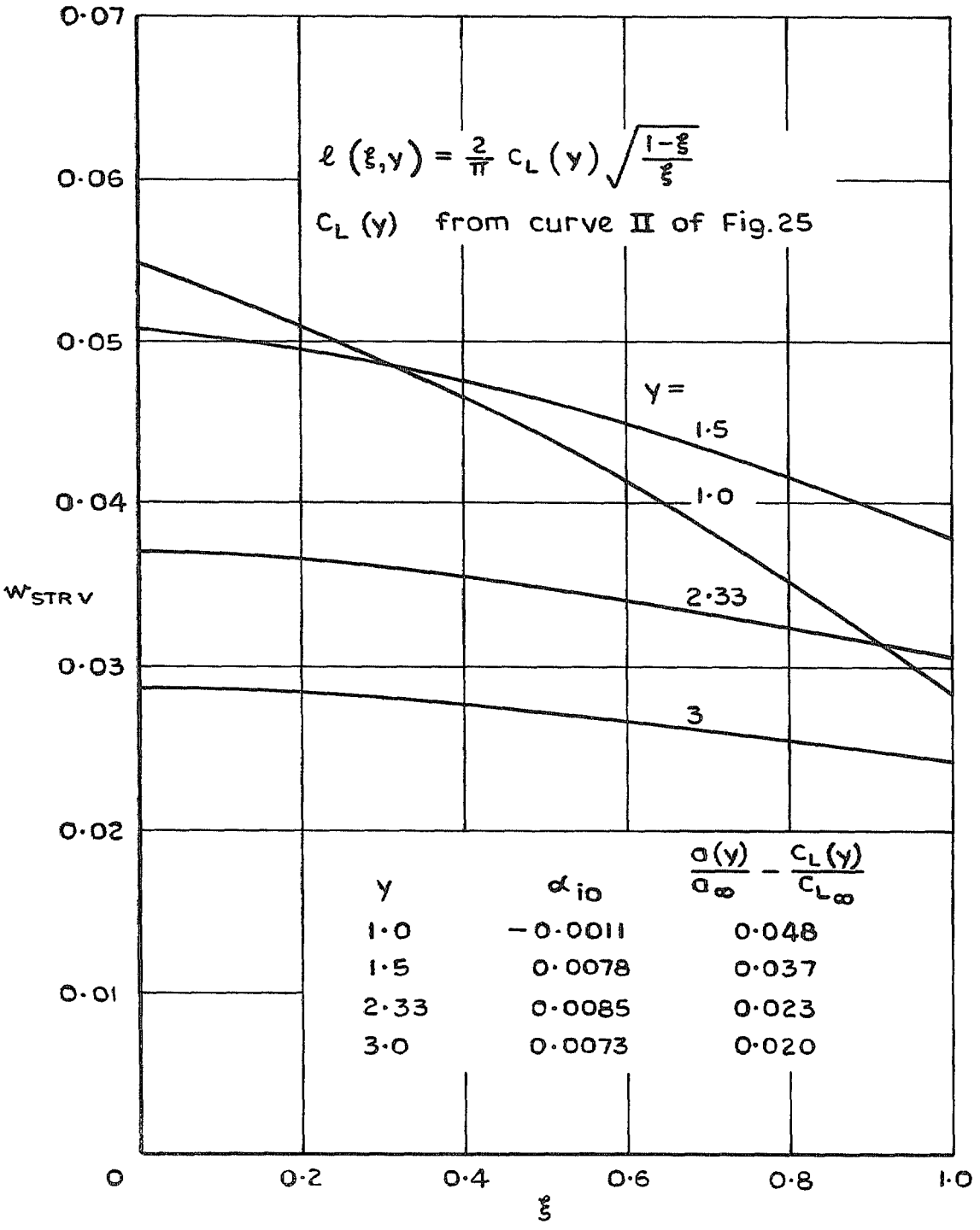

FIG. 28. Downwash induced by streamwise vorticity on infinite swept wing.

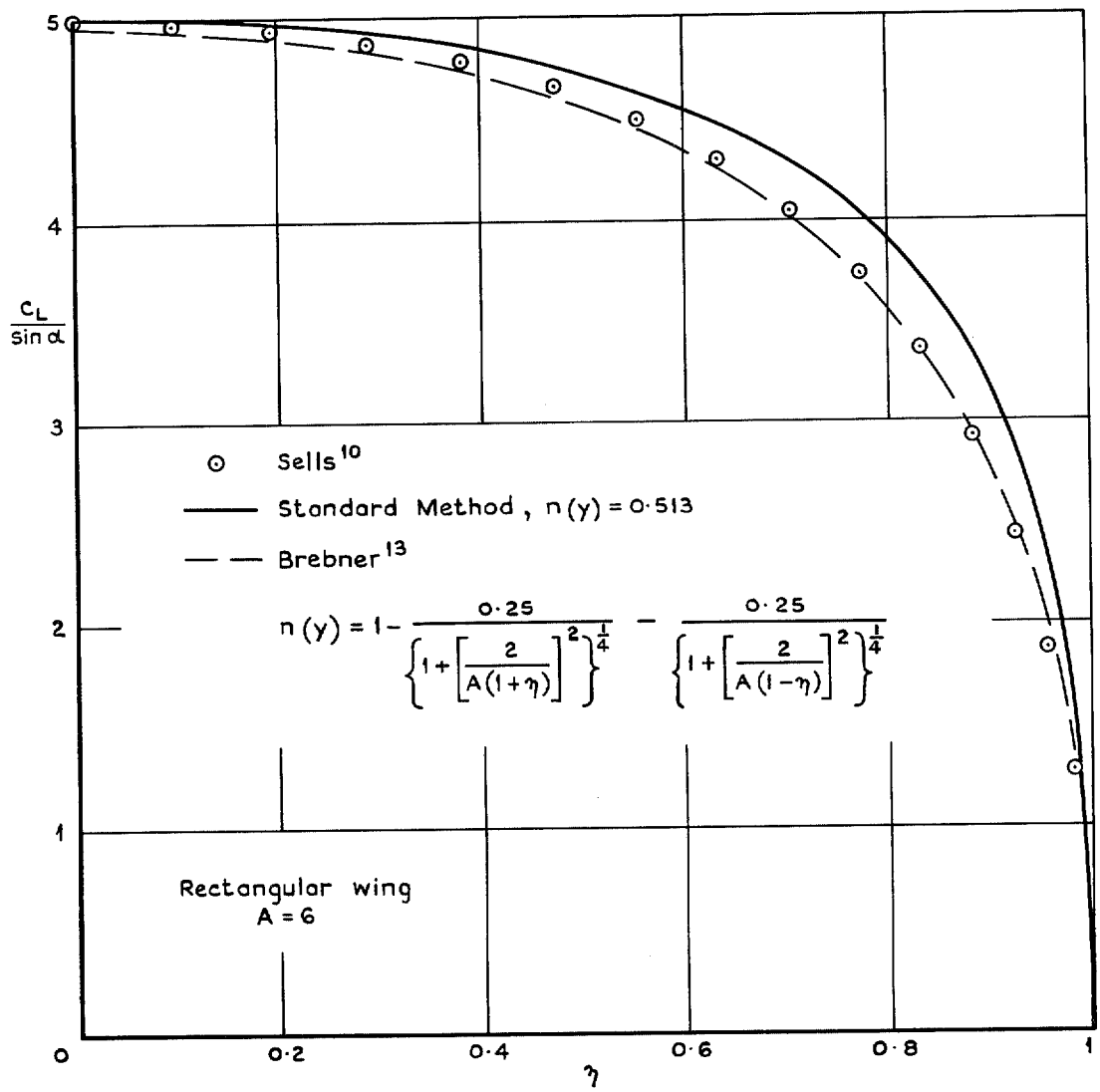

FIG. 29. Spanwise load distribution for a plane rectangular wing at an angle of incidence.

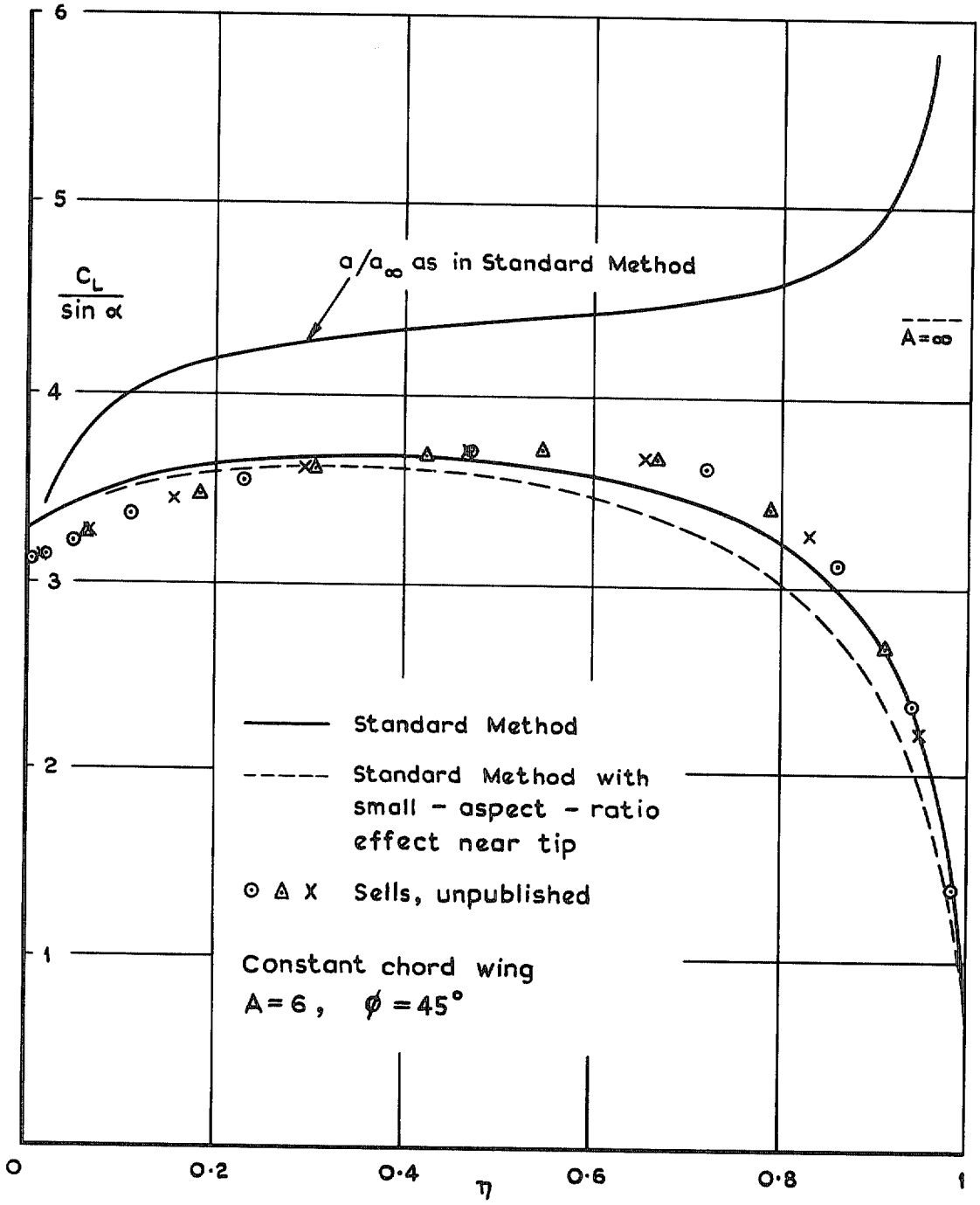

FIG. 30. Spanwise load distribution for a plane swept wing at an angle of incidence.

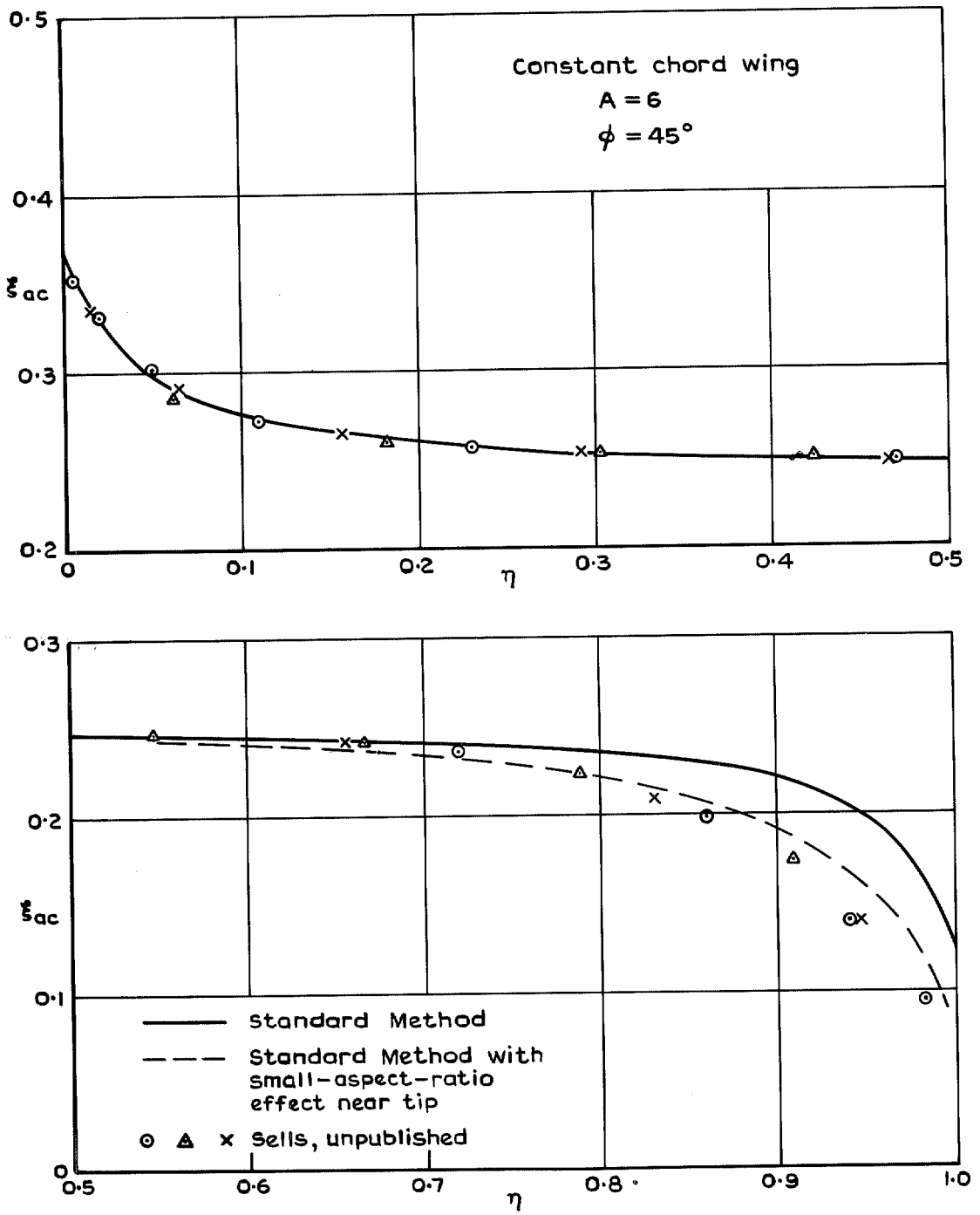

FIG. 31. Spanwise distribution of the position of the aerodynamic centre on a swept wing.

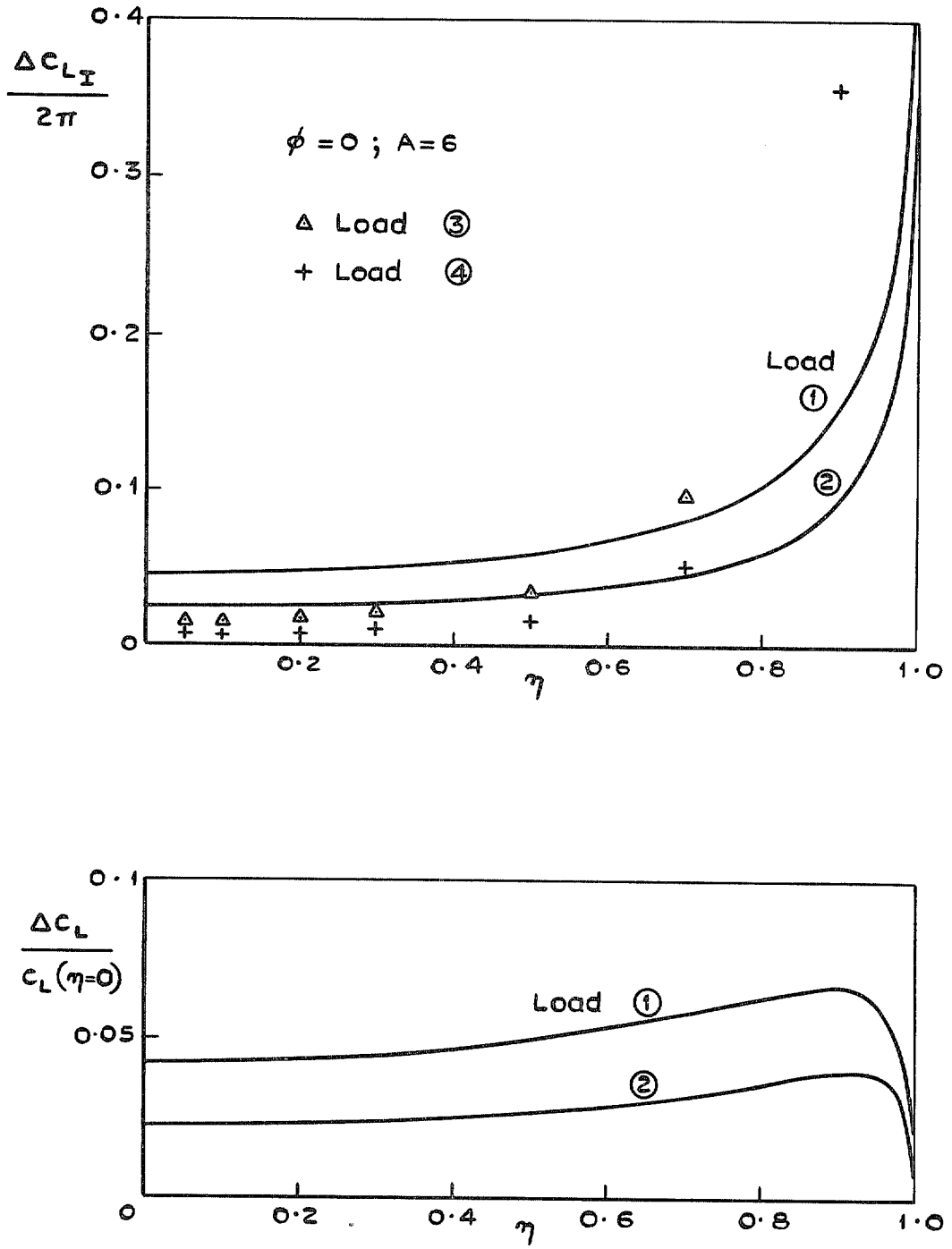

FIG. 32. C_L distribution for a rectangular wing with the slope $\partial z(x, y)/\partial x = -w_{\text{exact}}(x, y) + w_{\text{approx}}(x, y)$.

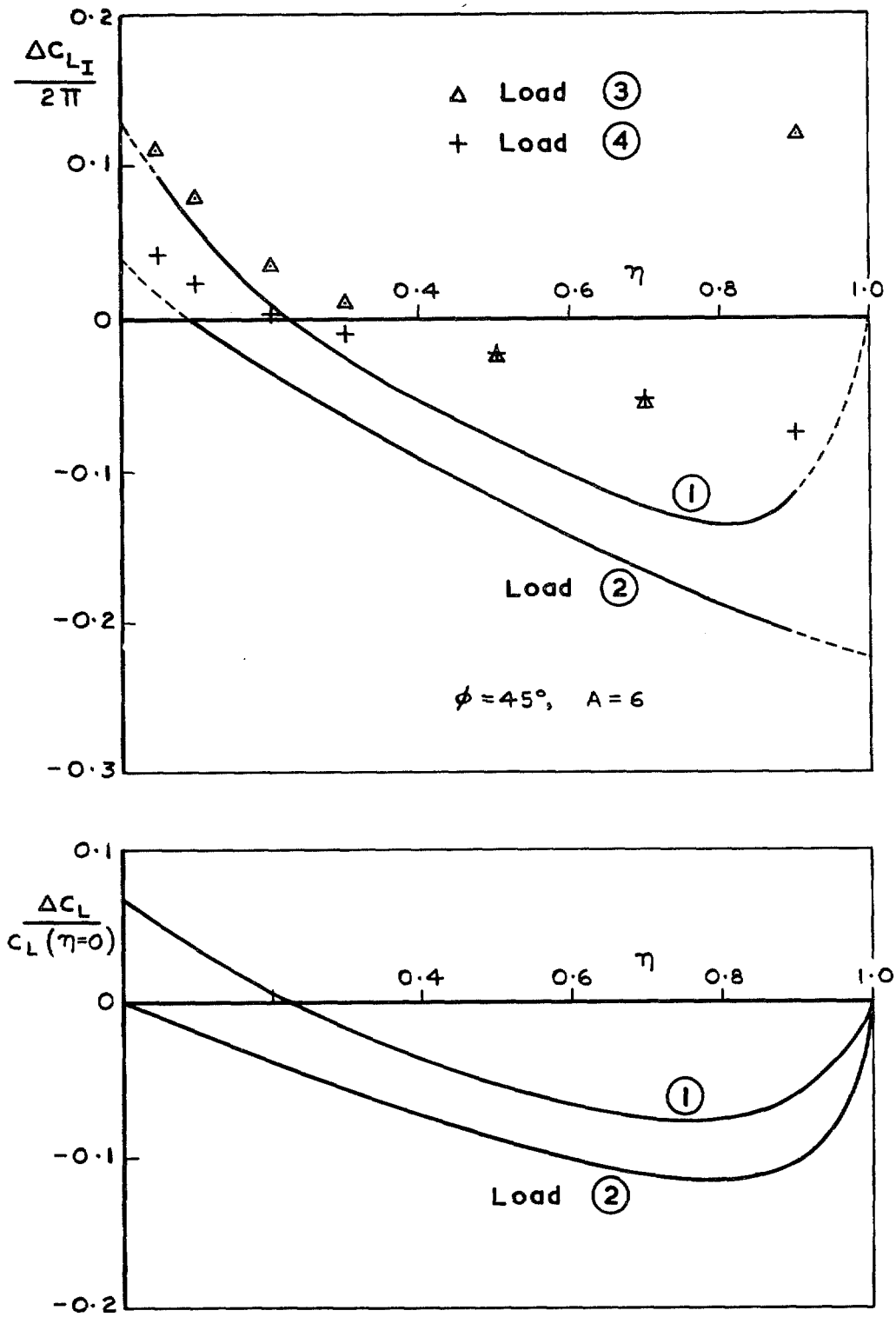

FIG. 33. C_L distribution for a swept wing with the slope $\partial z(x, y)/\partial x = -w_{\text{exact}}(x, y) + w_{\text{approx}}(x, y)$.

Printed in England for Her Majesty's Stationery Office by J. W. Arrowsmith Ltd., Bristol BS3 2NT
Dd. 505374 K5 8/74

HER MAJESTY'S STATIONERY OFFICE

Government Bookshops

49 High Holborn, London WC1V 6HB
13a Castle Street, Edinburgh EH2 3AR
41 The Hayes, Cardiff CF1 1JW
Brazennose Street, Manchester M60 8AS
Southey House, Wine Street, Bristol BS1 2BQ
258 Broad Street, Birmingham B1 2HE
80 Chichester Street, Belfast BT1 4JY

Government publications are also available through booksellers

ISBN 0 11 470845 2*